REPORT DOCUMENTATION PAGE

1a. REPORT SECURITY CLASSIFICATION Unclassified			1b. RESTRICTIVE MARKINGS		
2a. SECURITY CLASSIFICATION AUTHORITY			3. DISTRIBUTION / AVAILABILITY OF REPORT Approved for public release; distribution unlimited.		
2b. DECLASSIFICATION / DOWNGRADING SCHEDULE					
4. PERFORMING ORGANIZATION REPORT NUMBER(S)			5. MONITORING ORGANIZATION REPORT NUMBER(S) Appr elec dir		
6a. NAME OF PERFORMING ORGANIZATION The Johns Hopkins University Applied Physics Laboratory		6b. OFFICE SYMBOL *(If applicable)*	7a. NAME OF MONITORING ORGANIZATION Directorate of Physics and Geophysical Scienc Air Force Office of Scientific Research		
6c. ADDRESS *(City, State, and ZIP Code)* Laurel, Maryland 20723			7b. ADDRESS *(City, State, and ZIP Code)* Bldg 410, Bolling AFB Washington, DC 20323-6448		
8a. NAME OF FUNDING / SPONSORING ORGANIZATION Air Force Office of Scientific Research		8b. OFFICE SYMBOL *(if applicable)* NP	9. PROCUREMENT INSTRUMENT IDENTIFICATION NUMBER AFOSR-88-0101		
8c. ADDRESS *(City, State, and ZIP Code)*			10. SOURCE OF FUNDING NUMBERS		

			PROGRAM ELEMENT NO. 61102F	PROJECT NO. 2311	TASK NO. A1	WORK UNIT ACCESSION NO.

11. TITLE *(Include Security Classification)*

Final Report: Review of Research Performed Under AFOSR Grant 88-0101

12. PERSONAL AUTHOR(S)
Ching Meng and Barry Mauk

13a. TYPE OF REPORT Final	13b. TIME COVERED FROM 1/1/88 TO 12/31/90	14. DATE OF REPORT *(Year, Month, Day)* February 4, 1991	15. PAGE COUNT 60 pages

16. SUPPLEMENTARY NOTATION

17.	COSATI CODES		18. SUBJECT TERMS *(Continue on reverse if necessary and identify by block number)*
FIELD	GROUP	SUB-GROUP	Space Physics, Magnetosphere, Particle
			Precipitation, Aurora

19. ABSTRACT *(Continue on reverse if necessary and identify by block number)*

A final report on research conducted under AFOSR Grant 88-0101 is given. New scientific results and techniques developed towards an understanding of the Earth's space environment are given.

20. DISTRIBUTION / AVAILABILITY OF ABSTRACT ☒ UNCLASSIFIED/UNLIMITED ☒ SAME AS RPT. ☐ DTIC USERS	21. ABSTRACT SECURITY CLASSIFICATION Unclassified	
22a. NAME OF RESPONSIBLE INDIVIDUAL DR Henry K. Radoski	22b. TELEPHONE *(Include Area Code)* 2027624906	22c. OFFICE SYMBOL NP

DD FORM 1473, 84 MAR

83 APR edition may be used until exhausted.
All other editions are obsolete.

SECURITY CLASSIFICATION OF THIS PAGE

1. INTRODUCTION

2. THE CUSP AND BOUNDARY LAYERS

3. NIGHTSIDE PRECIPITATION IN THE EQUATORWARD PORTION OF THE AURORAL OVAL

4. MAGNETIC FIELD-ALIGNED PROCESSES WITHIN THE MIDDLE MAGNETOSPHERE

5. THE POLAR CAP AND QUIET TIME OVAL CONFIGURATION

6. AUTOMATED MONITORING OF THE SPACE ENVIRONMENT

7. SUMMARY AND CONCLUDING REMARKS

8. REFERENCES

9. FIGURES

10. GRANT SUPPORTED PUBLICATIONS (1987-1990)

1. Introduction

This is the official report describing the scientific results obtained from the three year grant AFOSR 88-0101. It is closely based on the detailed reviews of our earlier work which are contained in the proposal "An investigation of the Near Earth Space Environment" which sought a grant renewal. For the careful reader of that proposal, the present material may be repetitive.

The Earth's enormous, complex, and highly dynamic magnetosphere maps along magnetic field lines to a vastly smaller -- and hence easier to monitor -- region in the polar ionosphere. Our continuing research into understanding the plasma environment which surrounds our planet has an emphasis (although certainly not an exclusive one) on studying the charged particles which precipitate from various magnetospheric regions into the ionosphere, using auroral imagery and particle sensors. Particularly we have taken advantage of the large data sets available from operational Air Force satellites, such those in the DMSP series. The data set is unique in its continuous coverage and long duration. As the succeeding sections will make clear however, our efforts to study the complex processes in magnetospheric physics have in the past required the use of data from many sources -- ATS-6, SCATHA, ISEE-1,ISEE-3,IMP-8, HILAT, and POLAR BEAR.

To monitor the space environment with the DMSP data set of precipitating particles, it is first necessary to identify the magnetospheric source region of all types of precipitation observed at high latitude. This effort has been an ongoing campaign at APL, as described in several of the sections below. It is next necessary to teach a computer to make the same identifications the auroral researcher has developed. In the past we have relied on quantative algorithms for computer decision making; recently we

2

have been experimenting with sucess with a more general technique borrowed from the field of artificial intelligence, namely neural networks.

We have increasingly been collaborating with other researchers in need of data and expertise concerning auroral precipitation at the times of selected events (some of these are reflected in the publication list). Collaboraters have included those primarily using coherent radar, magnetometer chain, riometer, and ground based optical measurements; as well as researchers using AMPTE and other spacecraft. A major expansion of the effort to cooperate with researchers at other institutions seeking information concerning the state of the auroral oval has been completed. An online data base (available over SPAN) consisting of every DMSP F7 and F9 polar region crossing from December 1983 to present has been created. The data base consists of the neural network based identifications of the magnetospheric source of the precipitation (e.g., the cusp, LLBL, CPS, BPS, etc.), the flux and average energy measured, the boundaries of the precipitation of each type, and so forth. It is hoped that this data base will be of value to many magnetospheric researchers, and particularly to ground based observationalists.

The review subsection in each of our research categories illustrates the progress made in understanding fundamental questions of morphology and dynamics of the magnetosphere in the previous grant period; and there are excellent reasons to expect further progress. For example, although we have demonstrated (with fairly widespread acceptance) how the cusp proper may be defined [Newell and Meng, 1988a] and have compiled extensive statistics on its phenomenology [e.g., Newell et al., 1989], the basic question of the identification of magnetospheric mantle at low altitude has never been addressed, let alone questions of its behavior. Similarly the LLBL has not

3

been clearly distinguished from the dayside extension of the PSBL. Once these distinctions are established we can hope to accomplish the same extensive statistical resolution of outstanding questions as we have for the cusp.

Our interest is not merely confined to dayside phenomena. We have investigated the behavior of the equatorwardmost portion of the auroral oval precipitation, particularly that of the ions. We reported the first low altitude signature of dispersionless substorm injections [Newell and Meng, 1987]; and categorized the resulting ion dispersion signatures [Newell and Meng, 1988d].

We have a longstanding interest in the field-aligned coupling of the auroral regions to the distant magnetosphere, and we have been intrigued by evidence that the middle magnetosphere regions may have a more important role than conventional wisdom suggest. Along these lines we recently studied what appears to be field-aligned electric discharge phenomena occurring within the middle magnetosphere [Mauk and Meng, 1989], and have begun modeling a possible middle magnetosphere region discharge mechanism [Mauk, 1989].

We have long been interested in configurational questions concerning the polar cap and auroral oval, especially on the dayside [Meng and Lundin, 1986] or during very quiet times [Meng, 1981]. Both these topics are recently receiving renewed interest, including both collaborators [Lassen et al., 1988; Hones et al., 1989], and other researchers [e.g., Gussenhoven, 1989]. Other polar cap research of interest to us includes the study of unusual polar rain conditions. In the grant period reviewed here, we reported the first identification of ion polar rain [Newell and Meng, 1988c]; and the first cases of hemispherically symmetrical polar rain [Makita and Meng, 1987].

2. THE CUSP AND BOUNDARY LAYERS

Our first attempt at automated cusp identifications began in 1987 as an effort to quantify seasonal variation in cusp precipitation intensity [Newell and Meng, 1988b]. The criteria used in this first automated cusp identification were based on a wide band of intense soft precipitation from 0930 to 1330 magnetic local time (MLT). The algorithm selected precipitation regions as cusp if the ion average energy was below 6 keV, the electron average energy was below 500 eV, and the flux levels were sufficiently high. By late 1987, we had become convinced from an examination of a very large number of spectrograms that those researchers [e.g., Heikila, 1985; Lundin, 1988] arguing that there is a "cusp proper", a region limited in MLT near noon (a subset of the larger band termed the cleft), were correct.

We initiated a large scale project to make the cusp/cleft distinction as quantitatively and conceptually clear as possible [Newell and Meng, 1988a; Newell and Meng, 1989b]. Starting with the introduction of a simple conceptual definition of the cusp -- a localized region in which magnetosheath plasma entry is more direct, in the sense that more particles make it in to low altitudes and that their spectral characteristics are closer to magnetosheath values -- we developed a simple practical definition of the low-altitude cusp. Figure 2.1 shows how the average energy observed in the dayside soft band relates to the number flux; it is readily apparent how the high number fluxes are associated with energies closer to magnetosheath values. (Figure 2.2 shows how defining the cusp in terms of low average ion energy demarcates a statistically localized region near noon.) Because of the large number of passes that could be processed with the automated identifications (currently 12569), the results were more quantitative and have

5

apparently had a more widespread acceptance than have earlier attempts at making the cusp/cleft distinction [cf. Formisano, 1980].

The automated identifications have also been very fruitful in carrying out a variety of other morphology and phenomenology studies. We have quantified the early work of Burch [1973] showing the dependence of the cusp latitude on dipole tilt angles; our results [Newell and Meng, 1989a] show that for every degree shift in dipole tilt angle, the cusp latitude shifts by 0.06 degrees (the sense of the shift is towards lower latitudes in the winter hemisphere). This result is similar to the predictions of theoretical [Choe et al., 1973; Voigt, 1974] and empirical [Mead and Fairfield, 1975; Tsyganenko and Usmanov, 1983] magnetic field models. Still more recently we have shown more clearly than hitherto possible [e.g., Candidi, et al., 1983] that IMF B_y shifts the position of the cusp in local time; whereas IMF B_x does not affect the interhemispherical difference in cusp latitude [Newell et al., 1989] as might have been expected from some theoretical predictions [Cowley, 1981]

Our statistical work on the cusp has thus proven extremely fruitful.

3. NIGHT SIDE PRECIPITATION IN THE EQUATORWARD PORTION OF THE AURORAL OVAL

Geosynchronous satellite observations of the introduction of plasma into the middle magnetosphere suggest that the transport invariably occurs in association with highly time dependent impulsive "dispersionless injections" [McIlwain, 1975; Mauk and Meng, 1990]. These nearly energy independent boundaries, common to both electrons and ions, have long been indirectly inferred from high altitude satellites; but because of possible ambiguities associated with spatial and temporal effects, they have not been universally accepted. Because of the rapid L-shell crossing of the DMSP satellites, most observed variations in the fluxes can be interpreted as due to spatial effects. A

6

nearly dispersionless injection appears to the DMSP satellite as an abrupt equatorward shifting of the previously energy dependent equatorward edge of auroral precipitation to a common energy independent boundary. In the previous grant period, we reported the first low altitude evidence for dispersionless injections [Newell and Meng, 1987]. We thus established that clearly defined energy independent precipitation cutoffs are indeed seen shortly after the growth phase of a substorm (before the onset of the expansion phase).

There have been several reports of the energy dependence in the equatorward cutoffs in auroral electron precipitation. The sense of this latitude dispersion is that lower energy electrons reach further equatorward than do higher energy electrons, a result frequently held to be evidence for the existence of steady state Alfven convection layers [e.g., Horwitz et al., 1986]. During the current three year period we investigated the ion equatorward precipitation cutoffs [Newell and Meng, 1988d]. When viewed in spectrogram format, the ion cutoff latitudes form characteristic dispersion curves which vary with magnetic activity and local time, and proved to be more complicated than the electron cutoffs hitherto investigated. A study of 503 auroral oval passes over the dawn, dusk, and near midnight local time sectors revealed that the overwhelming majority (93%) of these curves can be classified into one of four categories of dispersion curves, with occurrence probabilities depending on the local time sector. Table I lists the types of dispersion curves observed, and their probability of observation as a function of local time. Certain features of these dispersion curves, including the coincidence of nearly zero energy electron and ion cutoffs, argue for the interpretation of these curves as the result of dispersion in a convection field.

However there is no existing model of magnetospheric convection which accounts for all the dispersion features observed in cutoff latitudes.

In addition to dispersion features, we also compared the simultaneous DMSP particle precipitations with the optical auroral observation made at Japanese Syowa, Antarctic Station. Two results were published in JGR and GRL (see publication list in section 10).

4. MAGNETIC FIELD-ALIGNED PROCESSES WITHIN THE MIDDLE MAGNETOSPHERE

It has become increasingly apparent that magnetic field-aligned processes have key roles to play in the transport processes that occur within the middle magnetosphere (~ geosynchronous) during dynamical periods. Most compelling are the geosynchronous observations of McIlwain [1975] of intense magnetic field-aligned electron beams in association with substorm injections. These beams are intense enough to drive discrete auroral processes, are reminiscent of beams observed in the vicinity of discrete aurora, and are often times coincident with East-West magnetic perturbations (e.g. "L-spikes") interpreted [e.g. Nakai, 1982] as resulting from magnetic-field-aligned electric currents [Mauk and Meng, 1987]. Moreover, direct observations of localized magnetic field-aligned currents have been made within the middle regions [Kelly et al., 1984; Robert el al., 1984; Roux, 1985]. More recent middle magnetosphere region electron beaming has been reported by Klumpar et al., [1988] and Kremser et al., [1988], and the possible relationship between those observations and the ones of McIlwain [1975] have been discussed by Mauk and Meng [1989].

The occurrence of magnetic field-aligned processes within the middle magnetosphere is an important issue in the context of present controversies surrounding the mapping of aurora! features to the distant magnetosphere. The controversies are summarized nicely by Siscoe [1988] in an <u>EOS</u> Meeting Report on the International Conference on Auroral Physics (July, 1988; St. John's College, Cambridge, U.K.). Notwithstanding the controversies concerning the so-called "Plasmoid" and Plasma Sheet Boundary Layer (PSBL) models of substorm processes, there is an additional question as to whether the outer plasma sheet boundary is where auroral breakups are initiated and even maintained. Galperin and Feldstein [1989] have presented clear evidence that the site of auroral breakup is near the inner boundaries of the plasma sheet, and recent AMPTE CCE observations tend to support that contention [Lui et al., 1988; Lopez et al., 1988].

Without taking a strong position on these controversies, it is clear that as interest shifts towards the middle magnetospheric regions with regard to discrete auroral processes, new thinking will have to emerge concerning how magnetic-field-aligned discharge phenomena can be initiated and maintained in regions where quasi-dipolar magnetic configurations prevail. While there are models that consider discharges within such regions [e.g. Rothwell et al., 1988; Kan et al., 1988] much work clearly remains to be done.

<u>Results from AFOSR Support</u>

Under the AFOSR grant (1988-1990), three papers have been written concerning this topic. They are:

9

Paper 1: Mauk, B. H., Generation of Macroscopic Magnetic-Field-Aligned Electric Fields by the Convection Surge Ion Acceleration Mechanism, JGR, 94, 8911, 1989.

Paper 2: Mauk, B. H., and C.-I. Meng, Macroscopic Magnetospheric Particle Acceleration, in AGU Geophysical Monograph 54, p. 319, 1989.

Paper 3: Mauk, B. H., and C.-I. Meng, The Aurora and Middle Magnetospheric Processes, in Auroral Physics, Cambridge University Press, 1990 (In Press).

The results of these works are summarized here.

Paper 1. This theoretical (simulation) work suggests a mechanism that can generate macroscopic, magnetic-field-aligned, multi-kilovolt potential drop electric fields within quasi-dipolar regions of the earth's magnetosphere. It was a follow-on to an earlier work [Mauk, 1986] in which the kinetic response of ion distributions was calculated in the environment of a dipolarizing magnetic flux tube (the so-called "Convection Surge" -- Quinn and Southwood, [1981]) This earlier modeling effort reproduced the bounce-phase bunch ion distributions reported by Quinn and McIlwain [1979], and explained the presence of magnetic-field-aligned ion distributions observed nominally within the geosynchronous magnetosphere at energies below ~1 to ~10 keV [Mauk and McIlwain, 1975; Kaye et al., 1981] and occasionally as high as ~40 keV [Figure 2, McIlwain, 1975].

In Paper 1 we extended the original modeling effort into a self-consistent simulation The field-aligned electric potential was calculated by imposing the quasi-neutrality condition using approximated electron distribution forms and by forcing the ions to respond self consistently to the resulting parallel electric fields.

Paper 2. The principal goal of this work was to explore the similarities between the guiding-center processes model in paper 1 and in Mauk [1986]

10

and the deep-tail neutral sheet processes discussed originally by Speiser [1965; 1967; 1970] and modeled and confirmed by Lyons and Speiser [1982] ([cf. Speiser, 1987]). In particular, in the vicinity of a narrow neutral sheet with a penetrating electric field, ions, on encountering the sheet, will execute a serpentine-like motion with the net effect that they are ejected from the neutral-sheet in an energized form and with a strongly magnetic-field-aligned beam-like distribution shape (forming, it is argued, the plasma sheet boundary layer).

The guiding-center convection-surge energization process is virtually identical to the neutral-sheet acceleration process in its consequences. In particular, it has been noted by Speiser [1970] and Sonnerup [1971] for special configurations, and now by Whipple et al. [1986] for more general configurations, that there exists a first adiabatic invariant for narrow neutral sheet interactions that is analogous to, but different from, the magnetic moment. This invariant reduces to the magnetic moment prior to and following the neutral sheet interaction, and so for the interaction as a whole, the magnetic moment μ is approximately preserved. Thus, the consequences of the neutral sheet acceleration process are fully constrained by conservation of energy (within the c $\mathbf{E}$ x $\mathbf{B}$/B, or deHoffman-Teller frame) and by the first adiabatic invariant. These constraints are identical to those that govern guiding center motions. For instance, had Lyons and Speiser [1982] invoked guiding processes in attempting to reproduce the plasma sheet boundary layer (PSBL) distributions, they would have obtained quantitatively the same results as they obtained using the neutral sheet acceleration processes. The convection surge process modeled in Mauk (1986) generates the same kind of strongly field-aligned ion beaming.

11

We proposed in Paper 2 an organizational scheme for the magnetotail, with the existence of an approximate first adiabatic invariant being the organizing parameter. In between the two adiabatic regions is a region of intermediate neutral sheet thicknesses, and within that region the ions are pitch angle randomized, and a first invariant may not be defined for individual particles [Propp and Beard, 1985; Martin, 1986; Whipple et al., 1986].

It is our thesis that macroscopic ion dynamics play a prominent role in the occurrence of auroral discharge phenomena. This thesis has precedent in the works of Kan [1975] and Stenzel et al. [1981]; and is supported by the observations of Lyons and Evans [1982] and Lyons et al. [1988]. In Paper 2 (and further in Paper 3) we have, in particular, drawn an analogy between the laboratory studies of the generation of electric potential double layers [Stenzel et al., 1981] and the modeling efforts of Paper 1 (The modeling efforts would require additional features to form detached double-layer-like structures). Our point concerning magnetotail organization is that, with regard to the macroscopic ion dynamics, there is little that is qualitatively different in the physics of the distant magnetotail that would favor it as a site of discrete auroral phenomena. The differences are likely to lie in the ability of the macroscopic system to supply an appropriate "cross-tail" electric field to the region. Intuitively, discharge phenomena occurring in the middle magnetosphere is likely to be transient in nature rather than sustained , and indeed middle magnetosphere observations identified with discharge phenomena have generally been transient in nature. Such transient phenomena could set up the conditions needed to sustain the processes modeled in Rothwell et al. [1988] or Kan et al. [1988].

Paper 3. A key goal of this paper was to lay a firmer foundation for some of the results that were taken somewhat for granted in the previous works. In particular, the claim that the McIlwain's [1975] electron beams exist on quasi-dipolar field-lines near the earthward boundary of the plasma sheet populations has been challenged at national and international scientific gatherings. These challengers contend that the beams actually reside near the plasma sheet boundary layer (PSBL). In Paper 3 we have analyzed one particular geosynchronous dispersionless injection, with associated magnetic-field-aligned electron beams, in substantial detail, and have provided what we consider to be overwhelming circumstantial evidence against the PSBL hypothesis. The evidence strongly supports the original contentions of McIlwain [1975], that the beams occur near the earthward boundary of the injected plasma sheet populations and are observed on quasi-dipolar field-lines.

Additionally, in Paper 3, we have reminded the reader of the prevalence of relatively low-latitude discrete-like auroral activity. In particular, an example was found, originally presented for other purposes, that shows discrete activity mapping earthward of the geosynchronous orbit and earthward of plasmas with central plasma sheet characteristics. The example, from Meng et al. [1979], is shown in Figure 4.1. The left panel shows a comparison between a spectrum sampled at geosynchronous orbit (ATS-6) and spectra sampled at very low altitudes by DMSP-32 near the magnetic foot-point of the geosynchronous satellite. The right panel shows the measured optical display (in negative), and the circle shows the calculated foot-point of the ATS-6 satellite. The foot-point is positioned within what is conventionally called "diffuse" aurora, equatorward of discrete auroral features. The low and high altitude spectra (both showing non-discrete

13

characteristics) match each other to a remarkable degree (a slight, 0.5° shift in DMSP sample latitude was needed to yield the "exact" match apparent with the "bars").

The interesting feature of Figure 4.1 is that clear discrete auroral features were observed equatorward of the ATS-6 magnetic foot-point and equatorward of populations with central plasma sheet characteristics. Equatorward of these discrete auroral features, the DMSP spectra were very different from the ATS-6 spectra. It is unknown how common this situation is. Many researchers [e.g. Galperin and Feldstein, 1989; Rothwell et al., 1988] have argued that discrete aurora observed at very low latitudes must map to the middle (e.g. geosynchronous) regions, but it is unusual to have the mapping confirmed by particle spectra. This DMSP/ATS-6 comparison motivated our previous suggestion that transient discrete activity could stimulate more sustained middle magnetosphere discrete activity.

5. THE POLAR CAP AND QUIET TIME OVAL CONFIGURATION

The term 'polar cap' has long been used rather loosely in the past with perhaps the most common definition being the region bounded by the average or statistical auroral oval. As a result, the polar cap has also been considered a dark and uninteresting region surrounded by the bright auroral oval along which all interesting magnetospheric and ionospheric processes take place. The only well-known exception is the so-called 'polar cap arcs' which appear from time to time across the area surrounded by the oval. However, such a view of the polar cap has been radically changed during the last five years.

When the north-south component B_z of the interplanetary magnetic field (IMF) has an appreciable southward component, the auroral oval is

14

larger than the average size and brighter, indicating that an auroral substorm is in progress. The region surrounded by the active auroral oval appears very dark, and there is no prominent feature which can be observed optically. However, drastic changes begin to take place as the IMF B_Z component begins to turn northward. As the IMF B_Z component remains positive for an extended period (say, >6 hrs), this highest latitude region of the earth becomes the stage of a variety of fascinating phenomena which are vital to understanding the solar wind-magnetosphere interaction.

We have long slighted auroral phenomena in this highest latitude region of the earth because our main interests have traditionally been concentrated in understanding magnetospheric substorms which are due primarily to the southward component of IMF B_Z. Actually, we have recognized for a decade that auroral phenomena in this highest region during periods of the IMF $B_Z > 0$ are at least as complicated and fascinating as those in the auroral oval during periods of the IMF $B_Z < 0$ (Meng, 1981a,b) Therefore, our understanding of the solar wind-magnetosphere interaction would be very incomplete without a detailed study of auroral phenomena during the periods of IMF $B_Z > 0$. Furthermore, the B_Z component is only one of the components of the IMF vector B, so that a full understanding of the solar wind-magnetosphere interaction requires a study of effects of the IMF components B_X and B_y as well. That is to say, we have been studying substorms which are only one aspect of the solar wind-magnetosphere interaction (namely, the effects of the IMF $B_Z < 0$). However, we must study effects of the IMF $B_Z > 0$, and B_y and B_X effects as well.

Results from AFOSR Support

There is little doubt that there exists a limited area in the polar region of the earth, from which the open field lines originate; here, the open field

15

lines are defined as the geomagnetic field lines which are 'interconnected' or 'reconnected' with IMF lines. Thus there is an area in which solar electrons impinge almost uniformly over the polar region, indicating that the solar electrons have an equal chance of access over a nearly circular area. The entry of solar electrons has been observed and the polar rain is the mostly common indicator. Thus, this area of polar rain is likely to be the open field line region. This is because the best available method to trace the open field lines is to use solar wind electrons of energies of the order of a few hundred electron volts. This area has a geometry which is similar to the area bounded by the auroral oval.

The DMSP (Defense Meteorology Satellite Program) series of satellites since the 1970's provide the most extensive observations of low energy particle precipitation observations and the simultaneous optical auroral images over dark hemisphere. Our investigations in solar-terrestrial physics (STP) have been very fruitful and cover several different aspects of STP as indicated in Section 10 Grant Supported Publications (1987-1990) of this proposal. In the following, only the polar cap morphology and the polar rain phenomenon are discussed.

5.1 Discovery of Ion Polar Rain

Although the comparatively featureless polar cap precipitation phenomenon of electron polar rain has been known and studied since the the work of Winningham and Heikila [1974], there had been no previous clear identification of the ion polar rain. We documented [Newell and Meng, 1988c] such an instance of ions at magnetosheath energy levels precipitating with characteristics of polar rain at flux levels near 10^9 eV/cm^2·s·sr. A Maxwellian distribution with a temperature of 230 eV and a density of 0.02/cm^3 fit the ion polar rain reasonable well. The clear ion polar rain signal

allowed verification that the strong dayside-nightside gradient expected and observed in electron polar rain was also for the ions, and that the sign of the dawn-dusk gradient was appropriate to the sign of IMF B_y. Conventional theories of polar rain [e.g., Fairfield and Scudder, 1985] would have had difficulty if no such ion polar rain signal could be measured.

5.2 Very Quiet Time Polar Region Morphology

During periods of relative magnetic quiescence the luminosity of auroral optical emissions is very weak and also the auroral display is not very dynamic. Thus, the studies of polar region are generally focused on the moderate and very active geomagnetic conditions associated with substorms and magnetic storms. Our attention to the quiet magnetosphere started in mid-1970's (for example, Meng et al., Auroral Circle: Delineating the poleward boundary of the quiet auroral belt, JGR, 82, 164, 1977; Meng, Polar cap variations and the interplanetary magnetic field, in Dynamics of the Magnetosphere, p. 23, 1979; Meng, Diurnal variation of the auroral oval size and the minimum oval, JGR, 84, 5319, 1979).

Based on case studies of quiet time auroral images and particle precipitations, we suggested that the so-called 'polar cap auroral arcs' are not located inside the instantaneous opened field line region (i.e. a narrower definition of the polar cap); instead they are in the poleward part of the widened auroral oval (Meng, Polar cap arcs and the plasma sheet, GRL, 8, 273, 1981). Since then, we have investigated the statistical distributions of the quiet time polar cap and auroral oval with results in a series of publications.

In addition to these polar cap studies, we also investigated the polar cusp region and dayside auroral display during very quiet geomagnetic conditions. Many interesting phenomena were also observed and many

17

publications can be found in the Section 10 of this proposal, AFOSR Grant Supported Publications List.

The quiet polar cap morphology can be summarized as follows:

The statistical distribution of precipitating auroral electrons does not have a well-known oval configuration. It has the shape of an irregular annular belt encircling a rather small polar cap. Optically, the auroral particle precipitation belt is characterized by a diffuse background of 6300-, 5577, and 3914-Å emissions with embedded discrete forms. The high-latitude, sun-aligned arcs in the dawn and dusk sector are in the region of the poleward expanded auroral oval.

Comparing the quiet time observations with previous established auroral features, we believe that the bright discrete auroras forming the classical oval are located in the poleward (most intense) part of the higher energy belt, the high-latitude dayside auroral arc-forms and sun-aligned so-called "polar cap arcs" are embedded in the high-latitude, low-energy belt. The high latitude sun-aligned arcs are observed poleward of the dayside oval, including both dawn and dusk parts. There is no obvious signature difference in the electron precipitation between the two high-latitude subgroups. Therefore, it is probable that the sun-aligned arcs are signatures of a poleward widening of the dayside auroral maximum during quiescence, as suggested by Meng (1981b).

The poleward area without significant precipitation (except the polar rain), encompassed by the electron precipitation belt is believed to be the polar cap proper. The instantaneous polar cap, thus defined, is very small and sometimes may be pear-shaped (or teardrop-shaped), with its largest extension in the noon-midnight direction, as seen occasionally in satellite images. The poleward boundary of the expanded oval can be much higher

18

than shown, and there is a dynamic variation of its shape and location, probably depending on the instantaneous orientation and magnitude of the interplanetary magnetic field.

6. AUTOMATED MONITORING OF THE SPACE ENVIRONMENT

It has now been three decades since rocket borne detectors first directly measured precipitating particle which cause the aurora [Meredith et al., 1958; Davis et al., 1960; McIlwain, 1960]. Enormous progress in understanding magnetospheric structure and auroral phenomena has been made since then. While the complexity of the magnetosphere insures that there is still a role for further case studies, we believe that statistical studies of a more sophisticated nature than hitherto will play an important role in making further progress. To accomplish this, we have been applying a pattern recognition technique from the field of artificial intelligence, namely neural networks, to develop a system for automatically monitoring high latitude precipitation -- and hence the space environment.

We have trained the neural network to identify the various types of precipitation observed in the DMSP F7 and F9 data sets (noon/midnight passes). As a result, an online data base consisting of the auroral oval boundaries, structure, and particle fluxes from December 1983 through the present for these satellites has been created. For each region the boundaries are specified in both geographic and geomagnetic coordinates, and the average and peak values of the particle flux is given, along with the average energies. This data base, which has recently been made available to the whole space physics community [Newell et al., 1990], should be of particular interest to

19

ground-based observers; although anyone interested in the state of the auroral oval may find it of value.

7. SUMMARY AND CONCLUDING REMARKS

Over the three year period covered by the previous grant (88-0101) we have continued our tradition of vigorous research and frequent publication (as documented in Section 10, Grant Supported Publications, 1987-1990). Particularly we are increasingly exploiting the enormous size of the data sets available to us to provide qualitative and quantitative answers to questions of morphology, such as which magnetospheric regions correspond to various types of precipitation and their spatial distributions. It should be emphasized that our statistical work does not involve binning of precipitation simply by MLAT and MLT (which invariably mixes different regions together); but rather always involves first recognizing the specific plasma regime, and subsequently compiling statistics.

We believe that a new, more quantitative period of space physics and solar-terrestrial interaction research is beginning, involving the use of larger data sets which are manipulated in a more sophisticated fashion. We are determined to be at the forefront of this effort.

8. REFERENCES

(Note: there is a separate bibliography of publications supported by AFOSR grant 88-0101 over the period 1987-1990).

Bosqued, J. M., J. A. Sauvaud, D. Delcourt, and R. A. Kovrazhkin, Precipitation of suprathermal ionospheric ions accelerated in the conjugate hemisphere, J. Geophys. Res., 91, 7006, 1986.

Burch, J. L., Rate of erosion of dayside magnetic flux based on a quantitative study of the dependence of polar cusp latitude on the interplanetary magnetic field, Radio Sci., 8, 955-961, 1973.

Burch, J. L., P. H. Reiff, J. D. Menietti, R. A. Heelis, W. B. Hanson, S. D. Shawhan, E. G. Shelley, M. Sugiura, D. R. Weimer, and J. D. Winningham, IMF B_y dependent plasma flow and Birkeland currents in the dayside magnetosphere 1. Dynamics Explorer observations, J. Geophys. Res., 90, 1577-1593, 1985.

Candidi, M., H. W. Kroehl, and C.-I. Meng, Intensity distribution of dayside polar soft electron precipitation and the IMF, Planet. Space Sci., 31, 489-498, 1983.

Candidi, M., and C.-I. Meng, The relation of the cusp precipitating electron flux to the solar wind and interplanetary magnetic field, J. Geophys. Res., 89, 9741-9751, 1984.

Cao, F. and J. R. Kan, Finite-Larmor-Radius Effect on Field-Aligned Currents in Hydromagnetic Waves, J. Geophys. Res., 92, 3397, 1987.

Carbary, J. F., and C.-I. Meng, Relations between the IMF B_z, AE index, and cusp latitude, J. Geophys. Res., 91, 1549, 1986a.

Carbary, J. F., and C.-I. Meng, Correlation of cusp latitude with B_z and AE(12) using nearly one year's data J. Geophys. Res., 91, 10047, 1986b.

Chen, F. F., Introduction to Plasma Physics and Controlled Fusion, Volume 1, Plenum Press, New York, 1984.

Chew, G. F., M. L. Goldberger, and F. E. Low, The Boltzmann equation and the one-fluid hydromagnetic equations in the absence of particle collisions, Proc. Roy. Soc., A236, 112-118, 1956.

Chiu, Y. T., and M. Schulz, Self-Consistent Particle and Parallel Electrostatic Field Distributions in the Magnetospheric-Ionospheric Auroral Region, J. Geophys. Res., 83, 629, 1978.

Choe, J. Y., and D. B. Beard, The compressed geomagnetic field as a function of dipole tilt, Planet. Space Sci., 22, 595-608, 1974.

Cowley, S. W. H., Asymmetry effects associated with the x-component of the IMF in a magnetically open magnetosphere, Planet. Space Sci., 29, 809-818, 1981.

Cowley, S. W. H., and W. J. Hughes, Observation of IMF sector effect in the Y magnetic field component at geostationary orbit, Planet. Space Sci., 31, 73, 1981.

Crooker, N. U., Dayside merging and cusp geometry, J. Geophys. Res., 84, 951-959, 1979.

Crooker, N. U., The half-wave rectifier response of the magnetosphere and antiparallel merging, J. Geophys. Res., 85, 575-578, 1980.

Crooker, N. U., J. Berchem, and C. T. Russell, Cusp displacement at the magnetopause for large IMF Y component, J. Geophys. Res., 92, 13467-13471, 1987.

Delcourt, D. C., B. L. Giles, C. R. Chappell, and T. E. Moore, Low-energy bouncing ions in the magnetosphere: a three-dimensional numerical study of Dynamics Explorer 1 data, J. Geophys. Res., 93, 1859-1870, 1988.

Dungey, J. W., Interplanetary magnetic field and the auroral zones, Phys. Rev. Lett., 6, 47-48, 1961.

Eastman, T. E., B. Popielawska, and L. A. Frank, Three-dimensional plasma observations near the outer magnetospheric boundary, J. Geophys. Res., 89, 9519-9539, 1984.

Fairfield, D. H., and J. D. Scudder, Polar rain: solar coronal electrons in the Earth's magnetosphere, J. Geophys. Res., 90, 4055-4068, 1985.

Formisano, V., HEOS-2 observations of the boundary layer from the magnetopause to the ionosphere, Planet. Space Sci., 28, 245-257, 1980.

Foster, J. C., and J. R. Burrows, Electron fluxes over the polar cap 2. Electron trapping and energization on open field lines, J. Geophys. Res., 82, 5165-5170, 1977.

Foster, J. C., J. M. Holt, R. G. Musgrove, and D. S. Evans, Solar wind dependencies of high-latitude convection and precipitation, Solar Wind-Magnetosphere Coupling, Y. Kamide and J. A. Slavin ed., 477-494, 1986.

Frahm, R. A., P. H. Reiff, J. D. Winningham, and J. L. Burch, Banded ion morphology: main and recovery storm phases, in Ion Acceleration in the Magnetosphere and Ionosphere, ed. by Tom Chang, pp. 98-107, American Geophysical Union, Washington, D. C., 1986.

Fraser, B. J., Observations of Ion Cyclotron Waves Near Synchronous Orbit and on the Ground, Space Science Reviews, 42, 357, 1985.

Fraser, B. J., and R. L. McPherron, Pc 1-2 Magnetic Pulsation Spectra and Heavy Ion Effects at Synchronous Orbit: ATS 6 Results, J. Geophys. Res., 87, 4560, 1982.

Friis-Christiansen, E., M. A. McHenry, C. R. Clauer, and S. Vennerstrom, Ionospheric traveling convection vortices observed near the polar cleft: a triggered response to sudden changes in the solar wind, Geophys. Res. Lett., 15, 253-256, 1988.

Galperin, Y. I., and Y. I. Feldstein, Auroral Luminosity and Its Relationship to Magnetospheric Plasma Domains, in Meng, Rycroft, and Frank ed., Auroral Physics, Cambridge University Press, In Press, 1990.

Goertz, C. K., and R. W. Boswell, Magnetosphere-Ionosphere Coupling, J. Geophys. Res., 84, 7239, 1979.

Gussenhoven, M. S., Low-altitude convection, precipitation, and current patterns in the baseline magnetosphere, Rev. Geophys., 26, 792-808, 1989.

Heikila, W. J., Definition of the cusp, in The Polar Cusp, J. A. Holtet, and A. Egeland, ed., 387-395, D. Reidel Publishing, Boston, 1985.

Heelis, R. A., The effects of interplanetary magnetic field orientation on dayside high-latitude ionospheric convection, J. Geophys. Res., 89, 2873-2880, 1984.

Heppner, J. P., and N. C. Maynard, Empirical high-latitude electric field models, J. Geophys. Res., 92, 4467-4489, 1987.

Hill, T. W., and P. H. Reiff, Evidence of magnetospheric cusp proton acceleration by magnetic merging at the dayside magnetopause, J. Geophys. Res., 82, 3623-3628, 1977.

Hones, E. W., J. D. Craven, L. A. Frank, D. S. Evans, and P. T. Newell, The horse collar aurora: A frequent pattern of the aurora in quiet times, Geophys. Res. Lett., 16, 37-40, 1989.

Horwitz, J. L., S. Menteer, J. Turnley, J. L. Burch, J. D. Winningham, C. R. Chappell, J. D. Craven, L. A. Frank, and D. W. Slater, Plasma boundaries in the inner magnetosphere, J. Geophys. Res., 91, 8861-8882, 1986.

Hughes, W. J., and S. W. H. Cowley, Observation of IMF-associated magnetic field perturbations in the GSM X component at geostationary orbit, in Solar Wind-Magnetosphere Coupling, 691-695, Y. Kamide and J. A. Slavin editors, 1986.

Iijima, T., R. Fuji, T. A. Potemra, and N. A. Saflekos, Field-aligned currents in the south polar cusp and their relationship to the interplanetary magnetic field, J. Geophys. Res., 83, 5595-5603, 1978.

Kan, J. R., Energization of Auroral Electrons by Electrostatic Shock Waves, J. Geophys. Res., 80, 2089, 1975.

Kan, J. R., L. Zhu, and S.-I. Akasofu, A Theory of Substorms: Onset and Subsidence, J. Geophys. Res., 93, 5624, 1988.

Kan, J. R., and W. Sun, Simulation of the Westward Traveling Surge and Pi 2 Pulsations During Substorms, J. Geophys. Res., 90 (10), 911, 1985.

Kaye, S. M., E. G. Shelley, R. D. Sharp, and R. G. Johnson, Ion Composition of Zipper Events, J. Geophys. Res., 86, 3393, 1981.

Kelly, T. J., C. T. Russell, and R. J. Walker, ISEE-1 and -2 Observations of an Oscillating Outward Moving Current Sheet Near Midnight, J. Geophys. Res., 89, 2745, 1984.

Klumpar, D. M., J. M. Quinn, and E. G. Shelley, Counter-Streaming Electrons at the Geomagnetic Equator Near 9 R_E, Geophys. Res. Lett., 15, 1295, 1988.

Kremser, G., A. Korth, L. Ullaland, S. Perraut, A. Roux, A. Pedersen, R. Schmidt, and P. Tanskanen, Field-Aligned Beams of Energetic Electrons (16 keV < E < 80 keV) Observed at Geosynchronous Orbit at Substorm Onset, J. Geophys. Res., 93, 14453, 1988.

Lanzerotti, L. J., L. C. Lee, C. G. Maclennan, A. Wolfe, and L. V. Medford, Possible evidence of flux transfer events in the polar ionosphere, Geophys. Res. Lett., 13, 1089-1092, 1986.

Lassen, K. C. Danielsen, and C.-I. Meng, Quiet-time average auroral configuration, Planet. Space Sci., 36, 791, 1988.

24

Lee, J. M., P. T. Newell, and C.-I. Meng, Observations of accelerated ions at the equatorward edge of the low altitude cusp, Eos, 70, p. 432 (abstract), 1989.

Lee, L. C., and J. R. Kan, Auroral Double Layers, Physics of Auroral Arc Formation, Geophysical Monograph 25, 245, American Geophysical Union, Washington, DC, 1981.

Levy, R. H., H. E. Petschek, and G. L. Siscoe, Aerodynamic aspects of magnetospheric flow, AIAA J., 2, 2065, 1964.

Lockwood, M. and M. F. Smith, Low-altitude signatures of the cusp and flux transfer events, Geophys. Res. Lett., 16, 879-882, 1989.

Lopez, R. E., A. T. Y. Lui, D. G. Sibeck, K. Takahashi, R. W. McEntire, L. J. Zanetti, and S. M. Krimigis, On the Relationship Between the Energetic Particle Flux Morphology and the Change in the Magnetic Field Magnitude During Substorms, J. Geophys. Res., In Press, 1988.

Lui, A. T. Y., R. E. Lopez, S. M. Krimigis, R. W. McEntire, L. J. Zanetti, and T. A. Potemra, A Case Study of a Magnetotail Current Disruption and Diversion," Geophys. Res. Lett., 15, 721, 1988.

Lyons, L. R., A simple model for polar cap convection patterns and generation of θ auroras, J. Geophys. Res., 90, 1561-1567, 1985.

Lyons, L. R., and D. S. Evans, An Association Between Discrete Aurora and Energetic Particle Boundaries, J. Geophys. Res., 89, 2395, 1984.

Lyons, L. R., J. F. Fennell, and A. L. Vampola, A General Association Between Discrete Auroras and Ion Precipitation from the Tail, J. Geophys. Res., 93, 12932, 1988.

Lyons, L. R., and T. W. Speiser, Evidence for Current Sheet Acceleration in the Geomagnetic Tail, J. Geophys. Res., 87, 2276, 1982.

Lyons, L. R., Electron Energization in the Geomagnetic Tail Current Sheet, J. Geophys. Res., 89, 5479, 1984.

Lyons, L. R., Processes Associated With Plasma Sheet Boundary Layer, Physica Scripta, T18, 103, 1987.

Lysak, R. L., and C. T. Dunn, Dynamics of Magnetosphere-Ionosphere Coupling Including Turbulent Transport, J. Geophys. Res., 88, 365, 1983.

Lundin, R., Acceleration/heating of plasma on auroral field lines: preliminary results from the Viking satellite, Annales Geophysicae, 6, 143-152, 1988.

Makita, K., and C.-I. Meng, Average electron precipitation patterns and visual aurora characteristics during geomagnetic quiescence, J. Geophys. Res., 89, 2861-2872, 1984.

Makita, K, and C.-I. Meng, Long-period polar rain variations, solar wind and hemispherically symmetric polar rain, J. Geophys. Res., 92, 7381-7393, 1987.

Martin, R. F., Jr., "The Effect of Plasma Sheet Thickness on Ion Acceleration Near a Magnetic Neutral Line, Ion Acceleration in the Magnetosphere and Ionosphere, Geophys. Monog. Ser., 38, edited by T. Chang, 141, AGU, Washington, DC, 1986.

Mauk, B. H., and C. E. McIlwain, UCSD Auroral Particles Experiment,: IEEE Trans. Aerosp. Electron. Syst., AES11, 1125, 1975.

Mauk, B. H., and R. L. McPherron, An Experimental Test of the Electromagnetic Ion Cyclotron Instability Within the Earth's Magnetosphere, Phys. Fluids, 23, 2111, 1980.

Mauk, B. H., C. E. McIlwain, and R. L. McPherron, Helium Cyclotron Resonance Within the Earth's Magnetosphere, Geophys. Res. Lett., 8, 103, 1981.

Mauk, B. H., J. Chin, and G. Parks, Auroral X-Ray Images, J. Geophys. Res., 86, 6827, 1981.

Mauk, B. H., Helium Resonance and Dispersion Effects on Geostationary Alfven/Ion Cyclotron Waves, J. Geophys. Res., 87, 9107, 1982b.

Mauk, B. H., Frequency Gap Formation in Electromagnetic Cyclotron Wave Distributions, Geophys. Res. Lett., 10, 635, 1983.

Mauk, B. H., and C. I. Meng, Dynamical injections as the source of near geostationary quiet time particle spatial boundaries, J. Geophys. Res., 88, 10011-10024, 1983.

Mauk, B. H., Quantitative Modeling of the 'Convection Surge' Mechanism of Ion Acceleration, J. Geophys. Res., 91, 3423, 1986.

Mauk, B. H., and C.-I. Meng, Plasma Injection During Substorms, Phys. Script., T18, 128, 1987.

Mauk, B. H., and C.-I. Meng, Macroscopic Magnetospheric Particle Acceleration, Solar System Plasma Physics; Geophysical Monograph, 54, 319, American Geophysical Union, Washington, DC, 1988.

Mauk, B. H., Generation of Macroscopic Magnetic-Field-Aligned Electric Fields by the Convection-Surge Ion Acceleration Mechanism, J. Geophys. Res., 94, 8911, 1989.

Mauk, B. H., and C.-I. Meng, The Aurora and Middle Magnetospheric Processes, Auroral Physics, Cambridge University Press, Cambridge, U.K., In Press, 1990.

McIlwain, C. E., Auroral Electron Beams Near the Magnetic Equator, The Physics of Hot Plasma in the Magnetosphere, B. Hultqvist and L. Stenflo, eds., Plenum, New York, 91, 1975.

McPherron, R. L., P. J. Coleman and R. C. Snare, ATS-6: UCLA Fluxgate Magnetometer, IEEE Trans. Aerospace and Electronic Systems, AES-11, 1110, 1975.

Mead, G. D., and D. B. Beard, Shape of the geomagnetic field solar wind boundary, J. Geophys. Res., 69, 1169-1179, 1964.

Mead, G. D., and D. H. Fairfield, A quantitative magnetospheric model derived from spacecraft magnetometer data, J. Geophys. Res., 80, 523-534, 1975.

Meng, C.-I., and K.A. Anderson, Magnetic field configuration in the magnetotail near 60 R_e, J. Geophys. Res., 79, 5143-5153, 1974.

Meng, C.-I., A.T.Y. Lui, S.M. Krimigis, S. Ismail, and D.J. Williams, Spatial distribution of energetic particles in the distant magnetotail, J. Geophys. Res., 86, 5682-5700, 1981.

Meng, C.-I., Latitudinal variation of the polar cusp during a geomagnetic storm, Geophys. Res. Lett., 9, 60-63, 1982.

Meng, C.-I., and R. Lundin, Auroral morphology of the midday oval, J. Geophys. Res., 91, 1572-1584, 1986.

Meng, C.-I., B. H. Mauk, and C. E. McIlwain, Electron Precipitation of Evening Diffuse Aurora and Its Conjugate Electron Fluxes Near the Magnetospheric Equator, J. Geophys. Res., 84, 2545, 1979.

Menietti, J. D., and J. L. Burch, Spatial extent of the plasma injection region in the cusp-magnetosheath interface, J. Geophys. Research, 93, 105-113, 1988.

Midgley, J. E., and L. Davis, Calculation by a moment technique of the perturbation of the geomagnetic field by the solar wind, J. Geophys. Res., 68, 5111-5123, 1963.

Nagai, T., Observed Magnetic Substorm Signatures at Synchronous Orbit, J. Geophys. Res., 87, 4405, 1982.

Newell, P. T., and C.-I. Meng, Energy dependence of the equatorward cutoffs in auroral electron and ion precipitation, J. Geophys. Res., 92, 7519-7530, 1987.

Newell, P. T., and C.-I. Meng, Low altitude observations of dispersionless substorm plasma injections, J. Geophys. Res., 92, 10063-10072, 1987.

Newell, P. T., and C.-I. Meng, The cusp and the cleft/LLBL: Low altitude identification and statistical local time variation, J. Geophys. Res., 93, 14549-14556, 1988a.

Newell, P. T., and C.-I. Meng, Hemispherical asymmetry in cusp precipitation near solstices, J. Geophys. Res., 93, 2643-2648, 1988b.

Newell, P. T., and C.-I. Meng, An event of distinct ion polar rain, Geophys. Res. Lett., 15, 1165-1168, 1988c.

Newell, P. T., and C.-I. Meng, Categorization of dispersion curves in the equatorward edge of the diffuse aurora, Planet. Space Sci., 36, 1031-1038, 1988d.

Newell, P. T., and C.-I. Meng, Dipole tilt angle effects on the latitude of the cusp and cleft/LLBL, J. Geophys. Res., 94, 6949-6953, 1989a.

Newell, P. T., and C.-I. Meng, On quantifying the distinctions between the cusp and the cleft/LLBL, in Electromagnetic Coupling in the Polar Clefts and Caps, ed. P. E. Sandholt and A. Egeland, Kluwer Academic Publishers, Dordrecht, 1989b.

Newell, P. T., Comment on "Low-altitude signatures of the cusp and flux transfer events" by Lockwood and Smith, accepted for publication in Geophys. Res. Lett., 17, 303-304, 1990.

Norris, A. J., J. F. E. Johnson, J. J. Sojka, C. L. Wrenn, N.{LS}Cornilleau-Wehrlin, S. Perraut, and A. Roux, Experimental Evidence For the Acceleration of Thermal Electrons by Ion Cyclotron Waves in the Magnetosphere, J. Geophys. Res., 89, 889-898, 1983.

Propp, K., and D. B. Beard, Cross-Tail Ion Drift in a Realistic Model Magnetotail, J. Geophys. Res., 89, 11013, 1984.

Quinn, J. M. and C. E. McIlwain, Bouncing Ion Clusters in the Earth's Magnetosphere, J. Geophys. Res., 84, 7365, 1979.

Quinn, J. M., Ion Bounce-Phase-Clusters in the Earth's Nightside Magnetosphere, PhD Dissertation, Dept. of Physics, University of California at San Diego, La Jolla, CA, 1981.

Quinn, J. M., and D. J. Southwood, Observations of Parallel Ion Energization in the Equatorial Region, J. Geophys. Res., 87, 10536, 1982.

Rijnbeek, R. P., S. W. H. Cowley, D. J. Southwood, and C. T. Russell, A survey of dayside flux transfer events observed by ISEE 1 and 2 magnetometers, J. Geophys. Res., 89, 786-800, 1984.

Robert, P., R. Gendrin, S. Perraut, A. Roux, and A. J. Pedersen, Geos 2 Identification of Rapidly Moving Current Structures in the Equatorial Outer Magnetosphere During Substorms, J. Geophys. Res., 89, 819, 1984.

Rothwell, P. L., L. P. Block, M. B. Silevitch, and C.-G. Falthammar, A New Model for Substorm Onsets: The Pre-Breakup and Triggering Regimes, Geophys. Res. Lett., 15, 1279, 1988.

Roux, A., N. Cornilleau-Wehrlin, and J. L. Rauch, Acceleration of Thermal Electrons by ICW's Propagating in a Multicomponent Magnetospheric Plasma, J. Geophys. Res., 89, 2267-2273, 1984.

Roux, A., Generation of Field-Aligned Current Structures at Substorm Onset, Proc. ESA Workshop on Future Missions in Solar, Heliospheric and Space Plasma Physics, 151-159, 1985.

Sanchez, E. R., PhD Dissertation, UCLA, Department of Atmospheric Sciences, 1989.

Sanchez, E. R., G. L. Siscoe, J. T. Gosling, E. W. Hones, Jr., and R. P. Lepping, Observations of rotational discontinuity-slow expansion fan structure of the magnetotail boundary, J. Geophys. Res., 95, 61-74, 1990a.

Sanchez, E. R., D. Summers, and G. L. Siscoe, Downstream evolution of an open magnetotail boundary, J. Geophys. Res., in press, 1990b.

Sanchez, E. R., and G. L. Siscoe, IMP 8 magnetotail boundary crossings: a test of the MHD models for an open magnetotail boundary, submitted to J. Geophys. Res., 1990c.

Sandholt, P. E., B. Lybekk, A. Egeland, R. Nakamura, and T. Oguti, Midday auroral breakup, submitted to J. Geomag. Geoelect., 1988.

Sauvaud, J. A., J. Crasnier, K. Mouala, R. A. Kovrazhkin, and N. V. Jorjio, Morning sector ion precipitation following substorm injections, J. Geophys. Res., 86, 3430-3438, 1981.

Sauvaud, J. A., J. M. Bosqued, R. A. Kovrazhkin, D. Delcourt, J. J. Berthelier, F. Lefeuvre, J. L. Rauch, Yu. I. Galperin, M. M. Mogilevsky, and E. E. Titova, Positive ion distributions in the morning auroral zone: local acceleration and drift effects, Adv. Space Res., 5, 73-77, 1985.

Sauvaud, J. A., and D. Delcourt, A numerical study of suprathermal ionospheric ion trajectories in three-dimensional electric and magnetic field models, J. Geophys. Res., 92, 5873-5884, 1987.

Sckopke, N., G. Paschmann, G. Haerendel, B. U. O. Sonnerup, S. J. Bame, T. G. Forbes, E. W. Hones, and C. T. Russell, Structure of the low-latitude boundary layer, J. Geophys. Res., 86, 2099-2110, 1981.

Sibeck, D. G., W. Baumjohann, and R. E. Lopez, Solar wind dynamic pressure variations and transient magnetospheric signatures, Geophys. Res. Lett., 16, 13-16, 1989.

Siscoe, G. L., and E. R. Sanchez, An MHD model for the complete open magnetotail boundary, J. Geophys. Res., 92, 7405-7411, 1987.

Siscoe, G. L., Meeting Reports: Auroral Physics, A Chapman Memorial, Eos Tran. AGU, 69, 1596, 1988.

Sonnerup, B. U. O., Adiabatic Particle Orbits in a Magnetic Null Sheet, J. Geophys. Res., 76, 8211, 1971.

Speiser, T. W., Particle Trajectories in Model Current Sheets, 1, Analytical Solutions, J. Geophys. Res., 70, 4219, 1965.

Speiser, T. W., Particle Trajectories in Model Current Sheets, 2, Applications to Auroras Using a Geomagnetic Tail Model, J. Geophys. Res., 72, 3919, 1967.

Speiser, T. W., Conductivity Without Collisions or Noise, Planet. Space Sci., 8, 613, 1970.

Speiser, T. W., Processes in the Magnetotail Neutral Sheet, Physica Scripta, T18, 119, 1987.

Spreiter, J. R., and S. S. Stahara, A new predictive model for determining solar wind-terrestrial planet interactions, J. Geophys. Res., 85, 6769-6777, 1980.

Stenzel, R. L., M. Ooyama, and Y. Nakamura, Potential Double-Layers in Strongly Magnetized Plasmas, Physics of Auroral Arc Formation Geophysical Monograph, 25, S.-I. Akasofu and J. R. Kan, eds., American Geophysical Union, Washington, DC, 226, 1981.

Stix, T. H., The Theory of Plasma Waves, McGraw-Hill, New York, 1962.

Svalgaard, L., Polar cap magnetic variations and their relationship with the interplanetary sector structure, J Geophys. Res., 78, 2064, 1973.

Swift, D. W., and L. C. Lee, The magnetotail boundary layer and energy transfer, Geophys. Res. Lett., 9, 527-530, 1982.

Swift, D. W., and L. C. Lee, Rotational Discontinuities and the structure of the magnetopause, J. Geophys. Res., 88, 111-124, 1983.

Tsyganenko, N. A., and A. V. Usmanov, Determination of the magnetospheric current system parameters and development of experimental geomagnetic field models based on data from IMP and Heos satellites, Planet. Space Sci., 36, 985-998, 1982.

Vasyliunas, V. M., Theoretical models of magnetic field line merging, 1, Rev. Geophys. Space Phys., 13, 303-336, 1975.

Vasyliunas, V. M., Interaction between the magnetospheric boundary layers and the ionosphere, Proceedings of Magnetosphere Boundary Layers Conference, Alpbach, 11-15 June, 1979, Eur. Space Agency Spec Publ., ESA SP-148, Aug., 1979.

Voigt, G.-H., Calculation of the shape and position of the last closed field line boundary and the coordinates of the magnetopause neutral points in a theoretical magnetospheric field model, J. Geophys. 40, 213-228, 1974.

29

Whipple, E. C., T. G. Northrop, and T. J. Birmingham, Adiabatic Theory in Regions of Strong Field Gradients, Geophys. Res., 91, 4149, 1986.

Winningham, J. D., and W. J. Heikkila, Polar cap auroral electron fluxes observed with Isis 1, J. Geophys. Res., 79, 949-957, 1974.

Winningham, J. D., J. L. Burch, and R. A. Frahm, Bands of ions and angular V's: a conjugate manifestation of ionospheric ion acceleration, J. Geophys. Res., 89, 1749-1754, 1984.

Yang, C. K., and B. U. O. Sonnerup, Compressible magnetic field reconnection: a slow wave model, Astrophys. J., 206, 570, 1976.

Yang, C. K., and B. U. O. Sonnerup, Compressible magnetopause reconnection, J. Geophys. Res., 82, 699-703, 1977.

9.0   FIGURES
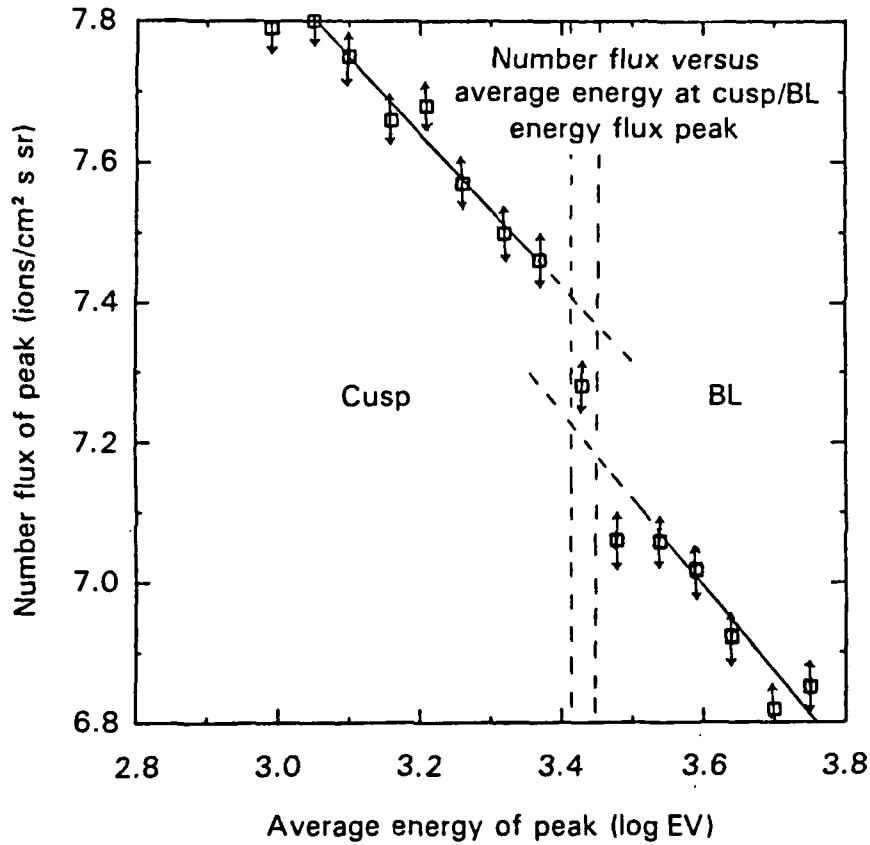
Figure 2.1   For each of 12569 dayside DMSP F7 passes, the point of peak ion energy flux was recorded irrespective of region type (cusp or boundary layer) and binned by average energy.   Plotted is the average number flux versus log energy bin.   The lower average energy passes have higher number fluxes; the clear break that occurs at about 3000 eV corresponds to the transition between regions that we classify as cusp and those that are classified as boundary layer.
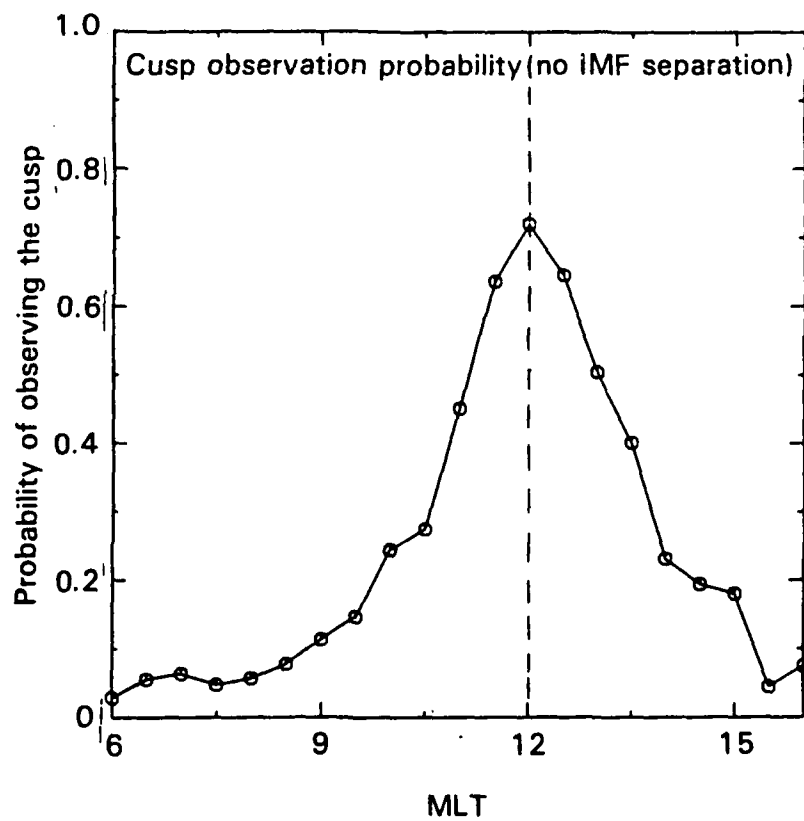
Figure 2.2   The probability as a function of MLT (in half hour bins) of observing the cusp on a given DMSP F7 dayside pass.
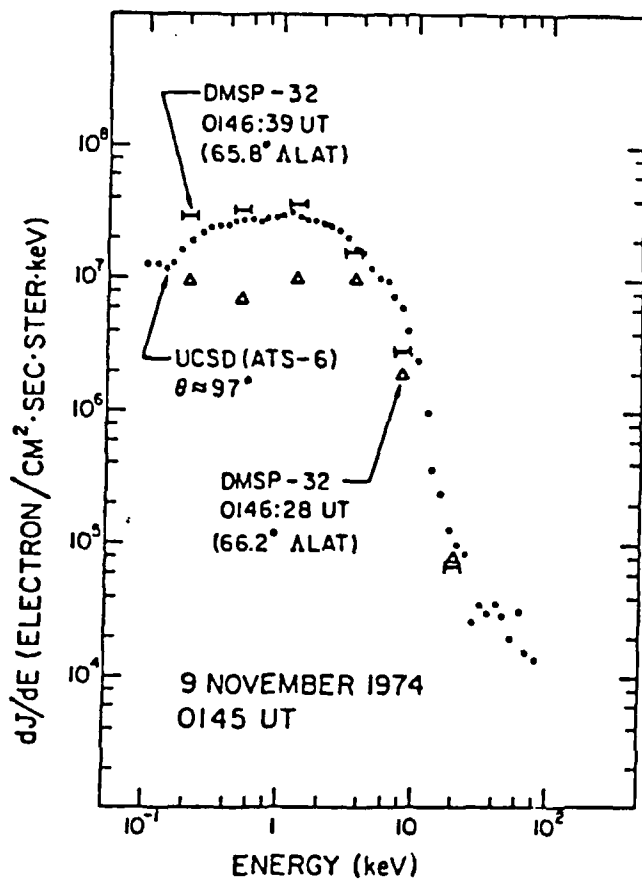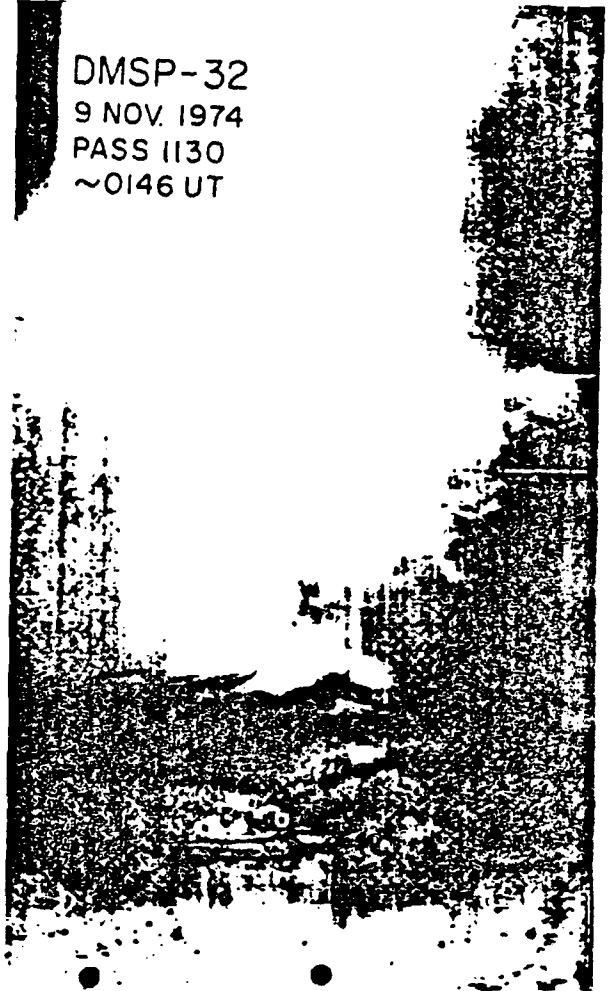
A coordinated observation between the plasma sheet electrons at geosynchronous orbit (ATS 6) and the auroral display and electron precipitation near its field-line conjugate observed by the DMSP 32 satellite with a circle for the calculated ATS 6 foot point.

Figure 4.1

10. <u>GRANT SUPPORTED PUBLICATIONS (1987-1990)</u>

1. Candidi, M., and C.-I. Meng, Low-altitude observations of the conjugate polar cusps, <u>J. Geophys. Res.</u>, <u>93</u>, 923-931, 1988.
2. Candidi, M., G. Mastrantonio, S. Orsini, and C.-I. Meng, Evidence of the influence of the interplanetary magnetic field azimuthal component on polar cusp configuration, <u>J. Geophys. Res.</u>, <u>94</u>, 13585-13591, 1989.
3. Carbary, J. F., and C.-I. Meng, Correlation of cusp width with AE(12) and B_z, <u>Planet. Space Sci.</u>, <u>36</u>, 157-161, 1988.
4. Engebretson, B. J. Anderson, L. J. Cahill, R. L. Arnoldy, P. T. Newell, C.-I. Meng, L. J. Zanetti, and T. A. Potemra, A multi-point case study of high-latitude daytime ULF pulsations, <u>J. Geophys. Res.</u>, <u>94</u>, 17143-17160, 1989.
5. Hones, E. W. Jr., J. D. Craven, L. A. Frank, D. S. Evans, and P. T. Newell, The horse-collar aurora: a frequent pattern of the aurora in quiet times, <u>Geophys Res. Lett.</u>, <u>16</u>, 37-40, 1989.
6. Lassen, K., C. Danielsen, and C.-I. Meng, Quiet-time average auroral configuration, <u>Planet. Space Sci.</u>, <u>36</u>, 791-799, 1988.
7. Lopez, R. E., H. Luhr, B. J. Anderson, P. T. Newell, and R. W. McEntire, <u>J. Geophys. Res.</u>,
7. Makita, K, and C.-I. Meng, Long-period polar rain variations, solar wind and hemispherically symmetric polar rain, <u>J. Geophys. Res.</u>, <u>92</u>, 7381-7393, 1987.
8. Makita, K., C.-I. Meng, and S.-I. Akasofu, Latitudinal electron precipitation patterns during large and small IMF magnitudes for northward IMF conditions, <u>J. Geophys. Res.</u>, <u>93</u>, 97-104, 1988.
9. Mauk, B. H., and C.-I. Meng, Plasma injections during substorms, <u>Phys. Script.</u>, T18, 128, 1987.
10. Mauk, B. H., Generation of macroscopic magnetic-field-aligned electric fields by the convection surge ion acceleration mechanism, <u>J. Geophys. Res.</u>, <u>94</u>, 8911-8920, 1989.
11. Mauk, B. H., and C.-I. Meng, Macroscopic magnetospheric particle acceleration, in <u>Solar System Plasma Physics</u> ed. by J. H. Waite and J. L. Burch, AGU monograph 54, 1988.
12. Mauk, B. H., and C.-I. Meng, The aurora and middle magnetospheric processes, in <u>Auroral Physics</u>, July, 1988, C.-I. Meng (ed), Cambridge University Press, Cambridge, England, 1989.
13. McHenry, M., C. R. Clauer, E. Friis-Christinsen, P. T. Newell, and J. D. Kelley, Ground observations of magnetospheric boundary layer phenomena, <u>J. Geophys. Res.</u>, <u>95</u>, 14995-15005, 1990.
14. Meng, C.-I., Auroral oval configuration during the quiet condition, <u>Electromagnetic Coupling in the Polar Clefts and Caps</u>, P. E. Sandholt and A. Egeland eds., D. Reidel Publishers, Dordrecht, 1989.

15. Menk, F. W., B. J. Fraser, H. J. Hansen, P. T. Newell, C.-I. Meng, and R. J. Morris, Multistation observations of Pc1-2 ULF pulsations between the plasmapause and polar cap, submitted to J. Geophys. Res., 1990.

16. Newell, P. T., and C.-I. Meng, Energy dependence of the equatorward cutoffs in auroral electron and ion precipitation, J. Geophys. Res., 92, 7519-7530, 1987.

17. Newell, P. T., and C.-I. Meng, Low altitude observations of dispersionless substorm plasma injections, J. Geophys. Res., 92, 10063-10072, 1987.

18. Newell, P. T., and C.-I. Meng, Cusp width and B_z: Observations and a conceptual model, J. Geophys. Res., 92, 13673-13678, 1987.

19. Newell, P. T., and C-I. Meng, Hemispherical asymmetry in cusp precipitation near solstices, J. Geophys. Res., 93, 2643-2648, 1988.

20. Newell, P. T., and C-I. Meng, An event of distinct ion polar rain, Geophys. Res. Lett., 15, 1165-1168, 1988.

21. Newell, P. T., and C.-I. Meng, Categorization of dispersion curves in the equatorward edge of the diffuse aurora, Planet. Space Sci., 36, 1031-1038, 1988.

22. Newell, P. T., and C.-I. Meng, The cusp and the cleft/boundary layer: Low-altitude identification and statistical local time variation, J. Geophys. Res., 93, 14549-14556, 1988.

23. Newell, P. T., and C.-I. Meng, Dipole tilt angle effects on the latitude of the cusp and cleft/LLBL, J. Geophys. Res., 94, 6949-6953, 1989.

24. Newell, P. T., C.-I. Meng, D. G. Sibeck, and R. Lepping, Some low altitude cusp dependencies on the interplanetary magnetic field, J. Geophys. Res., 94, 8921-8927, 1989.

25. Newell, P. T., C-I. Meng, On quantifying the distinction between the cusp and the cleft/boundary layer, Electromagnetic Coupling in the Polar Cleft and Caps, P. E. Sandholt and A. Egeland eds., D. Reidel Publishers, Dordrecht, 1989.

26. Newell, P. T., C.-I. Meng, and D. A. Hardy, Overview of statistical global electron and ion auroral precipitation, Auroral Physics, ed. by Meng, Rycroft and Frank, Cambridge University Press, Cambridge, England, 1990.

27. Newell, P. T., Comment on "Low altitude signatures of the cusp and flux transfer events" by Lockwood and Smith, Geophys. Res. Lett., 17, 303-304, 1990.

28. Newell, P. T., and C.-I. Meng, Intense keV polar rain, J. Geophys. Res., 13, 7869-7879, 1990.

29. Newell, P. T., W. J. Burke, C.-I. Meng, E. R. Sanchez, M. E. Greenspan, and C.-I. Meng, Identification and observations of the plasma mantle at low altitude, J. Geophys. Res., 96, 35-45, 1991.

30. Newell, P. T., S. Wing, C.-I. Meng, and V. Sigillito, A neural-network based system for monitoring the aurora, Johns Hopkins Univ. APL Technical Digest, 11, 291-299, 1990.

33

31 Ono, T., T. Hirasawa, and C.-I. Meng, Proton auroras observed at the equatorward edge of the duskside auroral oval, Geophys. Res. Lett., 14, 660-663, 1987.

32. Ono, T. T. Hirasawa, and C.-I. Meng, Weak auroral emissions and particle precipitations in the dusk auroral oval, J. Geophys. Res., 94, 11933-11947, 1989.

33. Ruohoniemi, J. M., R. A. Greenwald, J.-P. Villain, K. B. Baker, P. T. Newell, and C.-I. Meng, Coherent HF radar backscatter from small-scale irregularities in the dusk sector of the subauroral ionosphere, J. Geophys. Res., 93, 12871-12882, 1988.

34. Sanchez, E. R., and G. L. Siscoe, IMP 8 magnetotail boundary crossings: a test of the MHD models for an open magnetotail boundary, J. Geophys. Res. 95, 20771-20779, 1990.

35. Sanchez, E. R., D. Summers, C L. Siscoe, Downstream evolution of an open MHD magnetotail boundary, J. Geophys. Res., 95, 20743-20758, 1990.

36. Sandholt, P. E., B. Jacobsen, B. Lybekk, A. Egeland, C.-I. Meng, P. T. Newell, F. J. Rich, and E. J. Weber, Structure and dynamics in the polar cleft: coordinated satellite and ground-based observations in the prenoon sector, J. Geophys. Res., 94, 8928-8942, 1989.

37. P. E. Sandholt, B. Jacobsen, B. Lybekk, A. Egeland, C.-I. Meng, P. T. Newell, F. J. Rich, and E. J. Weber, Polar cleft structure at 09 MLT: Coordinated satellite and ground based observations, in Electromagnetic Coupling in the Polar Clefts and Caps, P. E. Sandholt and A. Egeland eds., D. Reidel Publisher, Dordrecht, 1989.

Selected Preprints

The Cusp and the Cleft/Boundary Layer: Low-Altitude Identification and Statistical Local Time Variation

PATRICK T. NEWELL AND CHING-I. MENG

The Johns Hopkins University Applied Physics Laboratory, Laurel, Maryland

Particles of roughly magnetosheath energies precipitate at low altitudes throughout the dayside, in a band referred to as the cusp or cleft. Recently it has been suggested that the cusp proper is a more limited region of the cleft localized near noon, although the criteria for distinguishing between the two regions have been unclear. An investigation into the distinction between the low-altitude cusp and the cleft (with the latter herein identified as the ionospheric signature of the low-latitude boundary layer (LLBL)) was performed on both a statistical and a case study basis. One year of DMSP F7 electron and ion data, comprising in all 5609 individual dayside passes, was employed. It was found that the average energy of precipitating particles allows for a clear morphological distinction between the cusp proper and the cleft/LLBL. Often both regions are observed on a given pass at the same MLT, each with its own characteristic properties. The probability of observing the cusp was found to be sharply peaked at 1200 MLT, while the probability of observing the cleft/LLBL was near unity away from noon and had a minimum at noon. The cusp was found to be 0.8°–1.1° magnetic latitude (MLAT) thick essentially independent of MLT, whereas the cleft was thinnest at noon and widened rapidly at local times away from noon. The ion number flux in the cusp was statistically 3.6 times higher than in the cleft. The peak flux within the cusp was located on average closer to the equatorward than to the poleward boundary. Yearly average composite spectrograms of precipitation in the two regions as a function of local time show that the properties of the cusp change comparatively little with local time, but that the peak ion energy flux in the cleft increases smoothly from roughly magnetosheath values close to noon to about plasma sheet boundary layer values near 0600 MLT.

1. HISTORICAL BACKGROUND ON "CUSP" IDENTIFICATION

Almost two decades ago, *Heikkila and Winningham* [1971] reported on low-altitude observations of electrons and ions of approximately magnetosheathlike character which precipitate in a wide band across the dayside, extending further than 0800 to 1600 MLT, and having a latitudinal width of a few degrees. They found that the equatorward boundary of this "cusp" precipitation could be determined by a sharp drop in the keV dayside electron plasma sheet precipitation. They reported that the electron count rates (which for electrostatic analyzers are proportional to differential energy flux) had a peak at 100 to 200 eV, while the ion differential number flux spectrum peaked at about 300 eV, with a total number flux of about 10^7 ions/cm^2 s sr.

At nearly the same time, *Frank* [1971] reported similar results at mid-altitudes. The cusp again was a wide band, essentially covering the dayside. Frank reported the ion number flux peaked at about 900 eV, with about the same total number flux as reported above. The spectral shape of the low-altitude ion cusp precipitation matched that in the magnetosheath, except that at low energies (below about 500 eV) the "cusp" had fewer ions than in the magnetosheath. Hence the cusp ions were unaccelerated (i.e., the peak is unchanged), but the average kinetic energy was higher than in the sheath, since fewer low-energy ions were present.

Burrows et al. [1972] and *McDiarmid et al.* [1976] have argued that part of the "cusp" (as defined above) lies on closed field lines, because energetic electrons, ordinarily greatly reduced in intensity, extend into the cusp, sometimes with a pitch angle distribution peaked at 90°. Most workers would agree that at times roughly magnetosheathlike plasma can be seen in the dayside on closed field lines. However, in view of recent results on the ease with

which magnetospheric plasma escapes into the sheath [e.g., *Lundin*, 1987; *Sibeck et al.*, 1987; *Williams et al.*, 1988] one should not be surprised to sometimes observe magnetospheric particles in the cusp, particularly at reduced intensities. Moreover, because of the magnetic mirroring effect, it is hard to understand why such particles when observed at low altitude are not more often peaked at 90°. One should thus be quite cautious in using the presence, especially at greatly reduced intensity, of energetic magnetospheric particles as a diagnostic of the open or closed nature of field lines.

Formisano [1980], using HEOS 2 electron data, sought to distinguish between the boundary layer and the region of more direct cusp entry. The HEOS 2 spectra contained only six points and were presented in "arbitrary units," but are of particular note because the same spacecraft and detector made sheath/boundary layer crossings both in the external magnetosphere and in the mid-altitude cusp. Both types of spectra are extremely easy to distinguish from plasma sheet (or radiation belt) populations, but the low-latitude boundary layer (LLBL) electrons are slightly more energetic than the sheath electrons, both in the external magnetosphere and in the cusp. Thus a distinction could be made between the cusp proper and the (still approximately magnetosheathlike) low-altitude signature of the LLBL. However, Formisano's cusp, although latitudinally narrower, still seemed very widespread in local time.

For many years the terms "cusp" and "cleft" were used interchangeably, with traditionalists arguing for the former and proponents of the latter arguing that it was a more apt description of the wide local time region of roughly magnetosheathlike particle entry. More recently there has been a tendency to consider the cusp to be a subset of the cleft, both in latitude and, especially, in local time, with the cusp confined closer to noon. *Heikkila* [1985] has offered the following definition (which he states is mostly due to G. Shepherd):

The cleft is the low altitude region around noon of about 100 eV electron precipitation associated with 6300 Å emission, but con-

taining also structured features of higher energy. The cusp is a more localized region near noon within the cleft characterized by low energy precipitation only, having no discrete auroral arcs, but often displaying irregular behavior, presumably associated with the magnetic cusp.

The above definition undoubtedly makes a differentiation many researchers today (but by no means all) believe to be useful; however, it must be admitted that as a practical matter it is not clear how to make the distinction in any particular case. If an inverted V does not happen to be present on a given cusp/cleft pass, there are no criteria for differentiating the regions, except perhaps how close in MLT the pass is to noon.

It is, however, of great interest to know whether there are in fact two different, morphologically distinct regions of approximately magnetosheathlike precipitation, or whether the cleft is a region smoothly varying with local time and which is called the cusp near magnetic local noon only because of the dictates of custom. The goals herein are, first, to establish the distinction between the two regions based on elementary arguments and a case examination of individual DMSP F7 cusp crossings; and having formalized the distinction in terms such that a computer can do the differentiating, to investigate the magnetic local time variations of the two regions—the cusp proper and the cleft/LLBL—statistically, using a base of 5609 individual dayside crossings.

2. IDENTIFICATION OF THE CUSP AND THE CLEFT/BL

The low-altitude cusp has been identified in a large number of different ways by workers using various types of observations. The discussion above gave only a small fraction of the methods used based on particle signatures alone. We therefore start by proposing a conceptual definition: "The low-altitude cusp is the dayside region in which the entry of magnetosheath plasma to low altitudes is most direct. Entry into a region is considered more direct if more particles make it in (the number flux is higher) and if such particles maintain more of their original energy spectral characteristics." The low-altitude cusp so defined is not therefore guaranteed to correspond to the external magnetic cusp, and since magnetic field mappings are notoriously tricky, it may be difficult to establish such a correspondence. However, our conceptual definition does correspond to the usual image of a region of comparatively unrestricted magnetosheath plasma access to low altitudes; and given the immense physical consequences of such entry, we believe that it is the "right" definition for the low-altitude cusp. It is of course only useful if it can indeed be established that within the broad band of roughly magnetosheathlike precipitation there is a localized region of more direct entry in the sense defined above.

The data used herein are from the electrostatic analyzers on board the Air Force DMSP F7 satellite, which measure electrons and ions from 32 eV to 30 keV. DMSP F7 is in a Sun-synchronous 838-km-altitude polar orbit in approximately the 1030–2230 LT meridian. The apertures always point toward local zenith with a field of view $< 8°$, so that at the latitudes of interest for auroral and cusp phenomena all particles observed are within the loss cone. *Hardy et al.* [1984] have provided detailed information concerning the detectors.

We start by showing representative dayside polar passes at different local times. (That they are indeed representative is a statistical question, to be addressed in the next section). Plate 1 shows a spectrogram of precipitating particles from a high-latitude pass of DMSP F7 near 1200 MLT, on December 24, 1983, from 1341

UT to 1345 UT. (Plate 1 can be found in the separate color section in this issue.) Note that the spectrogram displays differential energy flux (rather than number flux) which emphasizes higher-energy particles over lower-energy particles, and that the ion energy scale is inverted, so that 32-eV electrons and ions appear closest to the center. In Plate 1 the high number and energy fluxes (a quantitative discussion shortly follows), the ion energy flux peak near 1 keV (the number flux peak is always moderately lower), and the MLT location all suggest that if there is a cusp, the region shown in Plate 1 (between the arrows) should be included as a member of the species. For completeness we point out that the poleward plume of low-energy ions is simply a dramatic example of the energy-latitude dispersion sometimes observed in the cusp, particularly for southward B_z, and is a consequence of strong poleward convection [*Shelley et al.*, 1976; *Reiff et al.*, 1977] and a comparatively narrow cusp width, as indicated by the arrows denoting the cusp boundaries.

Continuing a preliminary investigation into the local time variation of dayside magnetosheath precipitation, we examine in Plate 2 (Plate 2 can be found in the separate color section in this issue), a pass near 0830 MLT on December 1, 1983, at 0756–0800 UT. Notice that the number fluxes are reduced by about an order of magnitude. Moreover, although the transition between dayside plasma sheet precipitation and roughly magnetosheathlike precipitation is still clear (the transition occurs at about $-75.2°$ MLAT), the average energies are higher (and further from magnetosheath energies) in Plate 2 as compared to the near-noon pass of Plate 1.

A critical question now arises. As the MLT varies between 0830 and 1200 MLT, how does the dayside cusp precipitation vary? *Is there one region which varies smoothly in MLT or two morphologically distinct regions?* Plate 3, which shows a pass near 1000 MLT on December 5, 1988 (1136–1141 UT), provides an answer. (Plate 3 can be found in the separate color section in this issue.) Three regions can be distinguished in Plate 3 moving equatorward to poleward (right to left): first the dayside plasma sheet precipitation characterized by keV electrons (from 72° to 76° MLAT); second a region quite similar to that observed at 0830 MLT (extending from 76° to 79°); and finally, furthest poleward, a region quite similar to the cusp as it appears at 1200 MLT (this region is marked by arrows). It is logical to identify the intermediate region as the ionospheric signature of the low-latitude boundary layer (LLBL). Thus the cusp is not simply the near-noon portion of the cleft/LLBL: at least some of the time both regions can be observed at the same MLT, with each region maintaining its independent characteristics. Plate 3 shows the cusp and the cleft/LLBL to be morphologically distinct regions.

The event shown in Plate 3 is by no means a unique pass; Plate 4 shows another example, also from December 5, 1983 (0457–0502 UT), in which the cusp and the cleft/LLBL can be clearly distinguished. (Plate 4 can be found in the separate color section in this issue.) Again the region further poleward, the cusp, can be distinguished from the boundary layer which lies equatorward of it (in this case the cusp has a low-energy poleward ion plume, marking strong tailward convection). In this example also the ion number flux in the region identified as cusp in Plate 4 far exceeds the number flux in the region marked cleft/LLBL (except at the highest energies, which are presumably of magnetospheric origin).

It is useful to compare the transition from the cusp to the cleft observed at low altitudes (Plates 3 and 4) with a crossing from the magnetosheath to the LLBL in the external magnetosphere. Figure 1 shows such a crossing by ISEE 1, as adapted from *Eastman et al.* [1985]. Eastman et al. term the crossing shown in Fig-
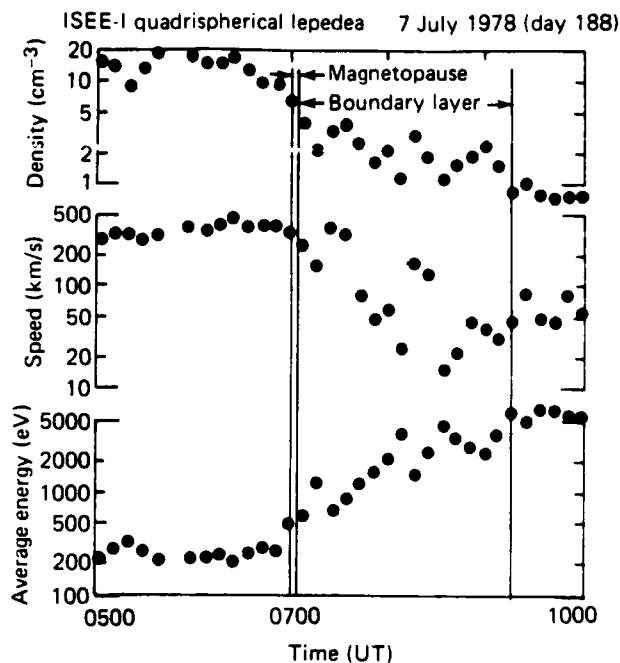
Fig. 1. Various plasma parameters from an ISEE 1 crossing from the magnetosheath into the LLBL at 16 R_e. Note the sharp drop in number flux, and the rise in total kinetic energy per ion as the crosses from the sheath into the boundary layer.

ure 1 "representative." Note first that as ISEE 1 moved from the sheath into the boundary layer the number density dropped by a factor of about 5. Eastman et al. concentrated on the flow velocity decrease, since they were addressing the possibility of enhanced flows in the boundary layer as many merging models would predict. (Other workers, such as Sonnerup et al. [1981] and Paschmann et al. [1986], have reported high-speed boundary layer flows suggestive of merging.) The DMSP observations, however, are only of the total kinetic energy, namely the sum of the energy associated with the bulk flow and the thermal energy. In the sheath, in this example, the kinetic energy per ion is a little less than 1 keV, whereas on the boundary layer side it rises to several keV (staying below about 5 keV). Thus in terms of the ions, there are two important characteristics associated with a sheath/boundary layer transition: the density decreases dramatically, and the average energy rises (a third characteristic, important for Eastman et al. [1985], namely the slower bulk flows typically associated with the boundary layer, will not be discussed here).

Fewer low-energy ions are present in the cusp than in the sheath [Frank, 1971] for simple physical reasons to be discussed in section 4. Still, the ion energy fluxes observed in Plates 1, 3, and 4 in the regions pointed out as cusp (by arrows) have a peak around 1 keV, as do magnetosheath fluxes. However, because of the relatively fewer particles at low energies, and because of a superthermal tail (present also in the magnetosheath, as shown, for example, by Williams et al. [1988]), the average ion energy in the cusp region is substantially higher. An examination of a large number of such spectrograms has led to the conclusion that the average ion energy in the cusp is < 3000 eV, while the average energy in the low altitude boundary layer is in the range 3000 eV to 6000 eV.

The observations of Formisano [1980] of HEOS 2 crossings from the sheath to the boundary layer (in the equatorial plane) show that the electron average energy also rises, although abso-

lute calibrations are not available. Again, the same effect is observed in Plates 3 and 4. Note that electrons with a temperature of, say, 80 eV would have an average energy of 120 eV, except that the always present superthermal tail (presumably due to magnetospheric leakage [Sibeck et al., 1987]) further raises the average energy. Our experience shows that the average electron energy in the cusp is always less than 220 eV (as shown in the next section, 145 eV is the typical value).

We are now able to propose a practical definition of the cusp and boundary layer, suitable for automated identifications, based on the average energies of electrons and ions in the two regions as given above. This allows for a large-scale statistical study of the local time variation as a function of MLT of the two different regions. In section 4, statistical evidence based on the completed study is also presented which tends to verify the dividing energy points chosen above.

3. STATISTICAL LOCAL TIME VARIATION OF THE CUSP AND CLEFT/LLBL

One year of DMSP F7 precipitating electron and ion data, from December 1983 (when the first F7 data collection began) through November 1984, was used to investigate the behavior of the cusp and the cleft/LLBL in the local time range 0600 to 1600 MLT. The investigation was extended further prenoon than postnoon simply because the satellite trajectory provides more coverage prenoon. On each pass the types of regions (cusp or cleft) encountered were recorded, along with their equatorward and poleward boundaries. Within each region the peak energy flux point was determined (based on a 3-s sliding average—about 0.3° MLAT width), and the various attributes, including the average spectrum, were recorded.

The determination as to whether a region was cusp, boundary layer, or neither was based on the following criteria, selected to give region and boundary determinations matching those found suitable on a case-by-case basis (e.g., the cases shown in Plates 1–4):

1. If the energy flux of the ions (electrons) was less than 10^{10} eV/cm^2 s sr (6×10^{10}), the region was neither cusp nor boundary layer.

2. If the energy flux in the 2- or 5-keV electron channel was greater than 10^7 eV/cm^2 s sr eV, the region was neither cusp nor boundary layer, since such fluxes would indicate plasma sheet presence.

3. If the first two criteria were met, the region was boundary layer if either 3000 eV < E_i < 6000 eV or 220 eV < E_e < 600 eV where E_i and E_e are the average electron and ion energies, respectively.

4. If the first two criteria were met and both 300 < E_i < 3000 eV and E_e < 220 eV, the region was identified as cusp.

Note that the flux level was not used to distinguish between the cusp and the cleft/LLBL. The flux level in the cusp (or boundary layer) varies dramatically with solar wind density [Candidi and Meng, 1984], leading us to believe that average energy is probably the more reliable indicator. However, this is not to say that flux is not an aid in making a cusp-cleft distinction; on the contrary, according to our conceptual definition, making a distinction between the two regions only makes sense if the cusp has the higher number flux. However, we wish to demonstrate statistically that the energy ranges chosen do indeed select the statistically higher number flux region, and we thus avoid biasing this result.

We note briefly that there have been several statistical maps of electron precipitation binned by MLT and latitude published (for

example, *McDiarmid et al.* [1972], *Candidi et al.* [1983], and most comprehensively, *Hardy et al.* [1985]). Besides including ion data, the present approach differs conceptually in that the precipitation is also binned by region (and thus only a subset of the precipitation data, namely that in the cusp or cleft, is included) rather than by *Kp*. The cusp can move at least 5° MLAT in 1 hour [*Meng*, 1984], so that in the statistical electron maps it can be difficult to distinguish the cusp. However, *Gussenhoven et al.* [1985] used the statistical maps of *Hardy et al.* [1985] to argue that the cusp could be distingushed from the cleft by the position of the minimum in electron average energy. The cusp as so defined changed in location from the 1100–1130 bin to the 1230–1300 bin as *Kp* varied from 0 to 5. The electron energy flux of their cusp was about 3–4 times lower and the average energy moderately higher than the results presented below. All these differences with the results presented herein are consistent with the statistical MLT/latitude maps representing a composite of cusp, boundary layer, and dayside hard precipitation.

On a given DMSP F7 dayside pass, one of five things could happen: (1) the cusp but not the cleft/LLBL could be observed; (2) the cleft/LLBL but not the cusp could be observed; (3) the cusp could be observed poleward of the cleft/LLBL; (4) the cleft/LLBL could be observed poleward of the cusp; or (5) the pass might not be useful for such sorting, because the magnetic local time could change by more than 1 hour from entering a region to exiting it, or a chaotic pattern of multiple regions could be found (this last was quite rare). Obviously occurrences of case 4 represent breakdowns in the simple identification scheme adopted rather than physical reality; but it is nonetheless important to keep statistics as a further check on the reliability of our identification scheme. In the plots presented below, the magnetic latitude was read directly from the World Data Center A (WDC-A) provided tapes and represents Gustafsson's magnetic latitude [*Gustafsson*, 1970]; the magnetic local time was calculated using an eccentric rotated dipole fit.

Figure 2 shows the probability as a function of local time (divided into half-hour bins) of each of the five cases above. The probability of seeing both the cusp and the cleft (in the proper order) at the same local time peaks at 1200 MLT, at about 25%. Among all cases where both regions were observed, the cusp was found to be the polewardmost region about 85% of the time. We examined a number of instances where the order was inverted. In no case were there two clear regions such as are shown in Plates 3 and 4 with a cleft region poleward of the cusp at nearly the same MLT. One common situation was that shown in Plate 5. (Plate 5 can be found in the separate color section in this issue.) Here at the poleward edge of a clear cusp region is a narrow feature of accelerated electrons, with enough intensity to be a visible arc. It is already known that at times Sun-aligned arcs cross the polar cap, so the occasional presence of discrete features poleward of the cusp (usually at subvisual levels) is to be expected. However, the most common "category 4" case was simply that DMSP F7 entered the cusp at, for example, 1245 MLT, and proceeding poleward encountered the cleft at 1330 MLT, still within the 1-hour tolerance permitted for sorting.

Next we consider normalized probabilities of observing the cusp and the cleft/LLBL. This is done based on two assumptions. The first is that if the satellite reaches high enough latitude on the dayside, it will always encounter some region of approximately magnetosheathlike particles. As *Heikkila* [1985] points out, this appears to be the viewpoint of essentially every worker who has investigated the cusp; and any deviations from this rule must be rare indeed.
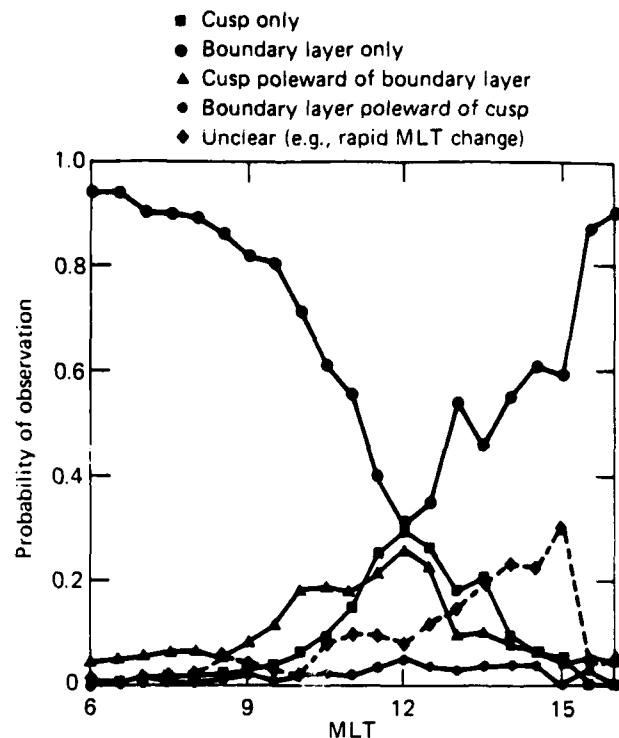

Fig. 2. The probability as a function of local time (in half-hour bins) of observing on a given DMSP F7 dayside pass (1) the cusp alone, (2) the cleft/LLBL alone, (3) the cusp poleward of the cleft, (4) the cleft poleward of the cusp, and (5) the MLT changing too rapidly to allow a determination. In this figure, probabilities sum to 1.

This first assumption is already included in the probabilities presented in Figure 2; that is, in cases where the DMSP F7 encountered neither region it is assumed that it did not reach high enough latitude, and such cases are not included in calculating the probabilities presented. The second assumption is that there are no gaps between the regions. This assumption is also one we are fairly confident of, based on examining a large number of cases. Therefore when, say, the cleft/LLBL is encountered at a certain latitude and local time and the satellite exits the cleft/LLBL at about the same local time headed toward higher latitudes without encountering the cusp, we can assume that the cusp was not present at that local time.

Figure 3 shows the normalized probability of encountering the cusp and cleft/LLBL as a function of local time. The cusp shows a sharp peak in occurrence in the half-hour bin centered around 1200 MLT, with the occurrence probability dropping off rapidly away from noon. The boundary layer (cleft), however, shows nearly 100% chance of observation well away from noon, but has a minimum in occurrence frequency for the bin centered at noon. There is therefore a satisfying agreement with intuitive but untested notions of the cusp position. We repeated the probability distribution with the bin size halved to 15 min, both to seek a further refinement and to test for consistency. The results are shown in Figure 4; although the finer bin size creates a few more wrinkles, once again the probability of observing the cusp shows a peak in the bin centered at 1200 MLT, with the peak now above 70%.

The question may arise as to why the cusp is sometimes not seen at 1200 MLT. There are three likely reasons: (1) the solar wind density is too low; (2) the solar wind velocity is too high;
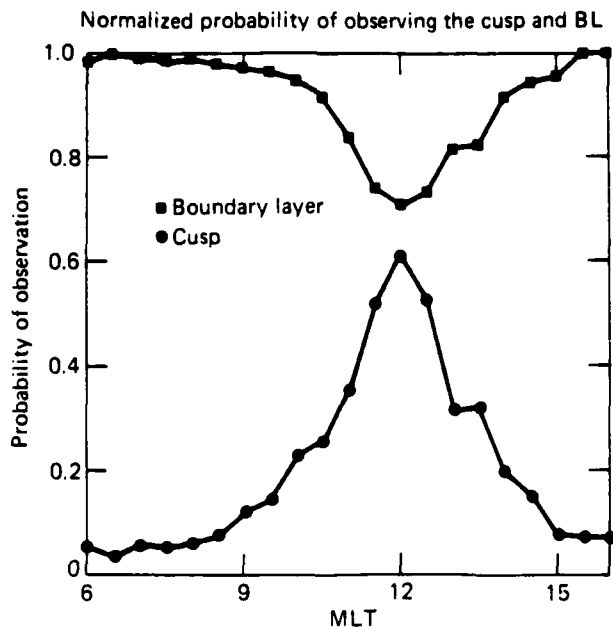
Normalized probability of observing the cusp and BL

Fig. 3. The normalized probabilities of detecting the cusp or the cleft as a function of MLT in half-hour bins. Probabilities sum to more than 1, since both regions may be observed.

and (3) the IMF B_y changes the cusp MLT position. The present paper is concerned with distinguishing the cusp from the cleft and determining their respective average local time behavior. Future work will investigate solar wind effects. However, checking several cases in which no cusp was identified on a pass near noon by our computer algorithm, we did find a few cases where possibility 2 held true, i.e., cases where the solar wind velocity was high (above about 700 km/s), causing the average ion kinetic energy
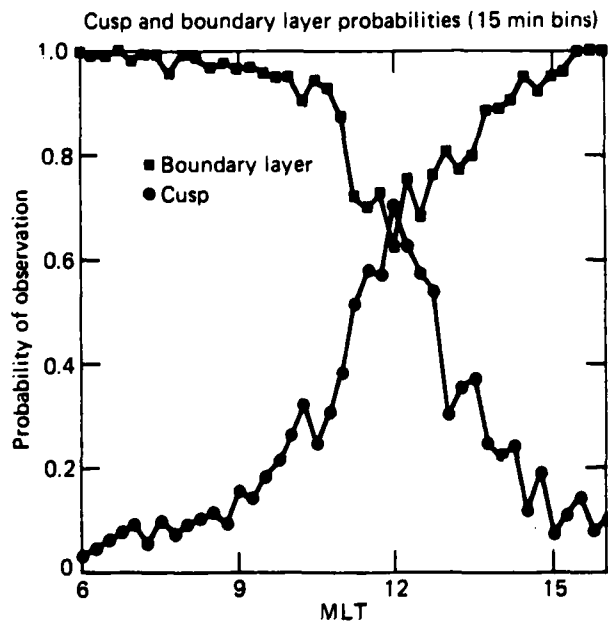
to rise above the value our algorithm used to distinguish cusp from cleft. The majority of cases are due to the third effect (the IMF B_y effect), as will be discussed in future work.

The above shows the probability of observing the cusp and cleft as a function of MLT. We now consider the local time variation of the average particle characteristics for those cases where the respective regions are observed. Plates 6 and 7 are composite spectrograms for the cusp and cleft/boundary layer, respectively, as a function of local time. (Plates 6 and 7 can be found in the separate color section in this issue.) In each half-hour local time bin an arithmetic average of particle spectra was taken for those individual passes in which a given region was observed. The individual spectra were themselves 3-s averages over the peak flux encountered in individual cusp passes. A comparison of the composite spectrograms for the two regions shows clearly the more direct magnetosheath origin of the plasma in the cusp. Both cusp electrons and cusp ions show energy flux peaks at appropriate values (about 40–150 eV and 400–2000 eV for electrons and ions, respectively). Over the MLT range 1000–1400, the ion number flux is 3.6 times higher in the cusp than in the boundary layer. For comparison, Sckopke et al. [1981] have reported that dayside boundary layer densities are about 4 times smaller than in the magnetosheath. Thus the statistical data presented here confirm that the energy criteria chosen in section 2 do indeed select a spatially confined region centered at noon in which the number flux is higher and more of the original magnetosheath spectral characteristics are maintained. Therefore, the cusp as herein defined is indeed the region of more direct magnetosheath entry.

Although the peak probability of observing the cusp is centered at noon, Plate 6 demonstrates that the 1400 MLT cusp, when observed, has a higher energy flux than the 1200 MLT cusp. The 1400 MLT region is, of course, the region of intense Birkeland currents and of auroral activity; however, any connection with the present results is obscure since the higher-energy electron precipitation associated with auroral arcs is reliably discriminated against by our algorithm for selecting the cusp.

Cusp and boundary layer probabilities (15 min bins)

Fig. 4. Probability of a given DMSP F7 pass observing the cusp and cleft as a function of MLT in 15-min bins. The maximum probability of observing the cusp (and minimum for observing the boundary layer) is still sharply peaked at 1200 MLT. In this figure, probabilities sum to more than 1, since both cusp and cleft may be observed in the same pass.
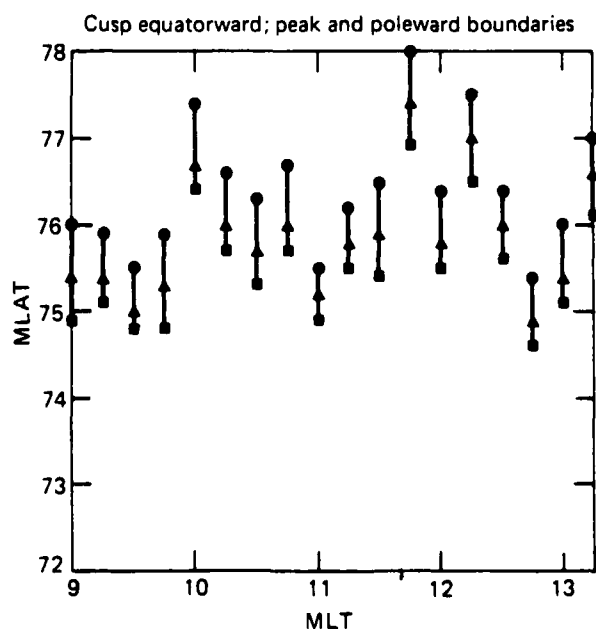
Cusp equatorward; peak and poleward boundaries

Fig. 5. The average latitudinal location of the equatorward and poleward boundaries and the point of peak ion precipitation for the cusp as a function of MLT.

As noted previously, statistics were kept on the boundaries of the two regions. Figure 5 shows the average equatorward and poleward boundaries of the cusp as a function of MLT and MLAT, along with the average point of peak ion flux. The cusp as herein defined is found to have a $0.8°-1.1°$ extent in latitudinal width, essentially independent of local time. Previous statistical studies have reported larger values for the cusp width [e.g., Burch, 1973; Carbary and Meng, 1986]. The difference is primarily due to the distinction made herein between the cusp and the cleft/LLBL. A secondary source of variability comes from the ill-defined nature of the poleward boundary of many cusp observations; in an open field line model of the cusp there is no reason to expect the poleward boundary to be sharply defined, and it frequently is not. In our algorithm this boundary is often determined when the flux falls below cusp levels (e.g., 10^{10} eV/cm s sr for ions).

Figure 6 shows the average position for the equatorward, poleward, and peak boundaries of the boundary layer as a function of MLT. Moving from noon to earlier local times, the boundary layer is observed to be latitudinally narrowest near noon, widens rapidly by 1030 MLT, and thereafter remains essentially constant. Moving to local times later than noon, the boundary layer again initially widens rapidly, up to 1315 MLT. DMSP F7 is Sun-synchronous in approximately the 1030–2230 MLT frame. As the dipole axis rotates with respect to the geographic axis under the satellite, the MLT varies; however, far from 1030 MLT, rapid changes in MLT with changing satellite latitude can occur. The latitude versus local time results are most meaningful within a few hours of 1030 MLT. Some of the behavior shown in Figure 6 is easy to understand theoretically, as is discussed in the next section.

4.   DISCUSSION AND INTERPRETATION

In section 2 we presented compelling evidence that the cusp is not simply the smooth continuation of the cleft/LLBL in the noon sector; for example, instances were presented in which both regions existed simultaneously and were clearly distinguishable at the same MLT. The results of section 3 also show various statistical differences between the two regions. However, it is possible to investigate whether the dividing energy chosen to separate the regions was in hindsight well chosen. Figure 7 plots the number flux into the cusp or cleft (at the same 3-s average peak used for all the statistics herein presented) as a function of the average energy. For the purposes of Figure 7, no distinction between regions was made; for each dayside pass, one point (the energy flux peak) is plotted. The general trend is for the ion number flux to drop off with increasing average ion kinetic energy approximately as E^{-2}; in addition there is apparently a break between the two vertical dashed lines separating the cusp from the cleft/LLBL. The dashed line further to the right is at 3000 eV and represents the ion average energy used by our computer algorithm to separate the cusp from the cleft; it was chosen based on case examinations. The line further to the left is at 2700 eV and represents a more conservative transition point based on the data in this figure. Note, however, that cases which fell in the transition region between the two dashed lines were not all taken to be cusp, since the average electron energy of many of these cases put them into the "cleft" category. Only if both the electron and ion criteria were met was a region of a given pass considered to be cusp. The various statistical results previously presented were recalculated excluding cases in the transition region (ion average energy 2700 eV to 3000 eV). The differences were small, and no improved consistency was

Boundary layer equatorward; peak and poleward boundaries
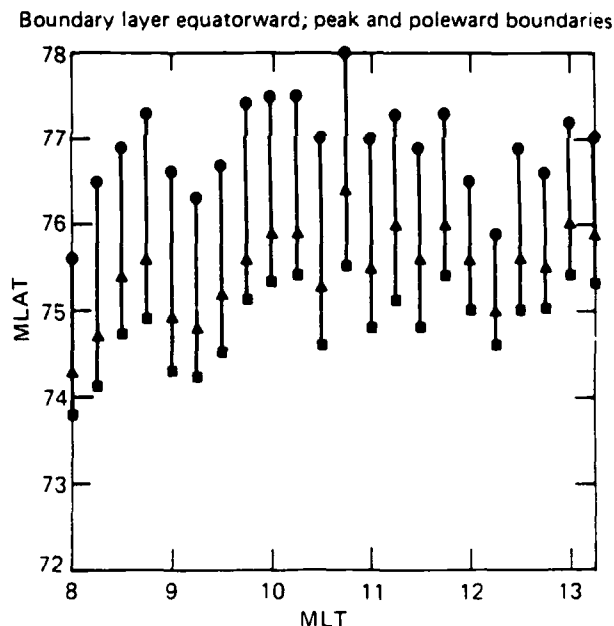

Fig. 6.   The average latitudinal location of the equatorward and poleward boundaries and the point of peak ion precipitation for the cleft/LLBL as a function of MLT.

found, apparently because cases in the transition region were largely already correctly classified based on their electron average energy. The apparent break in the number flux/average energy relationship of Figure 7 provides further evidence of the physical difference between the cusp and the cleft.

In the solar wind the statistical average number flux declines as the average ion kinetic energy increases [Mullan, 1983]: $\langle nV \rangle \sim 1/V \sim E^-$, since most of the kinetic energy is in the bulk velocity motion. Thus Figure 7 shows that the number flux drops off with increasing average energy faster in the cusp than in the solar wind. The magnetosheath is of course shocked (partially thermalized) solar wind, but most of the kinetic energy is still in the bulk motion, and one would not expect such a large change in the $\langle nV \rangle$ versus $\langle E \rangle$ slope on this basis. Fortunately there is a simple explanation as to why the number flux in the cusp drops off so rapidly with increasing average energy. A higher average ion kinetic energy in general implies a larger bulk flow velocity. The cusp probably consists of those dayside open field lines which thread the slow flow region of the magnetosheath, that is, to the region where the thermal velocity is comparable to the tailward flow velocity [Reiff et al., 1977; Hill and Reiff, 1977; Newell and Meng, 1987]. A progressively higher tailward bulk flow velocity allows progressively fewer low-energy ions to reach low altitudes before being convected tailward. Thus a larger average energy implying a larger bulk flow velocity would lead to a decline in density more rapidly than might be expected simply from the solar wind relationships. The original observations of Frank [1971] showed that although the energy flux peak in the cusp is the same as in the magnetosheath, lower-energy ions are often suppressed. This is also why the average ion energy in the cusp is often well above that in the magnetosheath even when the energy flux peaks coincide. Incidentally this model of a higher tailward velocity implying that fewer low-energy ions enter would imply a summer/winter asymmetry, since the winter cusp is further from the subsolar point and the tailward flow is larger. In fact the winter
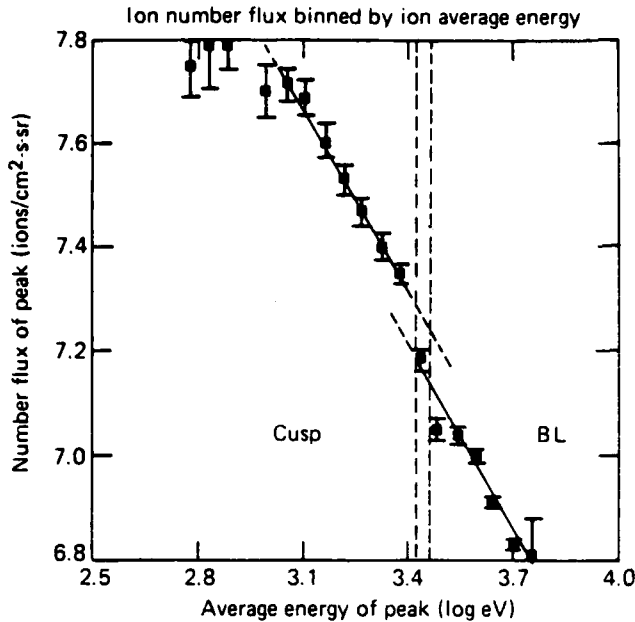
Ion number flux binned by ion average energy

Fig. 7. For each DMSP F7 dayside pass the point of peak ion energy flux was recorded irrespective of region (cusp or cleft) and binned by average energy. Plotted is the yearly average number flux versus log energy bin. The slope is about -2. The vertical dashed lines represent the transition between the cusp and cleft regions.

hemisphere cusp does indeed have fewer low-energy ions precipitating than does the summer [*Newell and Meng*, 1988].

For completeness we also present in Figure 8 a plot of electron number flux versus electron average energy. There is no obvious break at the typical dividing line between cusp and cleft. A careful examination of Plates 3 and 4 indicates why this is so. The electron characteristics are clearly different in the two regions, but there is considerable variability within the cleft/LLBL region. Our algorithm selected the peak energy flux from each region, and in many cases one can find brief intervals within the cleft in which the electron flux is comparable to that within the cusp. Almost certainly an algorithm which chose the electron flux at the same point as the ion flux (rather than allowing an independent peak anywhere within the regions) would have led to a clearer statistical difference between the two regions. Still, the general trend that lower average electron energy corresponds to more direct entry (in the sense that more particles make it in to low altitudes) is readily apparent in Figure 8. The ions are generally less variable and hence a better indicator of the nature of the region (cusp or cleft) than are electrons, although using both electron and ion data (as is done here) is better still.

From simple theoretical grounds it is likely that the entire dayside equatorial LLBL out to the dawn-dusk flanks usually maps into the ionosphere within 2 hours or less of noon [*Vasyliunas*, 1979]. Since the LLBL is thinnest at noon and widens rapidly by the dawn-dusk flanks, the behavior shown in Figure 6 for the low-altitude cleft is easily understandable. The observations at 0600-0800 MLT should (theoretically) generally map to the distant tail. Indeed, the cleft region composite spectrogram (Plate 6) shows a smooth transformation from an ion energy flux peak modestly higher than magnetosheath values near noon to a peak near several keV, a typical plasma sheet boundary layer value, near 0600 MLT.

It is interesting to consider whether the peak energy flux within the cusp occurs at the equatorward or the poleward boundary.

The standard open field line model of the cusp implies that the equatorward boundary should be the more intense, whereas diffuse entry onto closed field lines could give a source at the poleward boundary. Examination of individual spectrograms generally shows either no clear peak within the cusp (as in Plate 3) or a peak closer to the poleward edge (as in Plate 1). The statistical results of the previous section (Figure 6) show that the average ion energy flux peak within the cusp lies about two thirds of the way toward the equatorward boundary (i.e., the peak is further from the poleward boundary). Whether this result is important is not clear, since in most cases the flux within the cusp proper is roughly uniform.

5. SUMMARY AND CONCLUSIONS

Although the cusp has recently been thought of as a restricted region (near noon) of the cleft [e.g., *Heikkila*, 1985], the practical distinction has been unclear (note however that *Lundin* [1988] has recently used the isotropy or anisotropy of the electron precipitation as an indicator of cusp proper or cleft respectively). We have shown in this paper that a reasonable conceptual definition of the cusp—a localized region in which magnetosheath plasma entry is more direct (more direct meaning that more particles make it in to low altitudes and their spectral characteristics are closer to magnetosheath values)—is equivalent to a simple practical definition of the low-altitude cusp. If $E_e < 200$ eV, $E_i < 2700$ eV, $j_i > 10^{10}$ eV/cm^2 s sr, and $j_e > 6 \times 10^{10}$ eV/cm^2 s sr, the region is cusp (using slightly conservative criteria for average energies). Note that the energy flux peaks will be considerably lower than the values above; for example, the ion energy flux peak is generally below 1 keV. Low-energy ions do not make it into the cusp as well as higher-energy ions [*Frank*, 1971; *Newell and Meng*, 1988], which combined with a superthermal tail (also present in the magnetosheath) leads to the above cited average energies. Presumably the constraints of charge quasi-neutrality [*Burch*, 1985] lead to similar behavior for the electrons.

Number flux versus average energy at cusp/BL energy flux peak

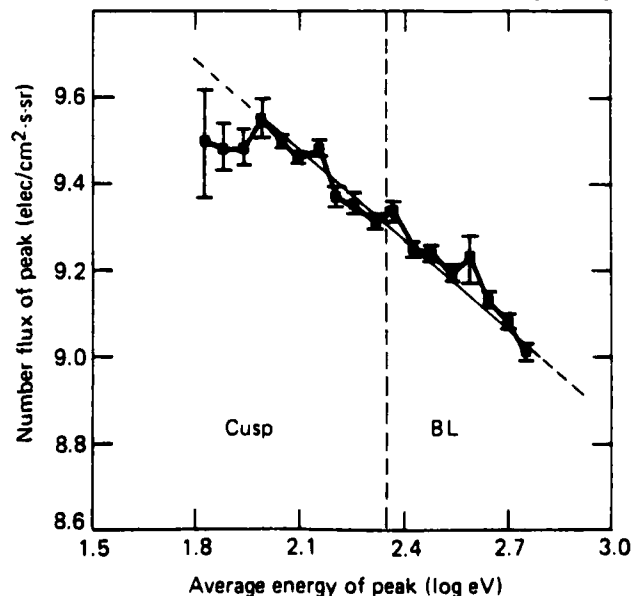## Electron number flux binned by electron average energy

Fig. 8. Same as Figure 7, but for electron number flux versus electron average energy. The highest number fluxes are associated with the lowest average energies.

The above algorithm for identifying the cusp has been applied to 1 year of DMSP F7 precipitating data (5609 individual passes) to investigate local time variations. The probability of observing the cusp is sharply peaked at noon and drops off rapidly away from noon. The probability of observing the cleft/LLBL is near unity a few hours away from noon, but has a pronounced minimum at noon. The cusp has a latitudinal width of $0.8°-1.1°$ MLAT essentially independent of local time, whereas the cleft is narrowest at noon and widens rapidly away from noon. The precipitating ion number flux in the cusp is about 3.6 times that of the cleft, which is nearly the same density factor found crossing from the magnetosheath into the boundary layer [Sckopke et al., 1981]. The spectral characteristics of the cusp vary comparatively little with MLT, but the peak in energy flux is observed near 1400-1430 MLT (however, the probability of observing the cusp at 1400 MLT is much smaller than at 1200 MLT). Individual cusp passes show either the ion flux peak near the equatorward edge (as often seems to be the case for southward IMF B_z) or an ion flux with no clear peak. The statistical yearly average shows the point of peak energy flux approximately twice as close to the equatorward boundary as the poleward boundary.

We end by noting that both an examination of individual cases (such as Plates 3 and 4) and a statistical study lead to the same conclusion, namely that the cusp and cleft are indeed morphologically distinct regions which can be differentiated in a practical way. Frequently both regions can be observed on the same pass at the same MLT (with the cusp immediately poleward of the cleft), showing that the cusp is not simply the near-noon portion of the cleft.

REFERENCES

Burch, J. L., Rate of erosion of dayside magnetic flux based on a quantitative study of the dependence of polar cusp latitude on the interplanetary magnetic field, *Radio Sci., 8*, 955-961, 1973.

Burch, J. L., Quasi-neutrality in the polar cusp, *Geophys. Res. Lett., 12*, 469-472, 1985.

Burrows, J. R., I. B. McDiarmid, and M. D. Wilson, Pitch angles and spectra of particles in the outer zone near noon, in *Earth's Magnetospheric Processes*, edited by B. M. McCormac, pp. 153-167, D. Reidel, Hingham, Mass., 1972.

Candidi, M., and C.-I. Meng, The relation of the cusp precipitating electron flux to the solar wind and the interplanetary magnetic field, *J. Geophys. Res., 89*, 9741-9751, 1984.

Candidi, M., H. W. Kroehl, and C.-I. Meng, Spatial intensity of dayside polar soft electron precipitation and the IMF, *Planet. Space Sci., 31*, 889, 1983.

Carbary, J. F., and C.-I. Meng, Correlation of cusp latitude with B_z and AE(12) using nearly one year's data, *J. Geophys. Res., 91*, 10047-10054, 1986.

Eastman, T. E., B. Popielawska, and L. A. Frank, Three-dimensional plasma observations near the outer magnetospheric boundary, *J. Geophys. Res., 90*, 9519-9539, 1985.

Formisano, V., HEOS 2 observations of the boundary layer from the magnetopause to the ionosphere, *Planet. Space Sci., 28*, 245-257, 1980.

Frank, L. A., Plasma in the Earth's polar magnetosphere, *J. Geophys. Res., 76*, 5202-5219, 1971.

Gussenhoven, M. S., D. A. Hardy, and R. L. Carovillano, Average electron precipitation in the polar cusps, cleft, and cap, in *The Polar Cusp*,

edited by J. A. Holtet and A. Egeland, pp. 85-97, D. Reidel, Hingham, Mass., 1985.

Gustafsson, G., Corrected geomagnetic coordinates for epoch 1980, in *Magnetospheric Currents, Geophys. Monogr. Ser.*, vol. 28, edited by T. A. Potemra, pp. 276-283, AGU, Washington, D.C., 1984.

Hardy, D. A., L. K. Schmitt, M. S. Gussenhoven, F. J. Marshall, H. C. Yeh, T. L. Shumaker, A. Hube, and J. Pantazis, Precipitating electron and ion detectors (SSJ/4) for the block 5D/flights 6-10 DMSP satellites: Calibration and data presentation, Rep. AFGL-TR-84-0317, Air Force Geophys. Lab., Hanscom Air Force Base, Mass., 1984.

Hardy, D. A., M. S. Gussenhoven, and E. Holeman, A statistical model of auroral electron precipitation, *J. Geophys. Res., 90*, 4229-4248, 1985.

Heikkila, W. J., Definition of the cusp, in *The Polar Cusp*, edited by J. A. Holtet and A. Egeland, pp. 387-395, D. Reidel, Hingham, Mass., 1985.

Heikkila, W. J., and J. D. Winningham, Penetration of magnetosheath plasma to low altitudes through the dayside magnetospheric cusps, *J. Geophys. Res., 76*, 883-891, 1971.

Hill, T. W., and P. H. Reiff, Evidence of magnetospheric cusp proton acceleration by magnetic merging at the dayside magnetopause, *J. Geophys. Res., 82*, 3623-3628, 1977.

Lundin, R., Acceleration/heating of plasma on auroral field lines: Preliminary results from the Viking satellite, *Annales Geophysicae, 6*, 143-152, 1988.

Lundin, R., K. Stasiewicz, and B. Hultqvist, On the interpretation of different flow vectors of different ion species in the magnetospheric boundary layer, *J. Geophys. Res., 92*, 3214-3222, 1987.

McDiarmid, I. B., J. R. Burrows, and E. E. Budzinski, Average characteristics of magnetospheric electrons (150 eV to 200 keV) at 1400 km, *J. Geophys. Res., 80*, 73-79, 1975.

McDiarmid, I. B., J. R. Burrows, and E. E. Budzinski, Particle properties in the dayside cleft, *J. Geophys. Res., 81*, 221-226, 1976.

Meng, C.-I., Dynamic variation of the auroral oval during intense magnetic storms, *J. Geophys. Res., 89*, 227-235, 1984.

Mullan, D. J., Momentum flux invariance in the solar wind, *Astrophys. J., 272*, 325-328, 1983.

Newell, P. T., and C.-I. Meng, Cusp width and B_z: Observations and a conceptual model, *J. Geophys. Res., 92*, 13673-13678, 1987.

Newell, P. T., and C.-I. Meng, Hemispherical asymmetry in cusp precipitation near solstices, *J. Geophys. Res., 93*, 2643-2648, 1988.

Paschmann, G., I. Papamastorakis, W. Baumjohann, N. Sckopke, C. W. Carlson, B. U. O. Sonnerup, and H. Lühr, The magnetopause for large magnetic shear: AMPTE/IRM observations, *J. Geophys. Res., 91*, 11099-11115, 1986.

Reiff, P. H., T. W. Hill, and J. L. Burch, Solar wind plasma injection at the dayside magnetospheric cusp, *J. Geophys. Res., 82*, 479-491, 1977.

Sckopke, N., G. Paschmann, G. Haerendel, B. U. O. Sonnerup, S. J. Bame, T. G. Forbes, E. W. Hones, and C. T. Russell, Structure of the low-latitude boundary layer, *J. Geophys. Res., 86*, 2099-2110, 1981.

Shelley, E. G., R. D. Sharp, and R. G. Johnson, He^{++} and H^+ flux measurements in the dayside cusp: Estimates of convection electric field, *J. Geophys. Res., 81*, 2363-2370, 1976.

Sibeck, D. G., R. W. McEntire, A. T. Y. Lui, R. E. Lopez, S. M. Krimigis, R. B. Decker, L. J. Zanetti, and T. A. Potemra, Energetic magnetospheric ions at the dayside magnetopause: Leakage or merging?, *J. Geophys. Res., 92*, 12097-12114, 1987.

Sonnerup, B. U. O., G. Paschmann, I. Papamastorakis, N. Sckopke, G. Haerendel, S. J. Bame, J. R. Asbridge, J. T. Gosling, and C. T. Russell, Evidence for magnetic field reconnection at the Earth's magnetopause, *J. Geophys. Res., 86*, 10049-10067, 1981.

Vasyliunas, V. M., Interaction between the magnetospheric boundary layers and the ionosphere, Proceedings of Magnetospheric Boundary Layers Conference, Alpbach, 11-15 June, 1979, *Eur. Space Agency Spec. Publ., ESA SP-148*, Aug. 1979.

Williams, D. J., D. G. Mitchell, L. A. Frank, and T. E. Eastman, Three-dimensional magnetosheath plasma ion distributions from 200 eV to 2 MeV, *J. Geophys. Res.*, in press, 1988.

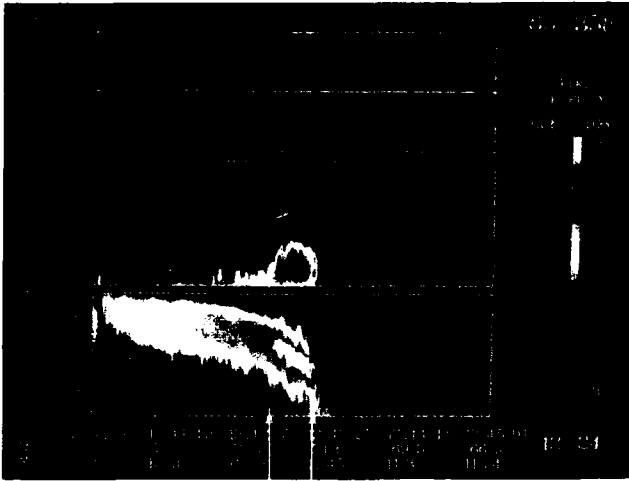C.-I. Meng and P. T. Newell, Johns Hopkins University Applied Physics Laboratory, Johns Hopkins Road, Laurel, MD 20707.

Plate 1. [*Newell and Meng*]. DMSP F7 spectrogram of the cusp near noon. The ion energy scale is inverted; differential energy flux (eV/cm^2 s sr eV) is displayed. The arrows indicate the cusp. Average energy is in eV; energy flux is in eV/cm^2 s sr.
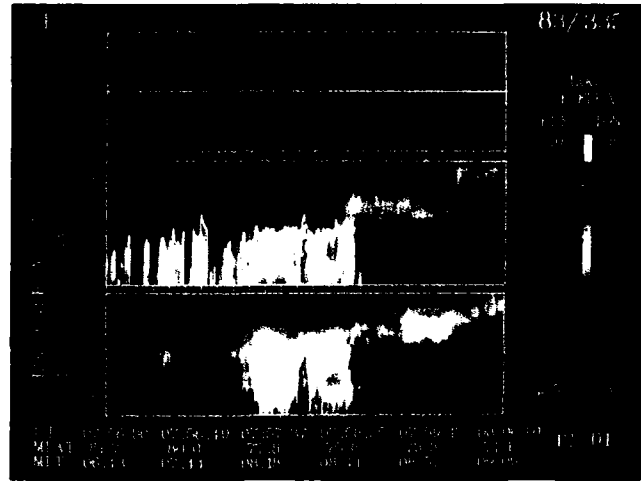

Plate 2. [*Newell and Meng*]. A cleft/LLBL pass near 0830 MLT. The precipitation is still roughly magnetosheathlike, but the number and energy flux is smaller and the average energy higher than near noon.
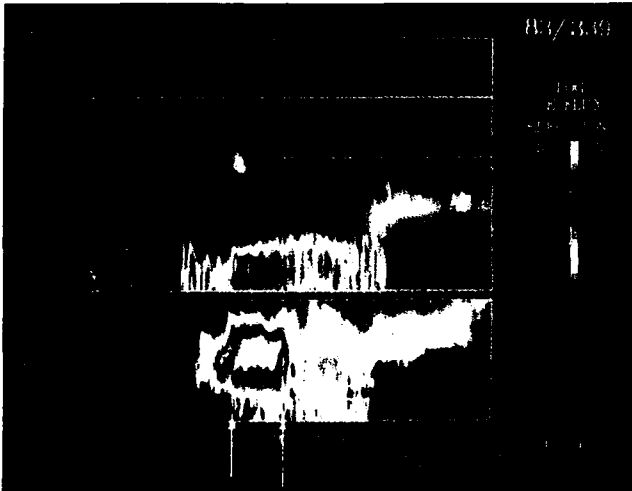

Plate 3. [*Newell and Meng*]. A DMSP F7 pass near 1010 MLT. The cusp and cleft/LLBL are both present at the same MLT. The flux is higher and the average energy lower in the cusp. The arrows indicate the cusp proper.
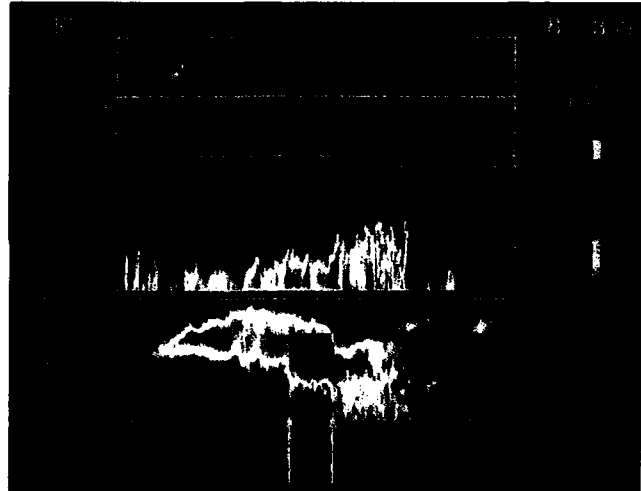
Plate 4. [*Newell and Meng*]. A DMSP F7 pass near 1000 MLT showing both the cusp and cleft at the same MLT. There is considerable variation within the cleft, but the number fluxes tend to be lower and the average energies higher than in the cusp. The arrows indicate the cusp proper.
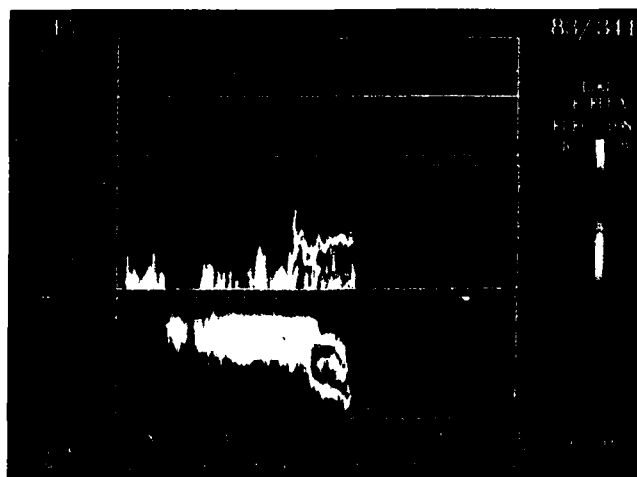
Plate 5. [*Newell and Meng*]. An example of a DMSP F7 pass with a highly localized burst of energetic electrons at the poleward edge of the cusp. Such an example would fall into category 4 as described in the text, but does not represent the LLBL poleward of the cusp.
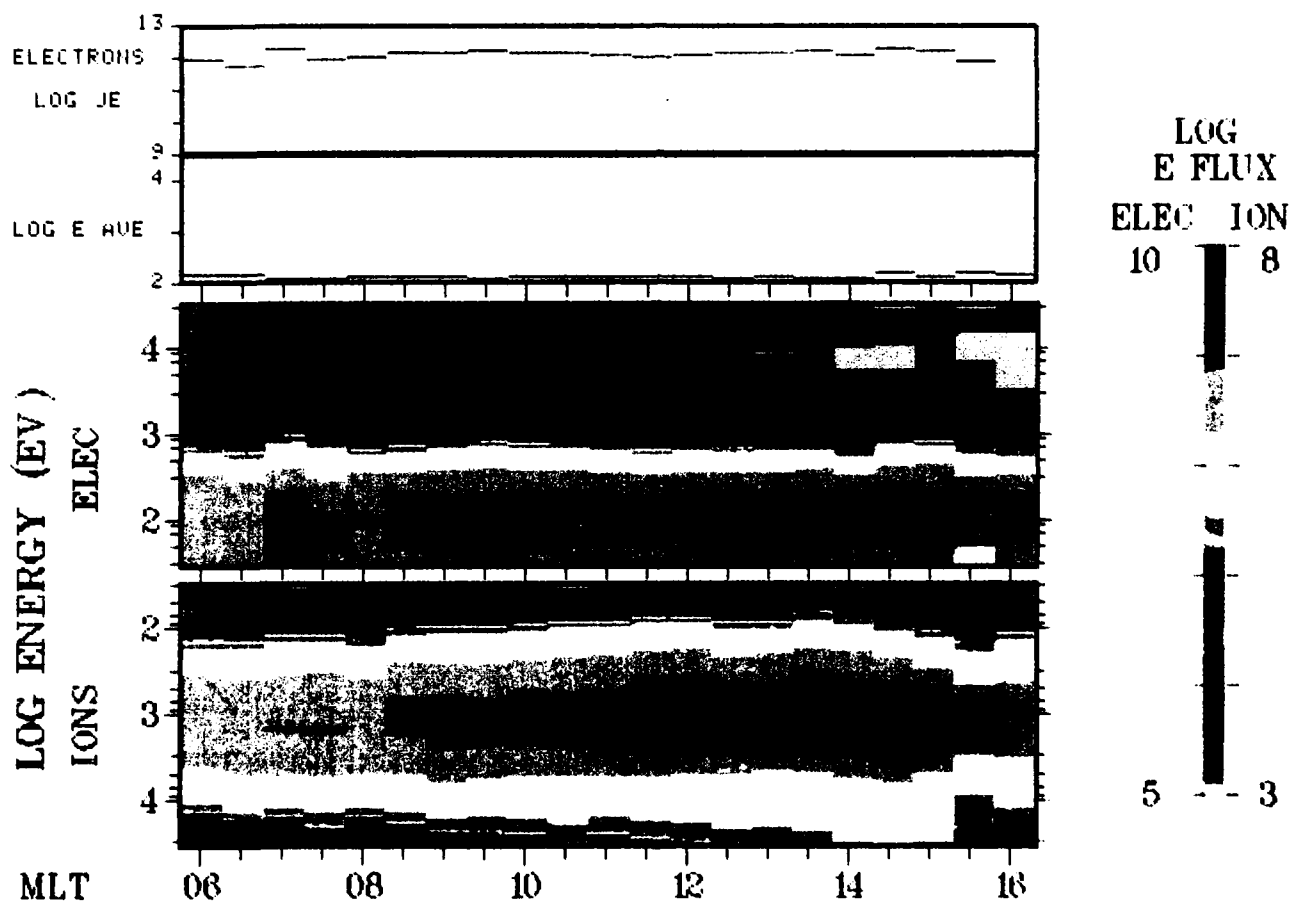
Plate 6.   [*Newell and Meng*]. A composite spectrogram showing the cusp on a yearly average basis as a function of MLT. Note that the cusp is often not observed away from noon; this plate shows the cusp characteristics when it is observed.
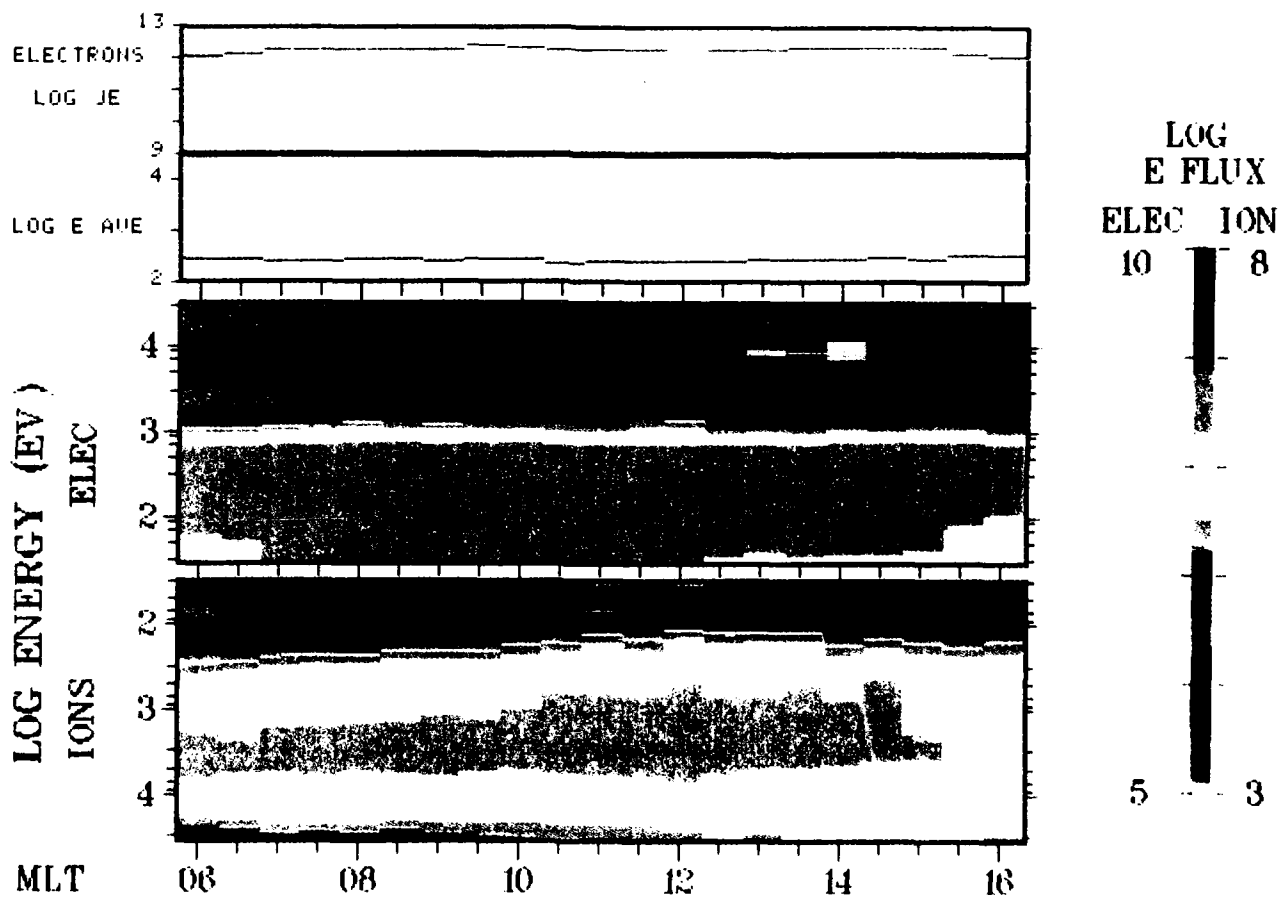
Plate 7. A yearly average composite spectrogram for the cleft/LLBL as a function of MLT.

Identification and Observations of the Plasma Mantle at Low Altitude

Patrick T. Newell ,[1] William J. Burke ,[2] Ching-I. Meng ,[1] Ennio R. Sanchez ,[1] and Marian E. Greenspan[3,4]

The direct injection of magnetosheath plasma into the cusp produces at low altitude a precipitation regime with an energy-latitude dispersion—the more poleward portion of which we herein term the "cusp plume." An extensive survey of the Defense Meteorological Satellite Program (DMSP) F7 and F9 32 eV to 30 keV precipitating particle data shows that similar dispersive signatures exist over much of the dayside, just poleward of the auroral oval. Away from noon (or more precisely, anywhere not immediately poleward of the cusp) the fluxes are reduced by a factor of about 10 as compared to the cusp plume, but other characteristics are quite similar. For example, the inferred temperatures and flow velocities, and the characteristic decline of energy and number flux with increasing latitude is essentially the same in a longitudinally broad ring of precipitation a few degrees thick in latitude over much of the dayside. We conclude that the field lines on which such precipitation occurs thread the magnetospheric plasma mantle over the entire longitudinally extended ring. Besides the location of occurrence (i.e., immediately poleward of the dayside oval), the identification is based especially on the associated very soft ion spectra, which have densities from a few times 10^{-2} to a few times $10^{-1}/cm^3$; on the temperature range, which is from a few tens of eV up to about 200 eV; and on the characteristic gradients with latitude. Further corroborating evidence that the precipitation is associated with field lines which thread the plasma mantle includes drift meter observations which show that regions so identified based on the particle data consistently lie on antisunward convecting field lines. Our observations indicate that some dayside high-latitude auroral features just poleward of the auroral oval are embedded in the plasma mantle.

1. Introduction

Much of the high-latitude magnetosphere is cloaked with a plasma "mantle," consisting of tailward flowing particles of magnetosheath origin. *Rosenbauer et al.* [1975] using Heos 2 data, and *Hardy et al.* [1975], using lunar-based observations, were the first to report the existence of the mantle. A mantle layer was identified in over 70% of the Heos 2 passes studied. Although *considerable* variability exists, as in most sections of the magnetosphere, typical temperatures are about 100 eV, typical densities are around a few times $10^{-2}/cm^3$ to $1/cm^3$, and typical flow velocities are 100–200 km/s. Usually, although not always, both the density and temperature decrease moving inward from the magnetosheath toward the magnetosphere.

The mantle is generally thicker for southward than northward interplanetary magnetic field (IMF) B_z , although great variability exists within all published data sets. *Sckopke et al.* [1976], using Heos 2 plasma and Imp 6 hourly IMF data reported that "the mantle is nearly always present when the IMF has a southward component . . . on the other hand, the mantle is thin or missing when the average IMF has a strong northward component." The data presented by Sckopke et al. show that the mantle was present for 8 out of 10 northward B_z passes, and 10 out of 11 southward IMF passes. *Hardy et al.* [1976], using lunar observations, found no clear correlation between hourly IMF B_z values and mantle thickness; however, *Hardy et al.* [1979] did find the appropriate correlation when higher time resolution IMF data was used.

The simplest explanation for the existence of the mantle, and its density and temperature gradients is that shown in Figure 1; adopt-

ed from *Rosenbauer et al.* [1975]. The essential argument is that lower energy ions (empty circles) spend a longer time transiting to and reflecting from the ionosphere than do higher energy ions (dark circles), and hence are transported a greater distance across field lines by the well-known velocity filter effect [e.g., *Shelley et al.*, 1976]. From this model, one would expect to find at low altitudes a population which was quite similar to the mantle directly poleward of the cusp; and which would be observable by the Defense Meteorological Satellite Program (DMSP), since those particles which are not mirrored are precipitated. This corresponds to a region which we term the "cusp plume," an example of which will be given in section 2. This region has previously been implicitly accepted as lying on field lines connected to the mantle [e.g., *Reiff*, 1979; *Erlandson et al.*, 1988]. Indeed, Reiff pointed out that the cusp proper—the region of direct magnetosheath entry—is intimately connected with the high-altitude mantle.

The purpose of the present paper is to document that a signature quite similar to the cusp plume—with greatly reduced densities, but the same ranges of temperature and flow velocity, and with the same characteristic dispersion signatures—occurs in a longitudinally broad ring just poleward of the dayside auroral oval. The time scale for the observed ions to transit from the dayside entry point to the ionosphere is much shorter than the time it takes ionospheric field lines to convect from the cusp around the polar cap and past the dawn-dusk flanks. We therefore infer that some additional direct entry—at levels 3 to 10 times lower than the fluxes seen in the cusp plume (poleward of the cusp proper)—must occur for a substantial interval while the field lines are convecting antisunward from the subsolar point.

Several years ago, *Vasyliunas* [1979] proposed a mapping from external magnetospheric regions to the ionosphere which has proven remarkably useful; this mapping is reproduced herein as Figure 2. In the course of the present paper, five DMSP dayside passes will be discussed explicitly. To orient the reader, and for reference in the remainder of the paper, the trajectories of these five passes are superposed onto the diagram. We particularly call attention to the fact that the mapping suggests that a substantial portion of the dayside ionosphere lies on field lines which thread the plasma mantle. The question of the low-altitude signature of the mantle ap-

---

[1]Applied Physics Laboratory, The Johns Hopkins University, Laurel, Maryland.

[2]Geophysics Laboratory, Hanscom Air Force Base, Massachusetts.

[3]Regis College Research Center, Weston, Massachusetts.

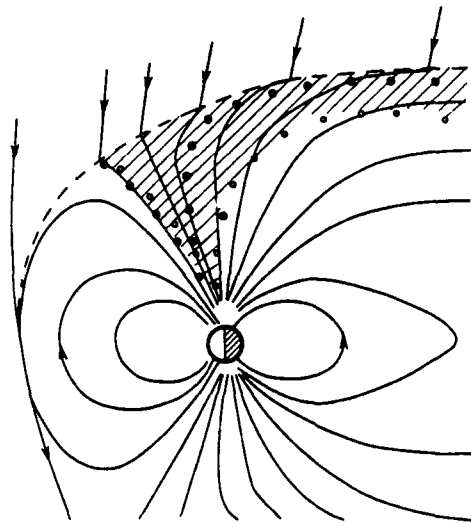[4]Now at Center for Space Physics, Boston University, Boston, Massachusetts.

Fig. 1. Adapted from *Rosenbauer et al.* [1975]. Low-energy ions (open circles) take longer to mirror from the ionosphere than do higher energy ions (closed circles), and are thus convected further across field lines, giving decreasing average energy and density with deeper penetration into the mantle (towards the magnetosphere).

Fig. 2. Adapted from *Vasyliunas* [1979]. One viewpoint of how various boundary layers map to the ionosphere.

pears to have been hitherto little addressed in magnetospheric research; and to our knowledge not addressed at all away from the cusp region.

Certain questions of the phenomenology of the low-altitude precipitation in the region lying on mantle field lines are also discussed. For example, we show that the mantle is the site of both small- and large-scale discrete auroral features. It is possible that the mantle is also the site of the "High-latitude dayside auroral features" reported by *Murphree et al.* [1990] to lie poleward of the auroral oval.

The present submission is one in a series of articles placing the ionospheric identification of magnetospheric regions based on particle signatures on a firmer basis. The initial papers dealt with quantifying the identification of the cusp proper [*Newell and Meng*, 1988; 1989]. The present work deals with establishing that a certain frequently occurring precipitation signature seen in the high-latitude dayside ionosphere lies on field lines which thread the magnetospheric plasma mantle.

2. DATA PRESENTATION

The data used in this investigation are from the DMSP F7 and F9 satellites. These DMSP satellites are in both sun-synchronous nearly circular orbits at about 835 km altitude, both in prenoon/-premidnight local time meridians with orbital inclinations of 98.7°. DMSP F7 (F9) have ascending and descending nodes at 1030 and 2230 LT (0930 and 2130 LT). F7 data is available from December 1983 to mid-1987, when F9, a currently operational satellite, replaced it. The SSJ/4 instrumental package included on both these flights measures electrons and ions from 32 eV to 30 keV in 20 logarithmically spaced steps [*Hardy et al.*, 1984]. The satellites are three-axis stabilized; and the detector apertures are always orientated toward local zenith. At the latitudes of interest in this paper, this means that only highly field-aligned particles well within the atmospheric loss cone are observed.

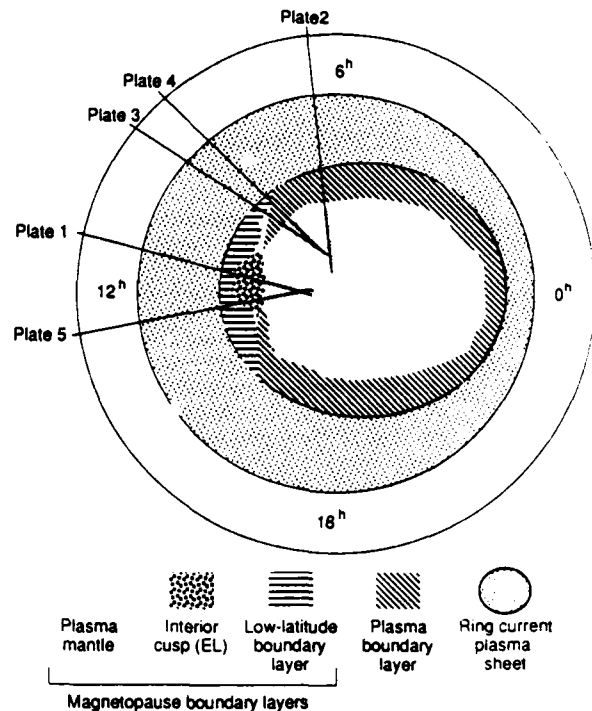DMSP F9 also carried an ion drift meter as one of four sensors

comprising the SSIES thermal plasma instrument (Special Sensor for Ions, Electrons, and Scintillation) [*Greenspan et al.*, 1986]. The other three sensors are an ion retarding potential analyzer, a total ion density trap, and a spherical electron Langmuir probe. The three ion sensors share a common aperture plane, which, when necessary, is biased away from the spacecraft potential to keep it close to the plasma potential. The drift meter is identical to the HILAT drift meter [*Rich and Heelis*, 1983] and similar to the drift meter flown on Dynamics Explorer 2 [*Heelis et al.*, 1981]. The components of the drift velocity perpendicular to the spacecraft are measured by determining the difference in currents to the top and bottom or left and right segments of the sensor.

2.1. Two Exemplary Cases

2.1.1. *Directly poleward of the cusp: the cusp "plume."* We begin our exposition in comparatively well known territory, namely, the dispersive magnetosheath precipitation seen directly poleward of the cusp—a region which we shall term the "cusp plume." Plate 1 shows an example, from January 26, 1984, at 1245 UT, of a DMSP F7 pass through the cusp proper [cf. *Newell and Meng*, 1988] with a clear well-developed energy latitude dispersion (the region labeled mantle is the cusp plume). Such smooth, continuous, fully developed cusp plumes monotonically decreasing in average energy and density with increasing latitude are, in our experience, an excellent indicator that the IMF B_z is southward (as it is indeed in this example, with an hourly average value of −2.2γ [*Couzens and King*, 1986]). In the schematic view presented by *Rosenbauer et al.* [1975] and reproduced herein as Figure 1, the precipitation poleward of the cusp should represent a sampling of the mantle population; since those electrons and ions not highly field aligned enough to precipitate should bounce and convect tailward to form the plasma mantle. There is no theoretical reason to believe that there should be a sharp boundary between the cusp proper and the
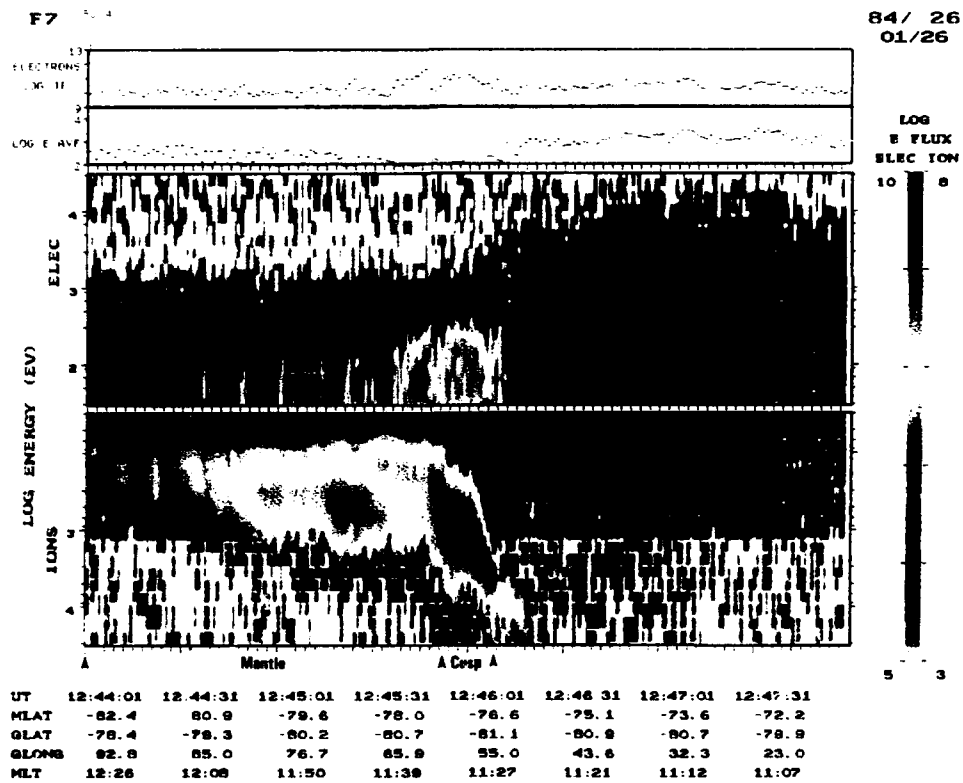
Plate 1. A DMSP F7 spectrogram showing a clear cusp and a classic "cusp plume" (mantle). The spectrogram shows differential energy flux from 32 eV to 30 keV in units of eV/cm^{2}s sr eV. The top line plot shows total energy flux (eV/cm^2 s sr); the lower line plot is of average energy (eV). Note that the ion energy scale is inverted.
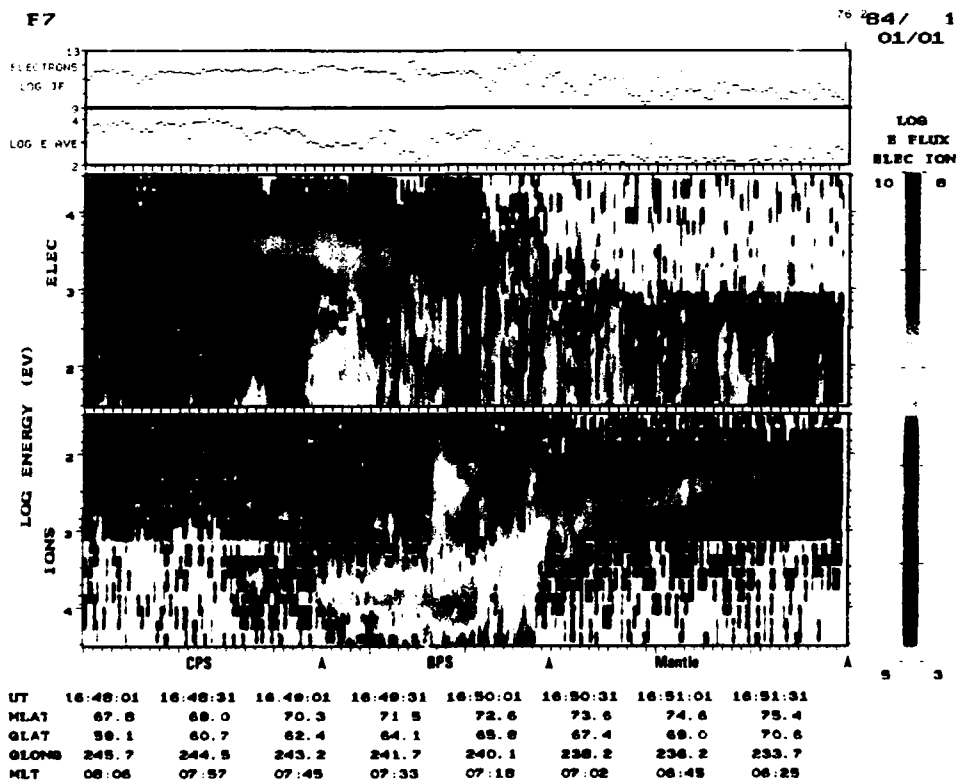

Plate 2. A DMSP F7 pass far away from noon, with no cusp precipitation observed, but with an extremely clear mantle signature. Note how the average ion energy and density falls with increasing latitude.

Temperature, density, and field-aligned velocity
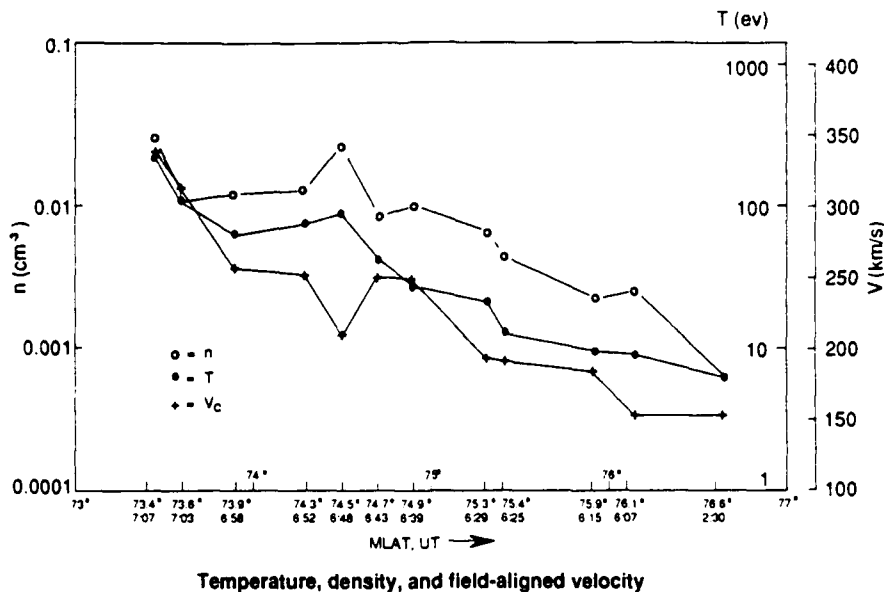
Fig. 3. Temperature, density, and field-aligned velocity with increasing magnetic latitude for the mantle region shown in Plate 2.

mantle (at least for B_z southward), and in general no sharp boundary is observed. Similarly, the cusp plume does not have a sharp poleward boundary but changes slowly into a pure (electron) polar rain.

It is apparent from Plate 1 that the usual properties of the mantle reported by Rosenbauer, namely, declining average energy and density with increasing distance from the magnetosheath source, are in evidence. (Other correlative evidence, including comparison of spectra, will be considered in section 2.2). Indeed, the low-altitude observation of such cusp plumes can be taken as tending to confirm Rosenbauer et al.'s hypothesis concerning the formation of the mantle as has previously been noted [Shelley et al., 1976; Reiff et al., 1977].

2.1.2. *Signatures well away from noon.* To our knowledge, no one has reported on whether such signatures exist away from the cusp. An extensive survey of DMSP F7 and F9 dayside crossings show that very similar signatures—often with the identical morphology, but always at reduced densities—do indeed exist over much of the dayside, just poleward of auroral oval region. A particularly clear example of such a dispersive region of magnetosheathlike precipitation observed well away from noon is given in Plate 2, which shows a DMSP F7 pass from January 1, 1984, around 1650 UT (B_z is not known for this case). The absolute values for the number flux are about 10 times lower than in the cusp plume of Plate 1 (a little less than 10^6 ions/cm^2 s sr versus 10^7 ions/cm^2 s sr, respectively). We have fit spectra by convecting Maxwellians for 12 different points within the region labeled as mantle in Plate 2; the results are shown in Figure 3 (Maxwellians were chosen primarily for convenience, as discussed in section 3.1; some individual sample fits are shown in section 2.2). If the temperature along magnetic field lines is lower than the temperature perpendicular to field lines the density inferred at low altitude will be systematically too low by the factor $T_{\parallel}/T_{\perp}$ (refer to section 3.1). Nonetheless, it is evident that the densities, temperatures, and velocities (although the latter is strictly the field-aligned velocity) are those appropriate to the mantle. Moreover, the mantle exhibits its characteristic declining density and falling temperatures with

increasing latitude (corresponding to deeper inside the magnetosphere within the high-altitude mantle—cf. Figure 1). The particles which we observe are precipitating and hence cannot themselves go on to populate the mantle, but presumably they represent a fair sampling of those which do.

We have examined several hundred spectrograms of dayside high-latitude precipitation in the DMSP F7 and F9 data; our conclusion is that in a large majority of cases some type of signature such as shown in Plate 2 can indeed be discerned. It would not be very surprising, after a little reflection, to occasionally see a portion of the cusp plume without observing the cusp itself; since depending on ionospheric convection patterns one can easily imagine satellite orbits well off noon in which this could happen. However what we observe is the routine, almost pervasive, observation of some variation of the signature shown in Plate 2, regardless of the dayside local time and sign of B_y (strong variations in intensity do occur and will be studied systematically in future work). To be sure, most such signatures (either poleward of the cusp or otherwise) are not as clear or simple as in Plates 1 and 2. Almost every magnetospheric plasma regime, whether encountered at low or high altitude, has structure beyond the simple monotonic declines in energy and density of those two examples. Two other factors are perhaps even more critical in identifying a plasma regime as mantle are: (1) The presence of very soft ions, generally with even lower energy than typical of the low-altitude cusp, generally with little or no precipitation above 1 keV; (2) The position, namely furthest poleward of the dayside auroral oval.

2.2. *Two Examples Which are More Typical and with Corroborating Evidence*

The examples presented in section 2.1 were "classic" examples; that is, the overall energy and density trends were very clear, and there were no complicating peculiarities. In this section we present two cases which are representative rather than exemplary; including some additional evidence to corroborate the mantle identification. One such less esthetic, but more typical, low-altitude mantle encounter is shown in Plate 3, which is a spectrogram of a DMSP

F9 pass from about 1205 UT on January 7, 1989. The various regions are demarcated by arrows and labels. We identify the region from 1206:30 to 1207:12 UT as BPS; i.e., the extension of the region of the discrete auroral oval into the dayside. The mantle extends from 1207:13 to 1207:48 UT. Within this region, ion average energy and density declines with increasing latitude, as can be seen in the line plots in the top two panels of Plate 3, although not so smoothly as in the previous examples. Note also that spiky electron acceleration events occur within the mantle as well as the traditional auroral oval; an important point which we will return to later.

Figure 4 presents the drift meter observations from the DMSP F9 on-board SSIES instrument. The region inferred to be mantle from the particle measurements (from 1207:13 to 1207:48 UT) is indicated on the spectrogram. Although there are some calibration uncertainties, in Figure 4, sunward is negative and antisunward is positive. Hence the drift meter observations confirm that the particle region which is identified as mantle in Plate 3 lies on antisunward convecting field lines (and indeed, the BPS/mantle boundary appears to lie near the sunward/antisunward convecting boundary). Poleward of the particle mantle signature in Figure 4 is a region of low velocity, apparently with slightly sunward convection. Most of this is due to the effects of corotation (160 m/s), which have not been corrected for in the figure; this correction would leave the velocity close to zero. We are not sure what physical significance to attach to the region of near-zero convection velocity (the drift turns significantly antisunward again poleward of Figure 4); at face value it would appear to imply a slight kink in the convection drifts if fitted to the Maynard-Heppner convection patterns.

A sample spectrum from the mantle region of Plate 3 is shown in Figure 5. To get an idea of the macroscopic parameters, various simple fits to convecting Maxwellians were tried; as shown in the figure a reasonable fit (the error bars are simply those due to Poisson statistics) was found with $n = 0.015/cm^3$; $kT = 110$ eV; $V_o = 210$ km/s (convection velocity). All these values are well within the range of typical mantle values; providing further confirmation of the identification.

A second representative example of a mantle identification away from noon is given in Plate 4. Plate 4 shows a DMSP F9 pass from April 23, 1989, starting at 0945:00 UT; the region which we identify as mantle is indicated by arrows, namely from 0945:18 to 0946:15 UT. (The region immediately equatorward we identify as LLBL; further equatorward is BPS and then CPS. The basis of the LLBL/BPS distinction on the dayside is simply the spectral properties compared to their high-altitude counterparts). The general trends for the density and average energy to decline are present within the mantle region, although there are considerable fluctuations, and a discrete electron acceleration event can be observed (0945:40 UT). Further evidence supporting the mantle identification is given in Figure 6, which shows the drift meter observations during the time interval given by the spectrogram. Once again, the region identified as mantle by the particle signature lies within a region of antisunward convection (positive Vhor). A sample spectrum is shown in Figure 7; in this case a reasonable fit is given by $n = 0.1/cm^3$; $kT = 100$ eV; and $V_o = 100$ km/s. These parameters all lie well within the range of normal mantle values. We have examined several further cases not shown here; the region identified as mantle by the particle precipitation characteristics lies with very good consistency on antisunward convecting field lines.

2.3. A Large-Scale Discrete Aurora in the Mantle

In this section we document the occurrence of discrete auroral features on mantle field lines. Some evidence for such features can be observed in the passes already presented; for example in the polar pass shown Plate 4, there is a small scale electron acceleration event at 0945:40 UT. In this section we present an example of a particularly intense and large-scale discrete auroral event. The event, shown in Plate 5, occurred on a DMSP F7 pass from January 26, 1984, around 1425 UT. The interplanetary magnetic field was southward for several consecutive hourly averages [Couzens and King, 1986]; for the hour ending 1500 UT, B_z-averaged -3.3 γ and B_y-averaged -6.2 γ (5-min IMF values were also consistently southward for more than an hour before the crossing). For the dayside pass shown in Plate 5 the mantle ions have an abrupt poleward cutoff at 1425:20 UT; precisely the latitude at which the electrons show signs of acceleration by an electrostatic potential. A sample spectrum is shown in Figure 8; the sharp cutoff above 2000 eV indicates a potential drop of this magnitude above the satellite and a low thermal temperature of the unaccelerated source population [Evans, 1968]. Of course, the value of the accelerating potential rises and falls over the course of the arc structure.

Plate 5 also includes the perturbation in the east-west (cross-satellite) component of the magnetic field. We wish to point out two results of interest from the magnetometer measurements. First, the region 1 current system corresponds to the cusp proper; whereas the mantle currents (as identified by Erlandson et al. [1988]) correspond to the particle signature which we also identify as mantle. Secondly, the discrete feature appears in a region of field-aligned currents which are flowing out of the ionosphere. Although Plate 5 is unusual in the scale size and clear structure (an inverted V) of the mantle arc, in our experience less dramatic electron acceleration events on smaller scales are quite common in the mantle region.

3. DISCUSSION

Two main topics are considered in this section: the possible mechanism for producing such a great longitudinal extent in the low-altitude mantle precipitation (section 3.1); and the occurrence of auroras within this mantle precipitation (section 3.2).

As a preface, there are clear limitations to the procedure we used to determine the parameters (flow velocity, density, and temperature) in the low-altitude plasma mantle. The DMSP particle detector apertures are always orientated toward local zenith; which at the latitudes of interest means only highly field-aligned precipitation is observed. Our procedure was simply to fit, by trial and error, a convecting Maxwellian to the ion spectrum. We tried Maxwellian fits first, because they are simple, rather than from any theoretical grounds. Indeed, the simple Rosenbauer picture (Figure 1) seems to imply that the observations at any localized point should be non-Maxwellian (a point that has been conveniently overlooked in previous studies of high-altitude observations). The fact that the Maxwellian fits worked well—the curves pass within error bars of far more than three points, which is the number of parameters in the fit—appears to us to be justification enough for using this functional form, at least to get approximate values for the integral parameters. If a more systematic investigation of spectra fits continued to show that Maxwellian fits worked well, some theoretical modification or improvement on the Rosenbauer cartoon would be necessary.

A limitation on our observations is that it is only possible to infer the field-aligned component of the velocity, and the field-aligned temperature. Moreover, if the parallel and perpendicular temperatures are not equal, as is quite likely for precipitation threading the mantle (both the inflow population from the subsonic magnetosheath [Crooker et al., 1976] and the outflow population in the external mantle [Rosenbauer et al., 1975] exhibit this property), then the density, n, inferred by such a low-altitude fit is only a fraction,
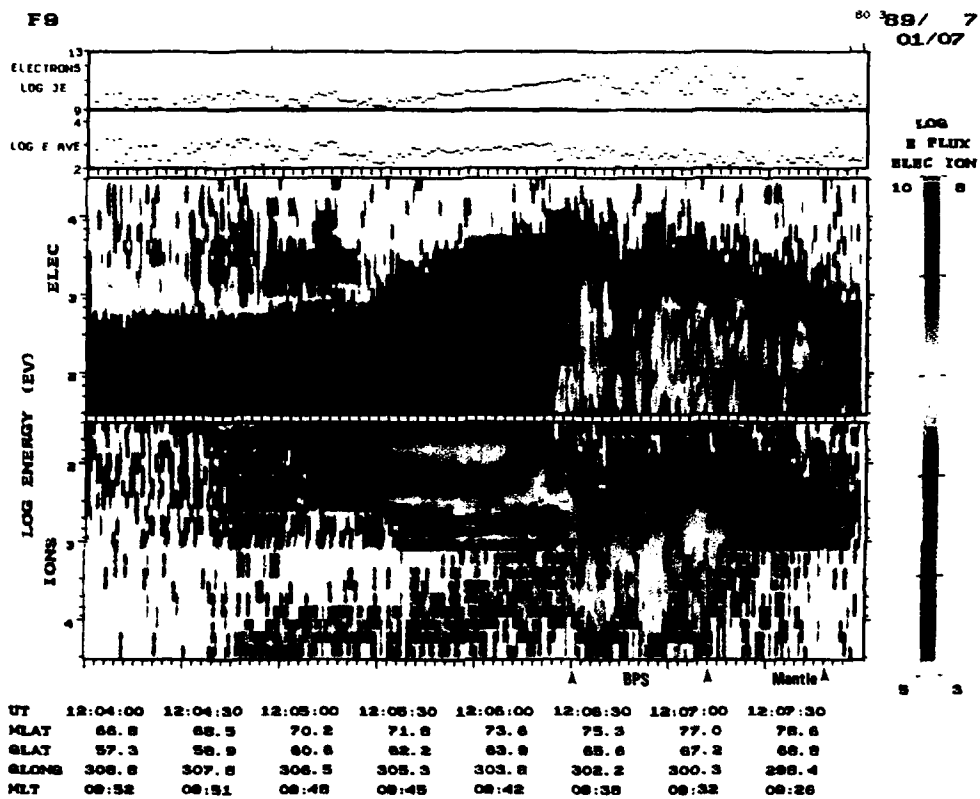
Plate 3. A DMSP F9 dayside polar pass showing a less classic but more representative mantle crossing.
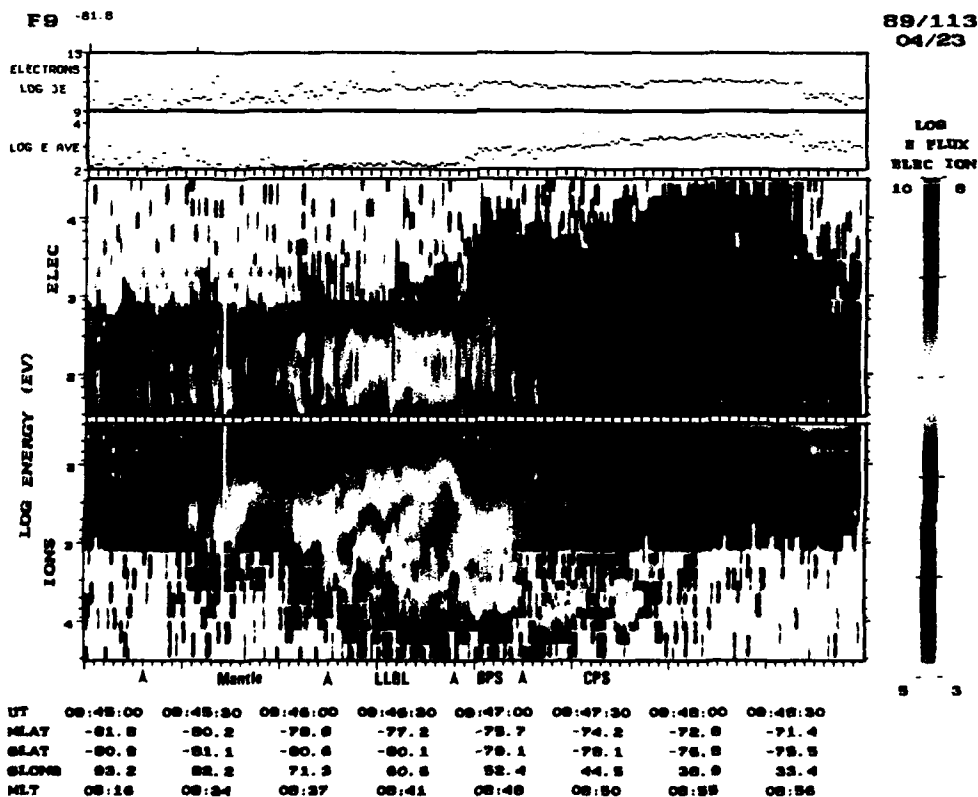

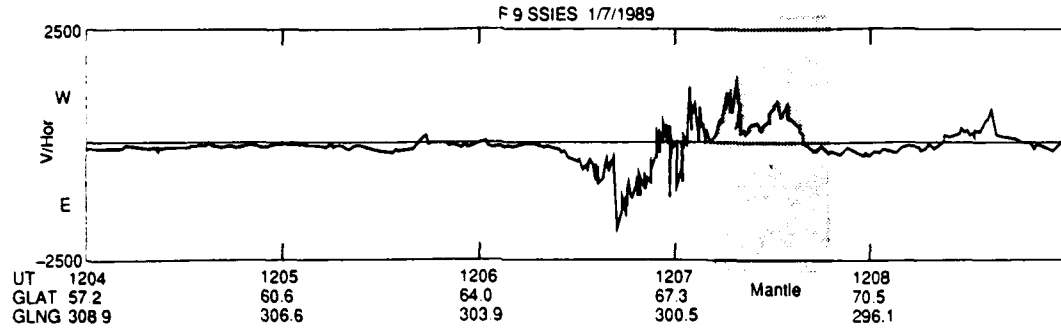Plate 4. A DMSP F9 spectrogram showing a representative mantle crossing.

Fig. 4. Drift meter observations corresponding to the DMSP F9 pass shown in Plate 3. The shaded region denotes the boundary of the mantle as determined from the particle data. Positive values indicate westward and antisunward convection; negative values eastward and sunward convection. The vertical scale is in meters per second.
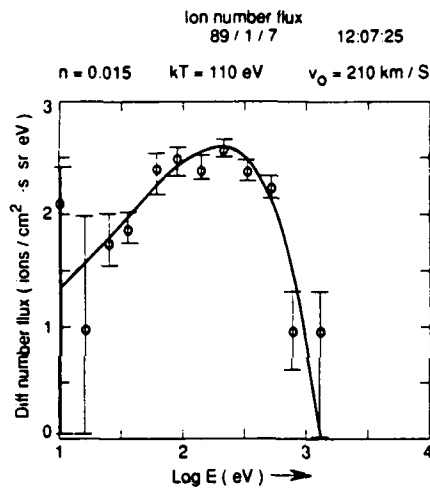
Fig. 5. A sample ion spectrum (differential number flux) from the mantle region for the pass shown in Plate 3. A reasonable fit is obtained from a convecting Maxwellian with parameters $n=0.015/$cm^3; $kT = 110$ eV; and $V_o = 210$ km/s.

namely, $T_\parallel/T_\perp n$, of the true density, as was worked out in the context of cusp precipitation by *Hill and Reiff* [1977; Appendix A]. The physical reason is quite simple: the higher the perpendicular temperature, the fewer highly field-aligned particles capable of reaching low-altitude exist; hence since only the parallel tempera-

ture is measured, one can infer an incorrectly low density if $T_\perp$ is actually larger than the measured $T_\parallel$. On the basis of value of this temperature ratio in published high-altitude mantle encounters [e.g., *Rosenbauer et al.*, 1975] and the dayside subsonic magnetosheath [*Crooker et al.*, 1976], one could project our inferred densities to be reduced below the true values by as much as a factor of 4.

3.1. Possible Mechanisms for Widespread Low-Altitude Mantle Precipitation

A basic question is whether all the mantle precipitation observed is in fact simply directly entering from the dayside magnetosheath (that is, the low-altitude mantle signature we observe represents that fraction of the entering plasma which precipitates rather than bouncing and heading tailward to form the magnetospheric mantle); or whether some of the precipitation is return flow from the distant tail regions. As the following considerations will show, it is probable that the bulk of the mantle precipitation observed is directly entering; although it is necessary that at least weak dayside entry occur over a region substantially more longitudinally extended than the cusp proper (where entry is essentially uninhibited and very intense).

The following essential facts must be accommodated: (1) Mantle precipitation is observed over a very wide longitudinal range, much larger than is the cusp. The cusp is only observed about 25% of the time as far away from noon as 10 MLT [*Newell and Meng*, 1989], whereas it is the norm to observe some type of mantle precipitation at this local time, and quite often out to the dawn and dusk flanks. (2) Fairly substantial (typically 100 km/s to 300 km/s) field-aligned flow velocities are observed. (3) The mantle signa-
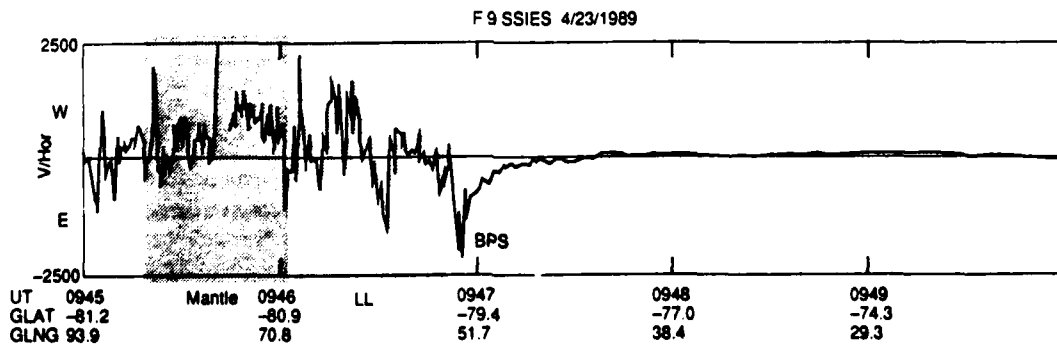

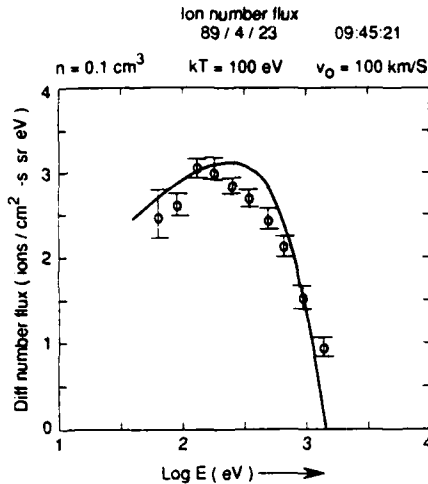Fig. 6. Same as Figure 4, except for the pass shown in Plate 4.

Ion number flux

89 / 4 / 23   09:45:21

$n = 0.1$ cm^3 $kT = 100$ eV $v_o = 100$ km/S

Fig. 7. A sample ion spectrum (differential number flux) from the mantle region for the pass show in Plate 4. A good fit is obtained from $n = 0.10/$cm^3; $kT = 100$ eV; $V_o = 100$ km/s.

ture is most intense (about 10^7 ions/cm^2 s sr) directly poleward of the cusp; and much less intense (10^6 ions/cm^2 s sr) away from the cusp.

Observation (2) is particularly difficult to explain if the source of the precipitation is the mantle at large |r| in the tail. Although the temperature is high enough compared to the bulk flow velocity that some back streaming component is possible (cf. Figure 9 of *Rosenbauer et al.* [1975]), we are not aware of reports that a sizable counterstreaming population with a appreciable bulk velocity toward the Earth exists.

However, the low-altitude dispersive mantle signature cannot owe simply to direct entry in the cusp region except in the cusp plume (near noon). This can be shown very simply. The signature is commonly observed as far away as the dawn flank (e.g., Plate 2). The time it takes a field line reconnected near the subsolar point to convect to the dawn flank is $t = \pi r/2v$, where r is the polar cap radius and v is the ionospheric convection velocity. Taking the polar cap radius to be 15°; and the ionospheric convection velocity to be a generous 400 m/s, it takes a field line 1 hour 48 min to make the trip. However, the time of flight from entry of magnetosheath plasma into the cusp until precipitation, given the measured flow velocities, is about 15 min. It is thus physically clear that the "mantle" precipitation signature observed away from noon is not an extension of the cusp plume but rather due to additional direct entry which occurs at a much weaker pace for field lines further away from noon (hence at increasingly long times since reconnection). This should not be surprising: there is no reason that dayside entry should go from essentially free access (in the cusp) to essentially no entry at all (for field lines which map deep down the tail) without going through any intermediate steps.

We are thus led to the opinion that the mantle precipitation likely represents a modified version of direct entry (Figure 1). The modification consists of assuming that as reconnected field lines convect around the polar cap boundary and poleward (downstream), some amount of particle entry continues, at a considerably lesser rate; indeed, there is probably some partial flow toward the Earth until after the reconnected field lines cross the dawn-dusk boundary. A proton with a 100 km/s velocity goes $10 R_e$ in about 10 min, so that (delayed) precipitation can occur over a somewhat

greater local time extent than direct entry does. We believe that a combination of these two effects, namely, entry occurring at a reduced rate for a longer time than does the intense, most direct entry near the cusp; and, to a lesser extent, the slow transit time from the magnetosphere boundary to the ionosphere for slow flowing ions, together probably account for the much larger longitudinal extent of mantle precipitation as compared to cusp precipitation.

Nonetheless, the magnetic field mapping can be extremely complicated in the high-latitude dayside region (as was illustrated, for example, by *Birn et al.* [1990]); and considering the scarcity of information on mantle distribution functions it is not possible at this time to preclude some component of mantle precipitation as being due to a return flow from the tail.

Finally, we note that our observations of a particle mantle signature which is not just confined to the near noon (poleward of the cusp) region but longitudinally extended over much of the dayside is in complete agreement with the recent magnetometer observations of *Erlandson et al.* [1988] of a "mantle" current system which is likewise longitudinally dispersed.

3.2. *Auroras Within the Region of Mantle Precipitation*

It is well established that most arcs occurring within the polar cap are associated with northward B_z [e.g., *Hardy et al.*, 1986; *Lassen et al.*, 1988]; and most polar cap arcs appear to be associated with poleward expansion of the dawn and dusk flanks of the auroral oval into the polar cap [*Meng*, 1981; *Gussenhoven et al.*, 1982; *Hones et al.*, 1989; *Makita et al.*, 1990]. Our present research shows that a different source of very high latitude dayside auroral arcs exists; namely that some dayside arcs occurring just poleward of the auroral oval are embedded in the low-altitude region which maps to the ionospheric mantle. A very clear example of this was given in Plate 5; although it is unusual in the scale size and clear structure of the mantle arc; less dramatic electron acceleration events on smaller scales are quite common in the mantle region. For example, in the polar pass shown Plate 4 there is a small scale electron acceleration event at 0945:40 UT. At this stage in our research it would only be speculation as to whether the great differences in scale size are due to intrinsic differences in the events, or merely the angle at which the satellite crosses the arcs.

The inverted V in Plate 5 occurred in a region of field-aligned mantle current out of the ionosphere. Although the observation is postnoon, it is consistent with the large IMF B_y value (-6.2 γ) that the region 1 current system is into the ionosphere [*Erlandson et al.*, 1988] and that the mantle current system (formerly known as the cusp current system) is out of the ionosphere [*Iijima* and *Potemra*, 1976]. Earlier work [e.g., *Lyons*, 1980] has shown that discrete aurora tend to occur in regions where the magnetospheric convection electric field satisfies $\nabla \cdot E < 0$, thus leading to the establishment of currents out of the ionosphere and field-aligned potential structure. The *Heppner* and *Maynard* [1987] convection model BC (the appropriate one for the observational conditions) would suggest $\nabla \cdot E < 0$ in the region where we observe the arc (refer to their Figure 3). Thus the observation of such a transoval inverted V on clearly open field lines should in hindsight perhaps not be too surprising.

Murphree et al. [1990] have recently reported on dayside high-latitude auroral features. These features are distinct from polar cap arcs, with which they are, however, connected. The features occur poleward of the visible oval ring, and are suggested by Murphree et al. (on the basis of latitude of occurrence) to be the result of merging occurring just poleward of the cusp. These high-latitude dayside features are observed primarily for northward B_z, when the antiparallel merging model [*Crooker*, 1979] would indicate that merging
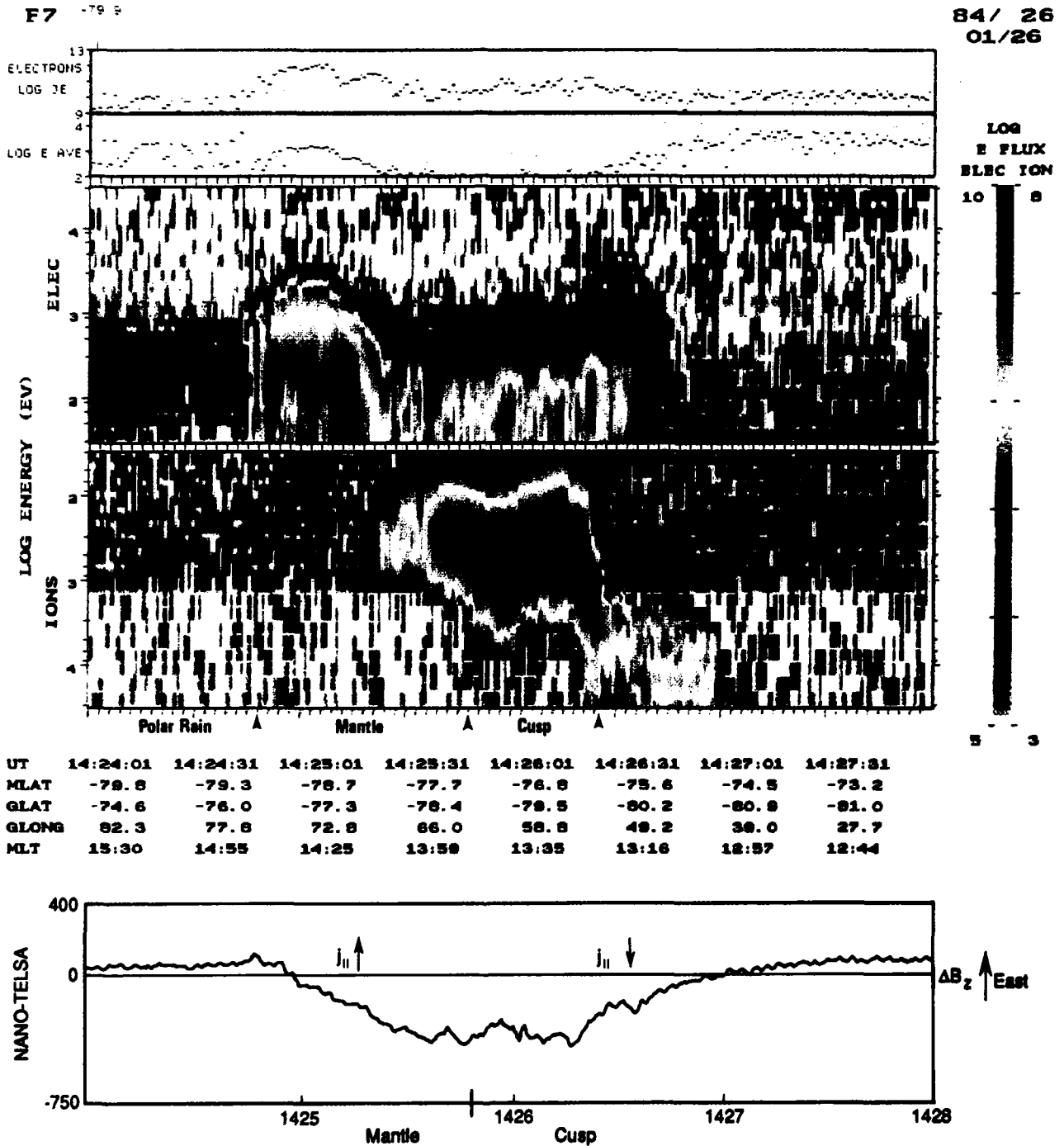
Plate 5. A spectrogram of a near noon dayside crossing which includes the cusp proper and the low-altitude mantle signature. A large-scale inverted V auroral structure is embedded in the mantle region. The line plot underneath the spectrogram shows the simultaneous magnetometer east/west magnetic perturbations. The "mantle" current system lies in the region identified as mantle based on the precipitating particle signature.

is most favored just poleward of the cusp. Because most of the events reported upon by *Murphree et al.* occurred for northward B_z while the event shown in Plate 5 happened during a prolonged interval of southward B_z, the relationship between the two categories of dayside transoval arcs is an open question. There is certainly room for distinct sources of such activity at high latitude on the dayside: For example—pressure pulses, Kevin-Helmholtz waves,

FTEs, impulsive solar wind penetration, etc.—and one should not be too hasty in identifying different observations as the same phenomenon.

Although it is probably unnecessary, we note briefly that the discrete arc structures embedded in the mantle as reported upon here, and also the structures identified in the Viking images by Murphree et al., are unrelated to the "mantle aurora" observed at much lower
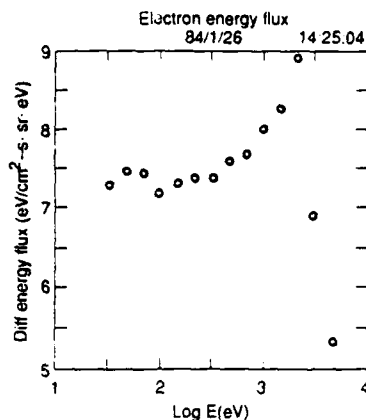
Electron energy flux
84/1/26   14 25.04

Fig. 8.   A sample electron spectrum (differential energy flux) showing a monoenergetic peak indicative of a 2000-V accelerating potential.
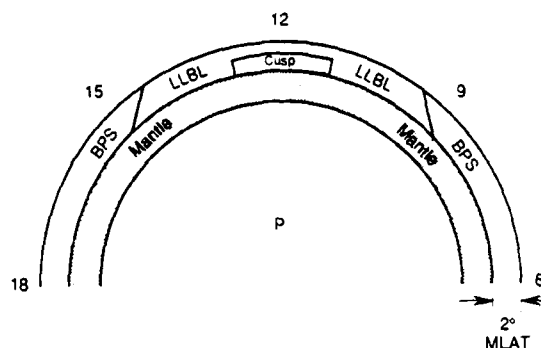

Fig. 9.   A modification of the figure of Vasyliunas based on our observations. The mantle forms a latitudinally narrow ring poleward of the other boundary layers.

latitudes [*Sanford*, 1964] which maps to the zone of hard (several keV) electron precipitation whose source is CPS electrons convected from the nightside [*Meng* and *Akasofu*, 1983].

4.   SUMMARY AND CONCLUSIONS

We have carried out what is, to our knowledge, the first identification of a low-altitude identification of the plasma mantle based on the precipitating particle signatures (away from the noon-time polar cusp—cf. *Reiff* [1979]). The identification is based on the following criteria: (1) Location, namely immediately poleward of the cusp or dayside auroral oval; (2) A general tendency for the density and average ion energy to decline with increasing latitude; (3) Drift meter measurements which indicate that the mantle as identified by the particle signature consistently lies on antisunward convecting field lines; and (4) Fitted convecting Maxwellian distributions which have ion densities and temperatures appropriate to the mantle (temperatures are a few tens of eV up to about 100 eV; densities are a few times 10^{-2} to a few times $10^{-1}/cm^3$).

We observe that discrete auroral features of varying size are at times found within the mantle region. Hence such features represent auroral forms which lie poleward of the main auroral oval. Since it is now fairly well established that discrete auroral forms are associated with field-aligned currents [e.g., *Kamide and Rostoker*, 1977; *Bythrow and Potemra*, 1987], it is not too surprising that the mantle—which has associated field-aligned currents [*Erlandson et al.*, 1988]—is also the site of discrete arcs, particularly when the current is out of the ionosphere [*Lyons*, 1980].

The particle signature of the mantle is observed over a very wide longitudinal range; although the latitudinal band over which mantlelike precipitation is observed is usually only a few degrees. Hence our observations are consistent with the schematic view of *Vasyliunas* [1979] (reproduced here as Figure 2), except that the precipitation signature of mantle field lines is a much narrower band in latitude than suggested in that schematic (presumably because most mantle field lines map to regions with only tailward flow). We offer Figure 9, a modification of Vasyliunas's schematic view, to summarize our research results to date on the magnetospheric source of ionospheric precipitation. In Figure 9, only the cusp size and positioning are currently statistically established, but we hope that the present work will be a prelude to a statistical study in which the morphology of mantle precipitation is statistically determined as well. The low-altitude mantle is observed under a vari-

ety of IMF conditions; but we leave it to future work to establish the role of B_z and B_y in shaping the low-altitude mantle phenomenology.

REFERENCES

Birn, J., E. W. Hones Jr., J. D. Craven, L. A. Frank, R. Elphinstone, and D. P. Stern, Open and closed field line regions in Tsyganenko's field model and their possible associations with horse-collar auroras, *Geophys. Res. Lett.*, in press, 1990.

Bythrow, P. F., and T. A. Potemra, Birkeland currents and energetic particles associated with optical auroral signatures of a westward traveling surge, *J. Geophys. Res.*, 92, 8691–8699, 1987

Couzens, D. A., and J. H. King, Interplanetary medium data book, *Suppl.* 3A 1977–1985, GSFC/NASA 86-04, Goddard Space Flight Cent., NASA, Greenbelt, Md., 1986.

Crooker, N. U., G. L. Siscoe, and R. B. Geller, Persistent pressure anisotropy in the subsonic magnetosheath region, *Geophys. Res. Lett.*, 3, 65–68, 1976.

Crooker, N. U., Dayside merging and cusp geometry, *J. Geophys. Res.*, 84, 951–959, 1979.

Erlandson, R. E., L. J. Zanetti, T. A. Potemra, P. F. Bythrow, and R. Lundin, IMF B_y dependence of region 1 Birkeland currents near noon, *J. Geophys. Res.*, 93, 9804–9814, 1988.

Evans, D. S., The observation of a near monoenergetic flux of auroral electrons, *J. Geophys. Res.*, 73, 2315–2323, 1968.

Greenspan, M. E., P. B. Anderson, and J. M. Pelagatti, Characteristics of the thermal plasma monitor (SSIES) for the Defense Meteorological Satellite Program (DMSP) spacecraft S8 through S10, Rep. AFGLTR-86-0227, Air Force Geophys. Lab., Hanscom Air Force Base, Mass., 1986.

Gussenhoven, M. S., Extremely high latitude auroras, *J. Geophys. Res.*, 87, 2401–2412, 1982.

Hardy, D. A., H. K. Hills, and J. W. Freeman, A new plasma regime in the distant geomagnetic tail, *Geophys. Res. Lett.*, 2, 169–172, 1975.

Hardy, D. A., J. W. Freeman, and H. K. Hills, Plasma observations in the magnetotail, in Magnetospheric Particles and Fields, edited by B. M. McCormac, p. 89, 1976.

Hardy, D. A., H. K. Hills, and J. W. Freeman, Occurrence of the lobe plasma at lunar distance, *J. Geophys. Res.*, 84, 72–78, 1979.

Hardy, D. A., L. K. Schmitt, M. S. Gussenhoven, F. J. Marshall, H. C. Yeh, T. L. Shumaker, A. Hube, and J. Pantazis, Precipitating electron and ion

detectors (SSJ/4) for the block 5D/flights 6-10 DMSP satellites: Calibration and data presentation, Rep. AFGL-TR-84-0317, Air Force Geophys. Lab., Hanscom Air Force Base, Mass., 1984.

Hardy, D. A., M. S. Gussenhoven, K. Riehl, R. Burkhardt, N. Heinemann, and T. Schumaker, The characteristics of polar-cap precipitation and their dependence on the interplanetary magnetic field and the solar wind, in *Solar Wind-Magnetosphere Coupling*, edited by Y. Kamide and J. A. Slavin, pp. 575–604, 1986, TERRAPUB, Tokyo, 1986.

Heelis, R. A., W. B. Hanson, C. R. Lippincott, D. R. Zuccaro, L. H. Harmon, B. J. Holt, J. E. Doherty, and R. A. Power, The ion drift meter for Dynamics Explorer-B, *Space Sci. Instrum.*, *5*, 511–521, 1981.

Heppner, J. P., and N. C. Maynard, Empirical high-latitude electric field models, *J. Geophys. Res.*, *92*, 4467-4489, 1987.

Hill, T. W., and P. H. Reiff, Evidence of magnetospheric cusp proton acceleration by magnetic merging at the dayside magnetopause, *J. Geophys. Res.*, *82*, 3623–3628, 1977.

Hones, E. W., J. D. Craven, L. A. Frank, D. S. Evans, and P. T. Newell, The horse-collar aurora: A frequent pattern of the aurora in quiet times, *Geophys. Res. Lett.*, *16*, 37–40, 1989.

Iijima, T., and T. A. Potemra, Field-aligned currents in the dayside cusp observed by Triad, *J. Geophys. Res.*, *81*, 5971–5979, 1976.

Kamide, Y., and G. Rostoker, The spatial relationship of field-aligned currents and auroral electrojets to the distributions of nightside auroras, *J. Geophys. Res.*, *82*, 5589–5608, 1977.

Lassen, K., C. Danielsen, and C.-I. Meng, Quiet-time average auroral configuration, *Planet. Space Sci.*, *36*, 791–799, 1988.

Lyons, L. R., Generation of large-scale regions of auroral currents, electric field potentials, and precipitation by the divergence of the convection electric field, *J. Geophys. Res.*, *85*, 17–24, 1980.

Makita, K., C.-I. Meng, and S.-I. Akasofu, Transpolar auroras, their particle precipitation, and IMF B_y component, submitted to *J. Geophys. Res.*, 1990.

Meng, C.-I., Polar cap arcs and the plasma sheet, *Geophys. Res. Lett.*, *8*, 273–276, 1981.

Meng, C.-I., and S.-I. Akasofu, Electron precipitation equatorward of the auroral oval and the mantle aurora in the midday sector, *Planet. Space Sci.*, *31*, 889–899, 1983.

Murphree, J. S., R. D. Elphinstone, D. Hearn, and L. L. Cogger, Large-scale high-latitude dayside auroral emissions, *J. Geophys. Res.*, *95*, 2345–2354, 1990.

Newell, P. T., and C.-I. Meng, The cusp and the cleft/LLBL: Low-altitude identification and statistical local time variation, *J. Geophys. Res.*, *93*, 14,549–14,556, 1988.

Newell, P. T., and C.-I. Meng, On quantifying the distinctions between the cusp and the cleft/LLBL, in Electromagnetic Coupling in the Polar Cleft and Caps, edited by P. E. Sandholt and A. Egeland, 87–101, Kluwer Academic, Dordrecht, Netherlands, 1989.

Reiff, P. H., Low-altitude signatures of the boundary layers, Proceedings of Magnetospheric Boundary Layer Conference, *Eur. Space Agency Spec. Publ.*, *148*, 1979.

Reiff, P. H., T. W. Hill, and J. L. Burch, Solar wind plasma injection at the dayside magnetospheric cusp, *J. Geophys. Res.*, *82*, 479–491, 1977.

Rich, F. J., and R. A. Heelis, Preliminary data processing plan for the thermal plasma experiment on the HILAT satellites, *Tech. Rep. AFGL-TR-83-0091*, Hanscom Air Force Base , Mass., 1983.

Rosenbauer, H. H. Grunwaldt, M. D. Montgomery, G. Paschmann, and N. Sckopke, Heos 2 Plasma observations in the distant polar magnetosphere: The plasma mantle, *J. Geophys. Res.*, *80*, 2723–2737, 1975.

Sanford, B. P., Aurora and airglow intensity variations with time and magnetic activity at southern high latitudes, *J. Atomos. Terr. Phys.*, 26, 749–769, 1964.

Sckopke, N., G. Paschmann, H. Rosenbauer, and D. H. Fairfield, Influence of the interplanetary magnetic field on the occurrence and thickness of the plasma mantle, *J. Geophys. Res.*, *81*, 2687–2691, 1976.

Shelley, E. G., R. D. Sharp, and R. G. Johnson, He^{++} and H^+ flux measurements in the dayside cusp: Estimates of the convection electric field, *J. Geophys. Res.*, *81*, 2363–2370, 1976.

Vasyliunas, V. M., Interaction between the magnetospheric boundary layers and the ionosphere, Proceedings of Magnetospheric Boundary Layer-Conference, *Eur. Space Agency Spec. Publ.*, *148*, 1979.

W. J. Burke, Geophysics Laboratory, Hanscom Air Force Base, MA.

M. E. Greenspan, Boston University, Center for Space Physics, Boston, MA.

C.-I. Meng, P. T. Newell, and E. R. Sanchez, The Johns Hopkins University Applied Physics Laboratory, Johns Hopkins Road, Laurel, MD 20723.

Some Low-Altitude Cusp Dependencies on the Interplanetary Magnetic Field

PATRICK T. NEWELL, CHING-I. MENG, AND DAVID G. SIBECK

The Johns Hopkins University Applied Physics Laboratory, Laurel, Maryland

RONALD LEPPING

Planetary Magnetospheres Branch, Goddard Space Flight Center, Greenbelt, Maryland

Although it has become well established that the low-altitude polar cusp moves equatorward during intervals of southward interplanetary magnetic field (IMF $B_z < 0$), many other important aspects of the cusp's response to IMF components are not as well investigated. An algorithm for identifying the cusp proper was applied to 12,569 high-latitude dayside passes of the DMSP F7 satellite (which is in a nearly circular polar orbit at ~838 km altitude), and the resulting cusp positioning data were correlated with the IMF (IMF data were available for about 25% of the cases). It was found that the peak probability of observing the cusp shifts prenoon for B_y negative (positive) in the northern (southern) hemisphere and postnoon for B_y positive (negative) in the northern (southern) hemisphere. The B_y induced shift is much more pronounced for southward than for northward B_z, a result that appears to be consistent with elementary considerations from, for example, the antiparallel merging model. No interhemispherical latitudinal differences in cusp positions were found that could be attributed to the IMF B_x component. As expected, the cusp latitudinal position correlated reasonably well (0.70) with B_z when the IMF had a southward component; the previously much less investigated correlation for B_z northward proved to be only 0.18, suggestive of a half-wave rectifier effect. The ratio of cusp ion number flux precipitation for B_z southward to that for B_z northward was 1.75 ± 0.12. The statistical local time (full) width of the cusp proper was found to be 2.1 hours for B_z northward and 2.8 hours for B_z southward.

1. INTRODUCTION

For many years the term "cusp" has been used loosely and variously, with the cusp having been identified in a variety of ways, many conflicting. It has become increasingly clear on the basis of particle signatures that there exists a "cusp proper," localized near noon in magnetic local time, in which magnetosheath plasma entry is more direct [*Formisano*, 1980; *Heikkila*, 1985; *Gussenhoven et al.*, 1985; *Lundin*, 1988]. *Newell and Meng* [1988a] have recently quantified the cusp-cleft distinction, showing statistically that a simple algorithm based primarily on the average energy of the electrons and especially the ions leads to a natural separation of the roughly magnetosheathlike precipitation that occurs on the dayside into two morphologically distinct regions, termed the cusp and the cleft/boundary layer. The cusp is a localized region near noon with spectral properties closer to the original magnetosheath plasma and a number flux approximately 4 times higher than that in the cleft/boundary layer (about the same ratio as observed in ISEE crossings from the magnetosheath into the boundary layer [cf. *Sckopke et al.*, 1981]). This paper presents the statistical dependence of the cusp, using this more restricted and quantitative definition, on IMF components. Three years worth of DMSP F7 dayside high-latitude passes were studied; we herein concentrate on the aspects of the cusp IMF dependency that are still comparatively less investigated, such as the B_x and B_y effects.

The existence and behavior of the low-altitude cusp are the clearest and most persistent signs of large-scale quasi-steady-state reconnection in magnetospheric physics. If the cusp is on closed field lines, it represents a region where (magnetosheath) plasma is steadily transported across lines of distinct magnetic field topology and hence fits one of the standard definitions of merging [e.g., *Vasyliunas*, 1975]. If, as we believe, the cusp lies on open field lines, it represents a site of merging by any definition. More-over, the cusp exhibits well-documented behavior consistent with merging theory, the most striking of which is its movement equatorward for southward IMF B_z [*Burch*, 1973; *Meng*, 1983; and most comprehensively to date, *Carbary and Meng*, 1986].

However, there are many theories of merging and a paucity of data for use in choosing between them. Indeed, the situation is still uncertain enough that the importance of merging in magnetospheric dynamics can still be questioned [e.g., *Eastman et al.*, 1984; *Heikkila*, 1984]. The persistency of the cusp (it is probably always present) requires that it be a steady-state merging phenomenon of some type, as opposed to, for example, the patchy unsteady merging that flux transfer events (FTEs) are often assumed to represent. FTEs are seen primarily only for southward IMF B_z [e.g., *Rijnbeek et al.*, 1984]. In this paper we consider the simplest model of merging, namely, the antiparallel hypothesis of *Crooker* [1979, 1988], and compare one of its most basic predictions, namely, the dependence of the location of merging sites on IMF B_z and B_y, with a large statistical data base giving the probability of observing the cusp as a function of MLT and the IMF parameters. We find excellent qualitative agreement between the predictions of the antiparallel model and our empirical cusp observation probabilities. We also investigate a predicted IMF B_x effect on the interhemispherical difference in cusp latitude [e.g., *Cowley*, 1981] with negative results; in the discussion section we show how the gasdynamic model of *Spreiter and Stahara* [1980] can explain the absence of a B_x effect. Finally, some other interesting effects of IMF on cusp behavior are reported.

There have been several previous studies of the effects of IMF B_y on related ionospheric effects, notably convection patterns and Birkeland currents. For example, *Heelis* [1984] found that the dayside convection throat was shifted toward dawn for a garden hose IMF, regardless of the sign of B_y, although B_y did control the dawn/dusk component of the flow poleward of the throat. *Burch et al.* [1985] presented B_y dependent high-latitude dayside convection patterns for B_z negative. They also found the southward B_z convection throat to be nearly stationary, although they lo-

cated the throat at noon. Recently, there has been considerable work on high-latitude convection patterns [e.g., *Heppner and Maynard*, 1987; *Foster et al.*, 1986; and others], a review of which would be outside the scope of the present work.

The signs of ionospheric currents in the general region of the cusp depend on IMF B_y [*Iijima et al.*, 1978; *Erlandson et al.*, 1988]. The Svalgaard-Mansurov effect shows that high-latitude ground-based measurements are affected by the interplanetary sector structure [*Svalgaard*, 1973]. The study most relevant to our own is that of *Candidi et al.* [1983]. They produced statistical contours of dayside 50-eV electron precipitation (from 2 months of DMSP F2 dayside passes) binned by MLAT and MLT with IMF B_z and B_y separation. They found that for B_z northward, a shifting of the contours appropriate to the sign of B_y was discernible, whereas for B_z southward, results were harder to interpret. They believed that the dynamical variations characteristic of the southward B_z situation obscured (smeared out) the B_y effect in the MLAT/MLT binning method.

It should be emphasized that our algorithm [*Newell and Meng*, 1988a] is based on pattern recognition rather than on the more traditional MLAT/MLT binning schemes. In the latter approach [*McDiarmid et al.*, 1975; *Candidi et al.*, 1983; *Hardy et al.*, 1985; *Gussenhoven et al.*, 1985; *Foster et al.*, 1986] all precipitation occurring at a given MLAT and MLT is put into a bin (usually with additional separation by Kp, but sometimes with separation by other factors such as solar wind conditions), and the result is then studied for the probable position of the cusp or other features. Because of the highly dynamic nature of the cusp location, particularly for southward B_z, and its dependence on many variables (e.g., dipole tilt angle [*Newell and Meng*, 1989]), the results are not always clear. Our algorithm attempts to identify the cusp position on each individual pass, and the statistics are performed subsequently. In short, the traditional approach first averages, then looks for the cusp; we look for the cusp, then average.

2. DATA PRESENTATION

The data used herein are from the electrostatic analyzers on the SSJ/4 package on the Air Force DMSP F7 satellites. These analyzers measure electrons and ions from 32 eV to 30 keV in 20 logarithmically spaced steps each. *Hardy et al.* [1984] has described the instruments and their calibration in detail. DMSP F7 is in a Sunsynchronous nearly circular polar orbit at about 838 km altitude in approximately the 1030-2230 LT plane. The detector apertures always point toward local zenith so that, at the high latitudes of interest here, only precipitating particles are observed.

The algorithm used for identifying the cusp proper (that is, the morphologically distinct and comparatively localized region about noon where the particles best maintain their original magnetosheath spectral characteristics, and the number flux is highest) was previously documented and justified [*Newell and Meng*, 1988a]. The following criteria are used, of which the most important is the ion average energy: (1) If the energy flux of the ions (electrons) is less than 10^{10} eV/cm^2 s sr (6×10^{10}), a region is neither cusp nor boundary layer. (2) If the previous criterion is met, the region is boundary layer if either 3000 eV < E_i < 6000 eV or 220 eV < E_e < 600 eV, where E_i and E_e are the average ion and electron energies, respectively. (3) If the first criterion is met and both 300 eV < E_i < 3000 eV and E_e < 220 eV, the region is identified as cusp.

The average energies given above should not be confused with the energy flux spectral peaks. There are several reasons why average energies significantly exceed spectral peak energies. The low-

altitude cusps in the DMSP F7 data as determined above have ion energy flux peaks near about 1 keV and electron energy flux peaks typically around 50 eV, values that are much closer to the original magnetosheath energies. However, the average energies (over the 32 eV to 30 keV range) are, generally speaking, somewhat higher, partly because fewer low-energy ions make it into the mid-altitude [*Frank*, 1971] and low-altitude [*Newell and Meng*, 1988a] cusp, and partly because some higher-energy ions are present that apparently escaped from the magnetosphere [e.g., *Sibeck et al.*, 1987; *Williams et al.*, 1988]. There may be additionally some acceleration of the magnetosheath flux peak prior to observation in the low-altitude cusp [*Hill and Reiff*, 1977], but this is still far from established. Figure 1 shows how the peak number flux observed on dayside passes varies as a function of the average energy (binned over a 3-year period). Figure 1 proves that the regions of lower average ion energies (and thus energies closer to the original magnetosheath values) are also the regions in which more particles are entering (the number fluxes are higher). In addition, the clear break in the average energy-number flux relationship is one of the pieces of evidence that indicate the existence of two morphologically distinct dayside regions of approximately magnetosheathlike particles, namely, the cusp proper and the boundary layer. The ion average energy that divides the two regions can be determined from Figure 1. A much more complete discussion is presented in *Newell and Meng* [1988a].

Three years worth of DMSP F7 dayside passes from December 1983 to December 1986, consisting in all of approximately 12,500 passes, were studied according to the above algorithm. The geomagnetic coordinate system used to organize the data was basically that of *Gustaffson* [1984]. Hourly averaged IMF data from IMP 8 were used via the Goddard NSSDC on-line OMNI program; IMF information was only available for approximately 25% of the passes. It is believed from simple arguments that B_y should produce mirror image effects in the two hemispheres. Because most of the 1000 MLT and earlier passes are in the northern hemisphere, and nearly all the passes at local times later than this are in the southern hemisphere, we could not separate by hemisphere as well
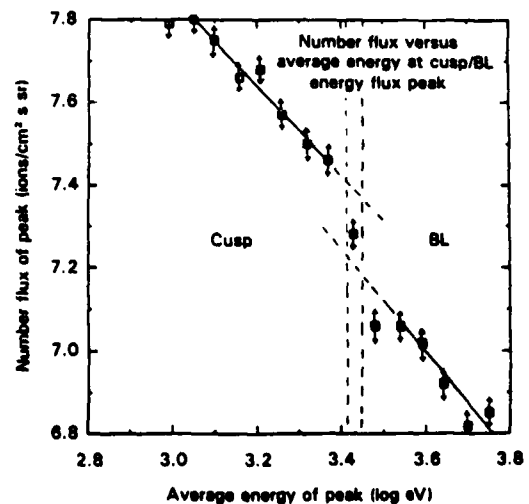

Fig. 1. For each DMSP F7 dayside pass, the point of peak ion energy flux was recorded irrespective of region (cusp or boundary layer) and binned by average energy. Plotted is the (3 year) average number flux versus log energy bin. The lower average energy passes have higher number fluxes; the clear break that occurs at about 3000 eV corresponds to the transition between regions that we classify as cusp and those that are classified as boundary layer.
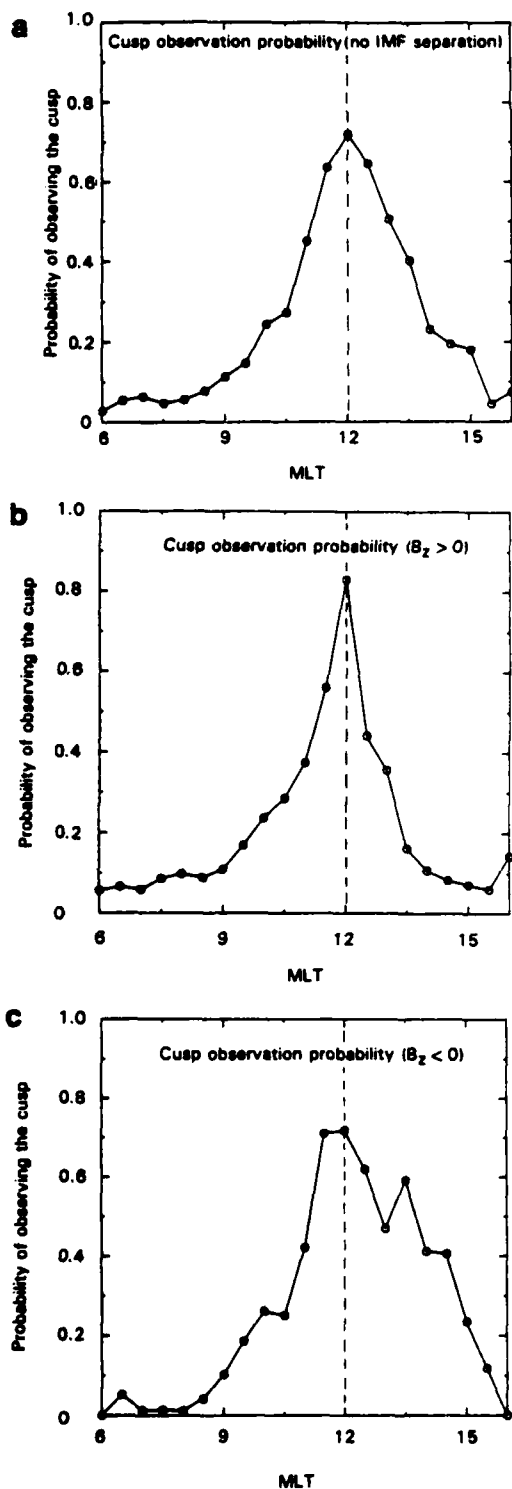
Fig. 2. The probability as a function of MLT (in half-hour bins) of observing the cusp on a given DMSP F7 dayside pass. (a) With no separation by IMF. Based on a total of 12,569 passes (which contain 2427 observations of the cusp) the peak probability of observing the cusp is at 1200 MLT. (b) The probability curve for B_z northward (2446 passes; 426 cusp observations). (c) The same for B_z southward (1972 passes; 450 cusp observations).

as by IMF sign. Thus northern hemisphere cases with B_y positive (negative) are always grouped with southern hemisphere cases with B_y negative (positive). A similar statement holds for B_x separations. Since this inversion is always applied, a statement in this paper applying for B_y positive always refers to the northern

hemisphere cases, with the reverse sign of B_y applying to the southern hemisphere cases.

Figure 2 shows the probability of encountering the cusp on a given dayside pass as a function of MLT for no IMF separation (Figure 2a), for IMF B_z northward (Figure 2b), and for IMF B_z southward (Figure 2c). In computing the probabilities, an assumption is made that if the satellite failed to encounter any type of dayside "oval" precipitation on a given orbit, it was because it did not reach high enough latitude. This assumption is believed to be reliable, since to our knowledge there has never been a pass by any satellite suitably instrumented and which reached high enough latitudes that did not encounter any dayside high-latitude precipitation region (*Heikkila* [1985] makes the same claim). This assumption was used to normalize the probabilities presented in Figure 2. Passes where the MLT changed by 1 hour or more from entering to exiting a precipitation region (i.e., a large slant angle cut through the oval) were also excluded and are also renormalized for in Figure 2.

Two clear effects can be discerned from Figure 2. First, the cusp longitudinal (local time) width is larger for southward than for northward B_z. This effect can be quantified by noting that the statistical width of the cusp, w, is given by $w = \int P_c(t)\, dt$, where P_c is the probability of observing the cusp as a function of MLT, denoted t. To keep the statistics reasonably meaningful, we restrict the area of integration to the bins from 0600 to 1500 MLT; over this range all IMF subgroupings (including groupings by both B_y and B_z) have at least 20 passes in each local time bin. For the case of no IMF separation, the cusp is statistically 2.6 hours wide in longitude. For B_z northward and southward, the local time width of the cusp is 2.1 and 2.8 hours, respectively. Thus the southward B_z cusp is longitudinally wider (but latitudinally narrower, as shown previously [*Newell and Meng*, 1987; *Carbary and Meng*, 1988]).

Notice, however, that the peak probability of observing the cusp, which occurs at noon for either sign of B_z, is larger for B_z northward than for B_z southward. One possible explanation is that for southward B_z the cusp has more of a tendency to move about. To investigate the most obvious cause, we subdivide further, by the sign of B_y in addition to the sign of B_z. Figures 3a-3d show the four B_y, B_z combinations. In these plots, only cases where $|B_y| \geq 3\gamma$ were included, a condition that makes the IMF dependence clearer. Thus our results are restricted to cases with a significant (but not necessarily large) B_y. It is fairly obvious in Figures 3c and 3d that B_y does indeed account for the movement of the cusp for southward B_z, whereas for northward B_z (Figures 3a and 3b) the cusp has less of a tendency to shift from magnetic noon. For southward B_z the peak probability of observing the cusp shifts by 0.5 hour (1.5 hours) toward dawn (dusk) for B_y negative (positive). Note also that for northward B_z some B_y effect is apparent; although the peak does not shift, there is an asymmetry in the distribution that is appropriate to the sign of B_y. In the discussion section we will interpret the greater B_y effect for southward B_z.

We next investigate the possibility of a B_x effect. A latitudinal asymmetry between the hemispheres has been proposed [*Cowley*, 1981] to result from the effects of B_x, with high-latitude features shifted toward midnight in the northern (southern) hemisphere for B_x positive (negative). Thus one might expect to find the cusp at higher latitudes for B_x positive than for B_x negative. To address this question, the average cusp latitude over the MLT range 1000-1300 has been determined for B_x positive (negative) in the northern (southern) hemisphere and compared to the cusp latitude for B_x negative (positive) in the northern (southern) hem-
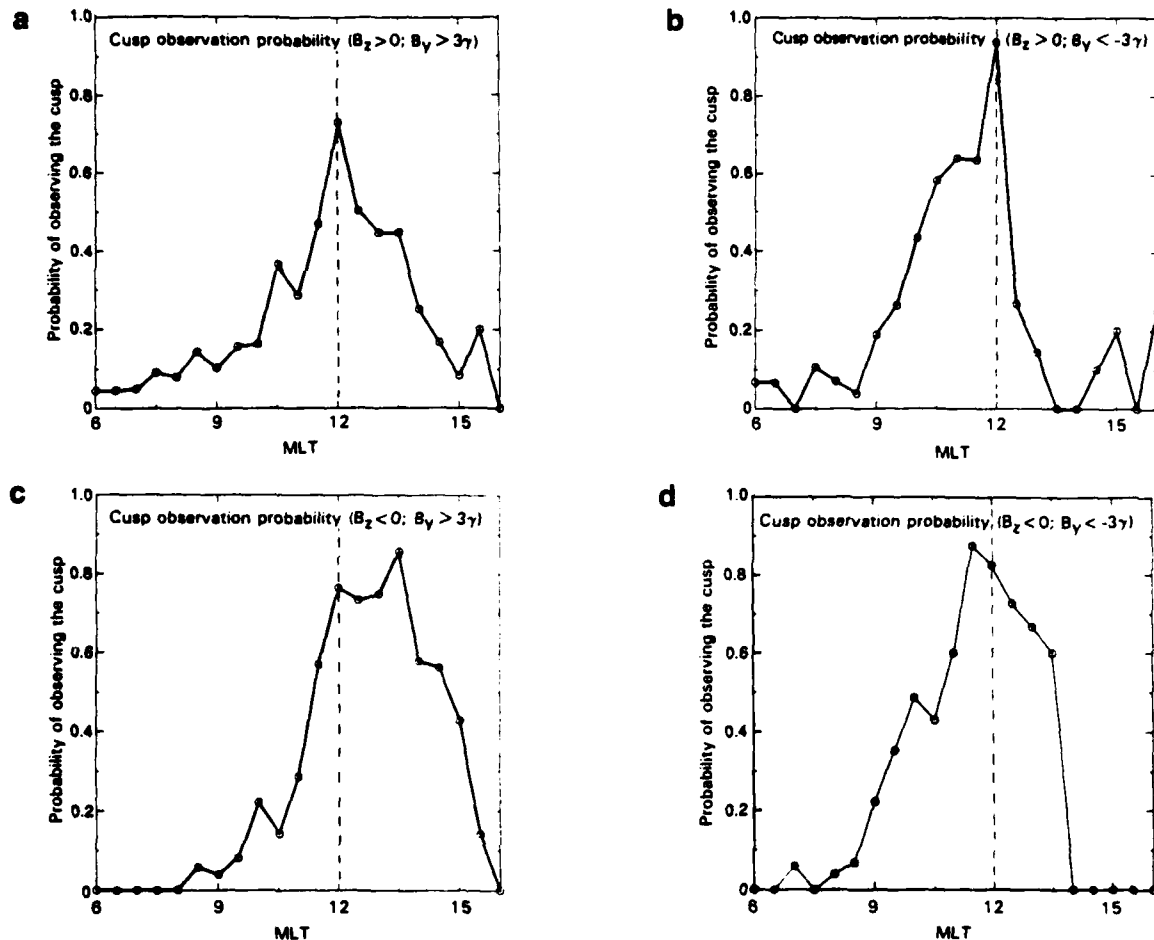
Fig. 3. (a) Same as Figure 2, for B_z northward and B_y > 3γ (total of 579 passes); (b) for B_z northward and B_y < −3γ (607 passes); (c) for B_z southward and B_y > 3γ (473 passes); (d) for B_z southward and B_y < −3γ (497 passes). The signs of B_y given apply to the northern hemisphere; the reverse sign is used in the southern hemisphere.

isphere. Figure 4a compares the position of the equatorward boundary of the cusp for the two B_x conditions (with no B_z separation). No dependence of the cusp latitude on the sign of B_x is apparent in this figure. To further investigate the question, plots were made with separation by B_z in addition to B_x. No clear latitude dependence was found in either case; Figure 4b presents the results for southward B_z. The equivalent of Figure 4 has also been calculated for the poleward cusp boundary (not presented here). Again, no pattern is discernible. In the discussion section we provide a possible explanation for the lack of a B_x effect.

It has become well established that the cusp latitude moves equatorward for B_z southward and, indeed, moves further south for increasingly negative B_z [Burch, 1973; Meng, 1983; Carbary and Meng, 1986]. Whether the cusp continues to move poleward for increasingly positive B_z is a question that has received comparatively little attention. In the original study of Burch [1973], it was found, based on about thirty points, that there was only a slight trend for the cusp to continue moving northward for increasingly positive B_z. The data in Figure 8 of Reiff et al. [1980] show that the four latitudinal positions in the large B_z bin do not lay poleward of the nine positions in the smaller northward B_z magnitude bin. The larger study of Carbary and Meng [1986] did not address this issue.

We believe it worthwhile to address this critical question explicitly and quantitatively. Figure 5 shows a scatterplot of the cusp

latitude as a function of both southward (5a) and northward (5b) B_z. In Figure 5, only cusp observations between 1100 and 1300 MLT were included, which reduces the scatter a bit. It is evident that there is little correlation for the northward B_z case. To quantify matters, the correlation between the cusp equatorward boundary and B_z is 0.70 for B_z southward (201 cases in the 1100–1300 MLT range) and 0.18 for B_z northward (148 cases). These correlations include a correction for dipole tilt angle of 0.06° MLAT/1° dipole tilt [Newell and Meng, 1989]. The results are almost identical for the cusp poleward boundary. Thus we are led to agree with the assertion [Burch, 1973] that for increasingly northward B_z, the cusp displays only a slight tendency to move to higher latitudes.

Coupling the present results with previous work, the general morphology of the cusp and its dependence on the IMF now appear to be fairly well established. A less investigated topic is the dependence of the cusp particle fluxes on the interplanetary magnetic field. Candidi and Meng [1984] reported that electron precipitation in the cusp was "roughly a factor of two" times larger for southward than for northward B_z. It is of interest to address this question again in a more precise manner, and using the availability of ion as well as electron data. On each DMSP pass through the cusp, the peak ion and electron energy flux was recorded on a sliding 3-s average. The statistical ratio of the ion (electron) number flux for southward B_z to northward B_z cases is 1.75 ± 0.12
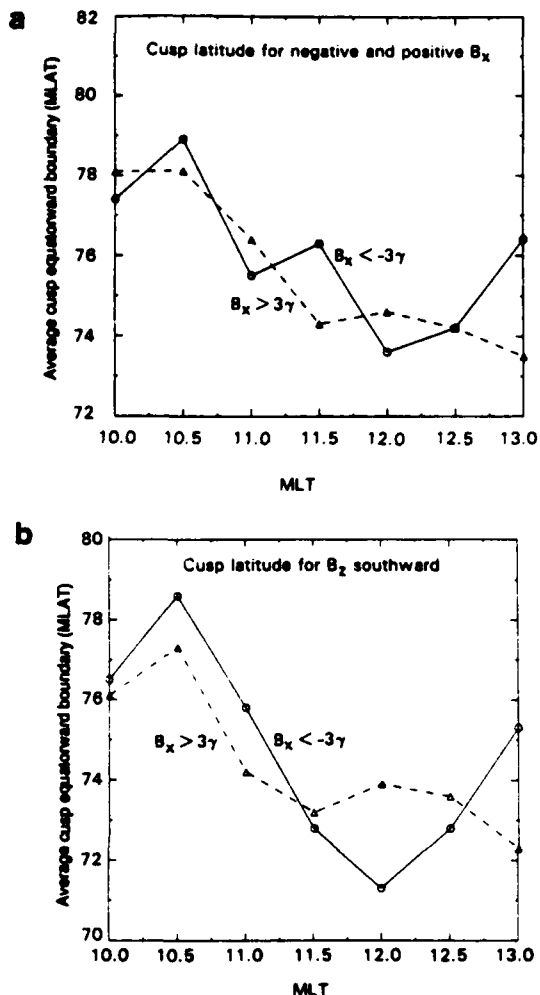
Fig. 4. The B_x dependence of the latitude of the equatorward boundary of the cusp as a function of MLT (a) for no B_z separation; (b) For B_z southward. The solid lines refer to $B_x < -3\gamma$ ($B_x > 3\gamma$) in the northern (southern) hemisphere; the dashed lines refer to $B_x < 3\gamma$ ($B_x < -3\gamma$) in the northern (southern) hemisphere.

(1.59 ± 0.10). The average energies changed comparatively little for the two cases; the southward to northward ratio for the ion (electron) average energy was 0.95 ± 0.02 (0.93 ± 0.01).

3. DISCUSSION AND INTERPRETATION

The results of the previous section showed that the local time position of the cusp depended much more strongly on IMF B_y when B_z was southward than it did for northward B_z. A possible explanation can be found in the antiparallel merging hypothesis, which holds that magnetic merging is most likely to occur at magnetopause locations where the IMF and the magnetospheric fields are antiparallel (instead of component merging models, which often consider only the B_z component). Figure 6, reproduced with permission from Crooker [1979], shows the location of the merging sites based on a shielded dipole field (i.e., including an image dipole) plus a uniform IMF. (The more recent antiparallel merging models give a result qualitatively very similar; see Figure 1 of Crooker [1988].) The view is in the YZ plane, from the Sun looking toward the Earth. The dashed lines show the direction of the IMF; the heavy lines are the merging sites based on the antiparallel hypothesis. It is clear from Figure 6 (for example, by comparing the IMF directions labeled 1 and 2) that the merging region has

a much wider latitudinal extent for B_z southward than for B_z northward, given the same B_y. Indeed, for B_z northward, the merging sites remain comparatively tightly clustered about noon, which appears to agree well with our observations (Figure 2b). While we do not suggest that the present results provide definitive evidence for any particular merging model, we are impressed that such a simple hypothesis seems to explain the behavior of the location of the most direct magnetosheath plasma entry (i.e., the low-altitude cusp).

The direction of the B_y shift we observe is consistent with elementary considerations, for example, the dipole plus uniform IMF model [Lyons, 1985]. It is also consistent with recent observations of the displacement of the external cusp (i.e., the magnetic cusp at the magnetopause) [Crooker et al., 1987]. However, there is a possible discrepancy with the work of Holzworth and Meng [1984]. They fit circles to DMSP photographs of the auroral oval and studied the dependence of the center of the fitted circles to IMF B_x and B_y. On the basis of 59 cases they found that in the northern hemisphere the shift was 0.0° ± 1.9°; in the southern hemisphere (78 cases) they found a duskward shift of 2.4° ± 1.8° when comparing cases of $B_y < -2\gamma$ with cases of $B_y > 2\gamma$. The shift of Holzworth and Meng [1984] is opposite that evident in Figure 3 of our work (i.e., their southern hemisphere observations would be expected to shift dawnward for positive B_y). It is also opposite the direction of the shift found in previ-
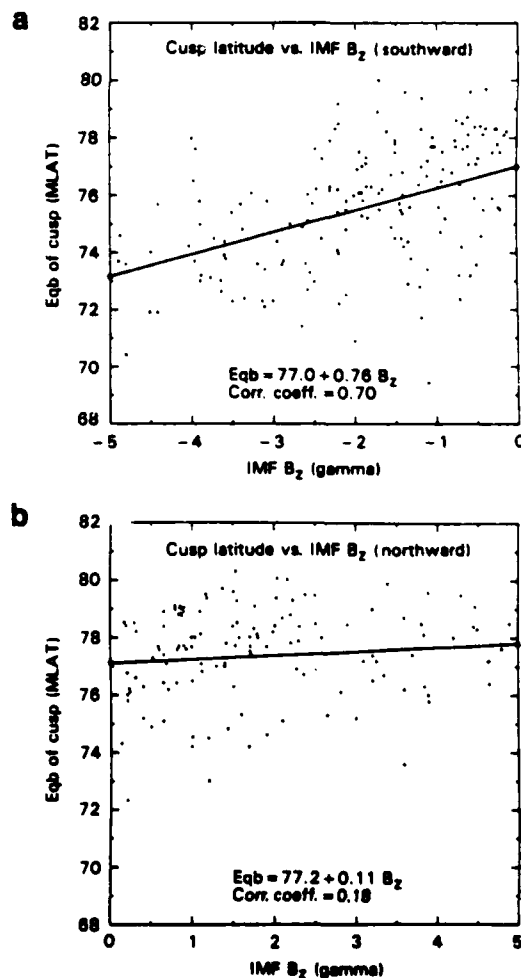

Fig. 5. The latitude of the cusp equatorward boundary as a function of IMF B_z (a) for southward B_z; (b) for northward B_z. The correlation coefficient in Figure 5a is 0.70; for Figure 5b it is only 0.18.
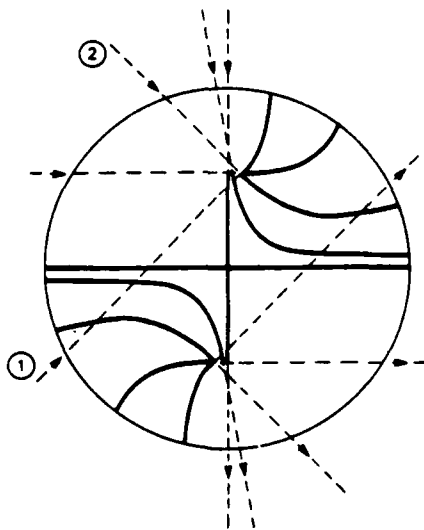
Fig. 6. (Adopted with permission from *Crooker* [1979].) The view is from the Sun toward the Earth. The dashed lines are IMF orientations; the connecting heavy lines are the resultant merging lines under the antiparallel hypothesis. The IMF orientations labeled 1 and 2 have the same B_y component but opposite B_z signs. Note that for southward B_z (2) the merging line is greatly extended toward dawn (in the northern hemisphere), whereas for northward B_z the merging line is more closely confined near noon (1).

ous studies in which low-altitude dawn–dusk effects were apparent [*Candidi et al.*, 1983; *Burch et al.*, 1985; *Iijima et al.*, 1978; etc.]. It is not clear why the centers of circular fits to the auroral oval differ from all these other studies and from elementary consi J rations. One possible reason is that since the circular fits to the visible aurora rely more heavily on the nightside than the dayside, the two regions may not respond in the same way to the IMF B_y. *Holzworth and Meng* [1984] did not find any surward/tailward shift due to B_x.

We consider next the absence of a B_x effect on the interhemispherical cusp latitudinal difference, as shown in our Figure 4. A simple explanation can be found from the predictions of gasdynamic theory [e.g., *Spreiter and Stahara*, 1980]. As the shocked solar wind approaches the magnetopause subsolar point, the plasma is compressed, and the density rises. The IMF B_y and B_z both are intensified (in the gasdynamic model they go to infinity); however, the magnetosheath B_x component is reduced (in the gasdynamic model it goes to zero at the subsolar point). Hence the field in contact with magnetopause differs greatly from the upstream IMF and indeed is different in such a way as to intensify the B_y and B_z coupling, while reducing the B_x coupling. The absence of an interhemispherical cusp latitude effect in our data due to B_x may result from this simple effect. We note that while *the evidence for the existence of a partial penetration of the IMF B_y* component into the magnetotail is clear [*Fairfield*, 1979; *Cowley and Hughes*, 1983], the evidence for a similar penetration of the IMF B_x effect is much more ambiguous [*Hughes and Cowley*, 1986].

To some extent, the present results are reminiscent of the "half-wave rectifier" concept of IMF-magnetosphere coupling [e.g., *Crooker*, 1980]. For B_z southward, both the latitudinal position (which follows B_z) and the longitudinal position (which follows B_y) are highly dependent on the IMF. For B_z northward, neither the magnitude of B_z nor the sign of B_y strongly affects the cusp position. This relatively poor correlation for northward B_z is evi-

dently true of the whole auroral oval; *Makita and Meng* [1984] similarly found very low correlation coefficients between the IMF B_z component and various auroral boundaries in various local time sectors for quiet time (mostly northward B_z) conditions.

4. CONCLUDING COMMENTS

The morphology of the cusp is now reasonably well established on a quantitative and statistical basis. The latitudinal width of the cusp is about 1° [*Newell and Meng*, 1988a], somewhat wider for northward B_z, and somewhat narrower for southward B_z [*Newell and Meng*, 1987]. From the present work, the longitudinal extent is about 2.1 hours for northward B_z and 2.8 hours for southward B_z. For northward B_z the cusp remains fairly confined near noon and at approximately 77°–79° MLAT, although B_y does cause a small local time shift. For southward B_z the cusp has a greater response to variations in both B_z and B_y, thus leading to larger longitudinal and latitudinal motions. The precipitating ion number flux in the cusp is 1.75 ± 0.12 times larger for southward than for northward B_z. There is no appreciable interhemispherical latitudinal difference resulting from B_x.

We choose to conclude with a few comments concerning the most promising directions for future cusp research. Recent accomplishments have been impressive; the relationship between particle precipitation and currents in the cusp region is now clearer [*Erlandson et al.*, 1988]; and the seasonal effects on the cusp latitude [*Burch*, 1973; *Newell and Meng*, 1989] and precipitation [*Newell and Meng*, 1988b] appear to be understood. The pitch angle structure within the low-altitude cusp [*Burch et al.*, 1982; *Lundin*, 1988] is known. There are still some very important outstanding questions concerning the low-altitude cusp: (1) Can FTEs be seen convecting through the cusp, as has been suggested [*Menietti and Burch*, 1988; *Sandholt et al.*, 1989]? (2) Under what circumstances is the peak of the ion flux accelerated compared to magnetosheath values as required by standard merging models? *Hill and Reiff* [1977] presented two cases of such apparent acceleration, but the issue seems not to have been further investigated in detail. (3) What is the causal multivariable relationship between AE, B_z, and cusp latitude? We suggest that the positive correlation between AE and cusp latitude [*Carbary and Meng*, 1986] may be deceptive. A southward B_z shifts the cusp latitude southward, leading to a flux transfer from the nightside to the dayside (i.e., the cusp latitude is lowered) after which substorm activity (AE) increases. The effect of the substorm activity (as measured by AE) should be to return flux from the nightside to the dayside, thus tending to *increase* cusp latitude.

In view of the steady progress being made in understanding cusp behavior, there is reason to be hopeful that some or all of these key remaining questions can be answered in the next few years.

REFERENCES

Burch, J. L., Rate of erosion of dayside magnetic flux based on a quantitative study of the dependence of polar cusp latitude on the interplanetary magnetic field, *Radio Sci.*, *8*, 955-961, 1973.

Burch, J. L., P. H. Reiff, R. A. Heelis, J. D. Winningham, W. B. Hanson, C. Gurgiolo, J. D. Menietti, R. A. Hoffman, and J. N. Barfield,

Plasma injection and transport in the mid-altitude polar cusp, *Geophys. Res. Lett.*, 9, 921-924, 1982.

Burch, J. L., P. H. Reiff, J. D. Menietti, R. A. Heelis, W. B. Hanson, S. D. Shawhan, E. G. Shelley, M. Sugiura, D. R. Weimer, and J. D. Winningham, IMF B_y dependent plasma flow and Birkeland currents in the dayside magnetosphere, 1, Dynamics Explorer observations, *J. Geophys. Res.*, 90, 1577-1593, 1985.

Candidi, M., H. W. Kroehl, and C.-I. Meng, Intensity distribution of day-side polar soft electron precipitation and the IMF, *Planet. Space Sci.*, 31, 489-498, 1983.

Candidi, M., and C.-I. Meng, The relation of the cusp precipitating electron flux to the solar wind and interplanetary magnetic field, *J. Geophys. Res.*, 89, 9741-9751, 1984.

Carbary, J. F., and C.-I. Meng, Correlation of cusp latitude with B, and $AE(12)$ using nearly one year's data, *J. Geophys. Res.*, 91, 10,047-10,054, 1986.

Carbary, J. F., and C.-I. Meng, Correlation of cusp width with $AE(12)$ and B, *Planet. Space Sci.*, 36, 157-161, 1988.

Cowley, S. W. H., Asymmetry effects associated with the x-component of the IMF in a magnetically open magnetosphere, *Planet. Space Sci.*, 29, 809-818, 1981.

Cowley, S. W. H., and W. J. Hughes, Observation of IMF sector effect in the Y magnetic field component at geostationary orbit, *Planet. Space Sci.*, 31, 73, 1983.

Crooker, N. U., Dayside merging and cusp geometry, *J. Geophys. Res.*, 84, 951-959, 1979.

Crooker, N. U., The half-wave rectifier response of the magnetosphere and antiparallel merging, *J. Geophys. Res.*, 85, 575-578, 1980.

Crooker, N. U., Mapping the merging potential from the magnetopause to the ionosphere through the dayside cusp, *J. Geophys. Res.*, 93, 7338-7344, 1988.

Crooker, N. U., J. Berchem, and C. T. Russell, Cusp displacement at the magnetopause for large IMF Y component, *J. Geophys. Res.*, 92, 13467-13471, 1987.

Eastman, T. E., B. Popielawska, and L. A. Frank, Three-dimensional plasma observations near the outer magnetospheric boundary, *J. Geophys. Res.*, 89, 9519-9539, 1984.

Erlandson, R. E., L. J. Zanetti, T. A. Potemra, P. F Bythrow, and R. Lundin, IMF B_x dependence of region 1 Birkeland currents near noon, *J. Geophys. Res.*, 93, 9804-9814, 1988.

Fairfield, D. H., On the average configuration of the geomagnetic tail, *J. Geophys. Res.*, 84, 1950-1958, 1979.

Formisano, V., HEOS-2 observations of the boundary layer from the magnetopause to the ionosphere, *Planet. Space Sci.*, 28, 245-257, 1980.

Foster, J. C., J. M. Holt, R. G. Musgrove, and D. S. Evans, Solar wind dependencies of high-latitude convection and precipitation, in *Solar Wind-Magnetosphere Coupling*, edited by Y. Kamide and J. A. Slavin, pp. 477-494, D. Reidel Co., Dordrecht, Holland, 1986.

Frank, L. A., Plasma in the Earth's polar magnetosphere, *J. Geophys. Res.*, 76, 5202-5219, 1971.

Gussenhoven, M. S., D. A. Hardy, and R. L. Carovillano, Average electron precipitation in the polar cusps, cleft, and cap, *The Polar Cusp*, edited by J. A. Holtet and A. Egeland, pp. 91-97, D. Reidel, Hingham, Mass., 1985.

Gustaffson, G., Corrected geomagnetic coordinates for epoch 1980, in *Magnetospheric Currents, Geophys. Monogr. Ser.*, vol. 28, edited by T. A. Potemra, pp. 276-283, AGU, Washington, D.C., 1984.

Hardy, D. A., L. K. Schmitt, M. S. Gussenhoven, F. J. Marshall, H. C. Yeh, T. L. Shumaker, A. Hube, and J. Pantazis, Precipitating electron and ion detectors (SSJ/4) for the block 5D/flights 6-10 DMSP satellites: Calibration and data presentation, *Rep. AFGL-TR-84-0317*, Air Force Geophys. Lab., Hanscom Air Force Base, Mass., 1984.

Hardy, D. A., M. S. Gussenhoven, and E. Holeman, A statistical model of auroral electron precipitation, *J. Geophys. Res.*, 90, 4229-4248, 1985.

Heelis, R. A., The effects of interplanetary magnetic field orientation on dayside high-latitude ionospheric convection, *J. Geophys. Res.*, 89, 2873-2880, 1984.

Heikkila, W. J., The electromagnetic field for an open magnetosphere, in *Magnetic Reconnection in Space and Laboratory Plasmas, Geophys. Monogr. Ser.*, vol. 30, edited by E. W. Hones, pp. 39-44, AGU, Washington, D.C., 1984.

Heikkila, W. J., Definition of the cusp, in *The Polar Cusp*, edited by J. A. Holtet and A. Egeland, pp. 387-395, D. Reidel, Hingham, Mass., 1985.

Heppner, J. P., and N. C. Maynard, Empirical high-latitude electric field models, *J. Geophys. Res.*, 92, 4467-4489, 1987.

Hill, T. W., and P. H. Reiff, Evidence of magnetospheric cusp proton acceleration by magnetic merging at the dayside magnetopause, *J. Geophys. Res.*, 82, 3623-3628, 1977.

Holzworth, R. H., and C.-I. Meng, Auroral boundary variations and the interplanetary field, *Planet. Space Sci.*, 32, 25-29, 1984.

Hughes, W. J., and S. W. H. Cowley, Observation of IMF-associated magnetic field perturbations in the GSM X component at geostationary orbit, in *Solar Wind-Magnetosphere Coupling*, edited by Y. Kamide and J. A. Slavin, pp. 691-695, D. Reidel Co., Dordrecht, Holland, 1986.

Iijima, T., R. Fuji, T. A. Potemra, and N. A. Saflekos, Field-aligned currents in the south polar cusp and their relationship to the interplanetary magnetic field, *J. Geophys. Res.*, 83, 5595-5603, 1978.

Lundin, R., Acceleration, heating of plasma on auroral field lines: Preliminary results from the Viking satellite, *Ann. Geophys.*, 6, 143-152, 1988.

Lyons, L. R., A simple model for polar cap convection patterns and generation of θ auroras, *J. Geophys. Res.*, 90, 1561-1567, 1985.

Makita, K., and C.-I. Meng, Average electron precipitation patterns and visual aurora characteristics during geomagnetic quiescence, *J. Geophys. Res.*, 89, 2861-2872, 1984.

McDiarmid, I. B., J. R. Burrows, and E. E. Budzinski, Average characteristics of magnetospheric electrons (150 eV to 200 keV) at 1400 km, *J. Geophys. Res.*, 80, 73-79, 1975.

Meng, C.-I., Case studies of the storm time variation of the polar cusp, *J. Geophys. Res.*, 88, 137-149, 1983.

Menietti, J. D., and J. L. Burch, Spatial extent of the plasma injection region in the cusp-magnetosheath interface, *J. Geophys. Res.*, 93, 105-113, 1988.

Newell, P. T., and C.-I. Meng, Cusp width and B_z: Observations and conceptual model, *J. Geophys. Res.*, 92, 13,673-13,678, 1987.

Newell, P. T., and C.-I. Meng, The cusp and the cleft LLBL: Low altitude identification and statistical local time variation, *J. Geophys. Res.*, 93, 14,549-14,556, 1988a.

Newell, P. T., and C.-I. Meng, Hemispherical asymmetry in cusp precipitation near solstices, *J. Geophys. Res.*, 93, 2643-2648, 1988b.

Newell, P. T., and C.-I. Meng, Dipole tilt angle effects on the latitude of the cusp and cleft LLBL, *J. Geophys. Res.*, in press, 1989.

Reiff, P. H., J. L. Burch, and R. W. Spiro, Cusp proton signatures and the interplanetary magnetic field, *J. Geophys. Res.*, 85, 5997-6009, 1980.

Rijnbeek, R. P., S. W. H. Cowley, D. J. Southwood, and C. T. Russell, A survey of dayside flux transfer events observed by ISEE 1 and 2 magnetometers, *J. Geophys. Res.*, 89, 786-800, 1984.

Sandholt, P. E., B. Lybekk, A. Egeland, R. Nakamura, and T. Oguti, Midday auroral breakup, *J. Geomagn. Geoelec.*, in press, 1989.

Sckopke, N., G. Paschmann, G. Haerendel, B. U. O. Sonnerup, S. J. Bame, T. G. Forbes, E. W. Hones, and C. T. Russell, Structure of the low-latitude boundary layer, *J. Geophys. Res.*, 86, 2099-2110, 1981.

Sibeck, D. G., R. W. McEntire, A. T. Y. Lui, R. E. Lopez, S. M. Krimigis, R. B. Decker, L. J. Zanetti, and T. A. Potemra, Energetic magnetospheric ions at the dayside magnetopause: Leakage or merging?, *J. Geophys. Res.*, 92, 12,097-12,114, 1987.

Spreiter, J. R., and S. S. Stahara, A new predictive model for determining solar wind-terrestrial planet interactions, *J. Geophys. Res.*, 85, 6769-6777, 1980.

Svalgaard, L., Polar cap magnetic variations and their relationship with the interplanetary sector structure, *J. Geophys. Res.*, 78, 2064, 1973.

Vasyliunas, V. M., Theoretical models of magnetic field line merging, 1, *Rev. Geophys.*, 13, 303-336, 1975.

Williams, D. J., D. G. Mitchell, L. A. Frank, and T. E. Eastman, Three-dimensional magnetosheath plasma ion distributions from 200 eV to 2 MeV, *J. Geophys. Res.*, 93, 12,783-12,794, 1988.

R. Lepping, Planetary Magnetospheres Branch, Goddard Space Flight Center, Greenbelt, MD 20771.

C.-I. Meng, P. T. Newell, and D. G. Sibeck, The Johns Hopkins University Applied Physics Laboratory, Johns Hopkins Road, Laurel, MD 20707.